Spring 5-4-2019

Evaluation of the Role of Microvascular Pathology on Peripheral Artery Disease

Constance Mietus
University of Nebraska Medical Center

EVALUATION OF THE ROLE OF MICROVASCULAR PATHOLOGY ON PERIPHERAL ARTERY DISEASE

By

Constance Mietus

A DISSERTATION

Presented to the Faculty of the University of Nebraska Graduate College in Partial Fulfillment of the Requirements for the Degree of Doctor of Philosophy

Medical Sciences Interdepartmental Area Graduate Program
(Surgery)

Under the Supervision of Professors Iraklis Pipinos and George Casale

March, 2019

Supervisory Committee:

Iraklis Pipinos, M.D., Ph.D

George Casale, Ph.D

Geoffrey Thiele, Ph.D.

B. Timothy Baxter, M.D.

Acknowledgements

My journey towards becoming a physician scientist has been quite an adventure. Over half of my life so far has been devoted to developing the skills and knowledge necessary to make that dream a reality. I've had a lot of help along the way. I'd like to thank my family for the sacrifices they have made, the constant support they've given, and the faith they had in me that has kept my own faith alive. I am exceptionally grateful to my mom for always, no matter what, being there for me; to my dad for encouraging me to be the best that I can be; to my grandmother who always believed with all of her heart that I could accomplish big things; and to my brother who never ceases to inspire and amaze me. Thank you to Alex, the love of my life, for being with me every step of the way. You most certainly are my better half. I am grateful to all of my friends, without whom I would be lost in life. Vanna, Christine, Larisa, thank you for always being there and being exceptional at life. I am also grateful for the unconditional love I've received from Pabst, Kawa, Sheep, and Lucky.

I am grateful to my mentors, Dr. Iraklis Pipinos and Dr. George Casale, for the time they have invested in my training. Not only have I been introduced to the exciting realms of translational research and vascular surgery, but I have grown tremendously as a researcher over the past four years. I am thankful for a wonderful graduate advisory committee. Thank you Dr. Thiele for all of the time you've invested in helping me develop my grant skills and life skills. Thank you to Dr. Baxter for helping me learn to think as both a clinician and a researcher. I am appreciative of the support that I have received from my colleagues, Panos, Eva, Dimitrios, Tim, Greg, Matt, Ryan, Hernan, Jen, Dr. Kim, Duy, Shuai, and Christina. I am also grateful to my many past mentors and colleagues who selflessly and patiently taught me how to be a better scientist. Thank you to Kacy Cullen

and Kevin Browne for all of the valuable experiences we had together, I would not be the scientist I am today without you.

Over the past six years, I have had the good fortune of working with amazing clinicians who have helped me to explore medicine and have offered me so much guidance in building my clinical career. In particular, I'd like to thank Dr. Michele Aizenberg and Dr. Sheritta Strong for absolutely everything you have done for me, I have learned so much from both of you, and cannot thank you enough for your support, encouragement, and the education I have received under your guidance. Thank you also to Dr. Surdell, Dr. MacTaggart, Dr. Thorell, Dr. Gillis, Dr. Follett, Dr. Torres, Dr. Balasanova, Dr. Che, and Dr. Sharma. Each of you have dedicated so much of your time to support and train me, and I truly appreciate the opportunities I have had working with you. Thank you also to the MD/PhD Scholars Program, both my peers and Drs. Shelley Smith, Debra Romberger, and Justin Mott, for your support and encouragement.

I have been truly blessed in life to have had the help of such amazing people . I do not know what the future will bring but because of you, it certainly looks a lot brighter.

EVALUATION OF THE ROLE OF MICROVASCULAR PATHOLOGY ON PERIPHERAL ARTERY DISEASE

Constance J. Mietus, Ph.D.

University of Nebraska, 2019

Supervisors: Iraklis Pipinos, M.D., Ph.D. and George Casale, Ph.D.

Background: Peripheral Artery Disease (PAD) begins with atherosclerotic narrowing of arteries, including those that supply the legs. Individuals with PAD experience pain during walking, which becomes increasingly limiting. Studies from our group and others have shown that a myopathy is present in the skeletal muscle of PAD patients, and is characterized by myofiber degeneration, fibrosis, and remodeling of vessels ranging from 50 – 150 μm in diameter. However, microvascular pathology, particularly of the smallest microvessels (5 – 15 μm in diameter) remains poorly characterized. Furthermore, little is known about the relationships between microvascular architecture, microperfusion, and patient walking performance. We hypothesize that microvascular pathology is present in the terminal microvasculature of PAD muscle compared to control and worsens with PAD severity. Additionally, we hypothesize that microvascular architecture is associated with deficits in micro- and macro- perfusion and walking performance in PAD patients with intermittent claudication (IC).

Methods: Gastrocnemius biopsy specimens were collected from control, PAD patients with IC, and PAD patients with critical limb ischemia. Microvascular architecture, microvascular fibrosis, total collagen, and the abundance and phenotype of pericytes were quantified. Microvascular perfusion was assessed by Contrast Enhanced Ultrasonography (CEU). Gardner walking protocols were used to assess claudication

onset time (COT) and peak walking time (PWT). Patients also completed the Walking Impairment Questionnaire (WIQ).

Results: Microvascular pathology increased with advancing PAD severity and included progressive increases in basement membrane thickening, abundance of αSMA^+ pericytes, and microvessel density. In advanced PAD muscle, increases were observed in total fibrotic burden and peri-microvascular Collagen I and IV deposition. αSMA^+ pericytes expressed TGF-β1. Relationships were observed between microvascular architecture and microperfusion both at rest and after ischemic stress. Microvascular architecture was associated with macrovascular hemodynamic restrictions. Microvascular architecture was associated with COT, PWT, and patient self-reports of walking speed, walking distance, and stair climbing ability.

Conclusions: Microvascular pathology worsens with PAD severity in association with fibrosis. Alteration of microvascular architecture contributes to microperfusion deficits and walking limitations in PAD.

Table of Contents

List of Tables

List of Figures

List of Abbreviations

ABI	Ankle Brachial Index
ACE	angiotensin converting enzyme
ADP	adenosine di-phosphate
ALK	alkaline phosphotase
ANG2	angiotensin 2
αSMA	α-smooth muscle actin
ATP	adenosine tri-phosphate
BM	basement membrane
BOLD	blood oxygen level dependent
C/EBPδ	CCAAT enhance binding protein-δ
CEU	contrast enhanced ultrasonography
CLI	critical limb ischemia
COT	claudication onset time
CTA	computed tomography angiography
CTT	contrast transit time
CTV	contrast transit velocity
DKK-1	Dickkopf-related protein 1
DM	Diabetes Mellitus
ECM	extracellular matrix
eNOS	endothelial nitric oxide synthase
ET-1	endothelin-1
ET_A	endothelin receptor A
ET_B	endothelin receptor B
$FADH_2$	flavin adenine dinucleotide

FAK	focal adhesion kinase
FGF	fibroblast growth factor
FSP-1	fibroblast specific protein-1
HIF-1α	hypoxia inducible factor-1α
IC	intermittent claudication
ICAM	intracellular adhesion molecule
ICC	interclass correlation coefficient
IQR	Interquartile Range
MBF	microvascular blood flow
MCID	minimal clinically important difference
MCP-1	monocyte chemoattractive protein-1
MCTD	Mixed Connective Tissue Disease
MI	myocardial infarction
MIF	macrophage migration inhibition factor
MRA	magnetic resonance angiography
MRI	magnetic resonance imaging
MSC	mesenchymal stem cell
NADH	nicotinamide di-nucleotide
NFKB	nuclear factor-KB
NG2	neuro/glial antigen 2
NO	nitric oxide
PAD	Peripheral Artery Disease
PAH	Pulmonary Arterial Hypertension
PDGFβ	platelet derived growth factor β
PDGFRβ	platelet derived growth factor receptor β

PDK4	Pyruvate dehydrogenase Kinase 4
PET	positron emission tomography
PHD	prolyl hydroxylase domain
PWT	peak walking time
RGS-5	regulator of G-protein signaling-5
ROS	reactive oxygen species
SF-36	short form-36
SLE	systemic lupus erythematosus
SOD	superoxide dismutase
SPECT	single photon emission computed tomography
TGF-β1	transforming growth factor-β1
TIC	time intensity curves
TNFα	tumor necrosis factor α
TTP	time to peak
VCAM	vascular cellular adhesion molecule
VEGF	vascular endothelial
VSMC	vascular smooth muscle cells
WIQ	Walking Impairment Questionnaire

Chapter I: Introduction and Background

Atherosclerosis

Atherosclerosis, a leading cause of morbidity and mortality worldwide,[1,2] is a systemic disease that affects susceptible sites in large and medium sized arteries. During atherogenesis, the arterial endothelial layer becomes perturbed, generating a transient inflammatory response. Several events may lead to this endothelial damage. Physical damage can be induced by direct trauma, stress, or hypertension. Circulating factors can aggravate damage, notably the reactive oxygen species (free radicals) that are present in air pollution and cigarette smoke. Additionally, it is believed that hyperlipidemia, chronically elevated blood glucose, and elevated levels of homocysteine exacerbate arterial endothelial damage. Early atherosclerotic lesions appear as fatty streaks and are observed in post mortem aortas of individuals as young as 10 years of age. It is believed that with chronic damage and inflammation these fatty streaks evolve into atherosclerotic plaques that are composed of accumulated lipid and fibrous material between the intimal and medial layers of vessels. As atherosclerotic plaques grow in size, the lumen of the affected artery stiffens and narrows, often with deleterious consequences to the downstream tissues. Slowly growing plaques tend to be more stable due to compensatory remodeling of the artery through migration and proliferation of vascular smooth muscle cells (VSMC). Rapidly growing plaques are thought to contain the inflammatory and lipid aggregations within the vessel by coverage with a fibrous cap. These unstable plaques are more prone to rupture which results in rapid blood clot occlusion (full or partial), which may abruptly occlude the artery, subsequently inducing tissue ischemia. Fragments of these blood clots can dissociate from the lesion and travel to distal vasculature, where smaller caliber vessels may also become occluded. Several organs are susceptible to the

consequences of atherosclerotic disease, including the heart (coronary artery disease & myocardial infarction), brain (transient ischemic attack & stroke), and kidney (renal artery stenosis & kidney failure). Peripheral vasculature is often involved and may lead to Peripheral Artery Disease (PAD). Plaques in PAD are most commonly found in the aortoilliac and femoropopliteal regions of the vasculature that supplies the lower limbs.[3]

Peripheral Artery Disease

PAD is a progressive disease that begins with the atherosclerotic narrowing of arteries leading to a partial or complete failure of the arterial system to deliver oxygenated blood to peripheral tissues including the legs.[4] PAD is estimated to affect approximately 202 million individuals globally, including 8.5 million Americans,[5,6] and the prevalence of PAD is anticipated to rise as populations age.[3] It is estimated that 12-20% of all individuals above the age of 60 have PAD [7]. Additionally, the total cost of PAD in the United States exceeds $21 billion dollars annually.[8,9] PAD impairs quality of life[10-12] and increases the patient's 5-year mortality rate by up to 30%,[13-18] however the pathophysiologic mechanisms are not known.

The Fontaine scheme clinically classifies PAD into four stages. In the early stages of PAD, a reduction in blood flow is present but the individual is asymptomatic (Fontaine Stage I).[4,19] Claudication is the most common symptomatic manifestation of PAD, presenting as ischemic leg muscle pain and gait dysfunction (Fontaine Stage II).[19,20] In later stages, PAD patients experience pain at rest (Fontaine Stage III)[19,21,22] and many patients progress to developing ulcerations that range from trophic lesions to gangrene which may require limb amputation (Fontaine Stage IV).[19,21]

The development of intermittent claudication (IC) is insidious, and in very mild PAD, IC symptoms only develop during intervals of high physical activity.[23] Intensity of

physical activity fluctuates very little throughout the day of an average claudicating patient. Additionally, a recent study from our laboratory demonstrated that PAD patient activity rarely exceeded a light intensity level. Patients with IC spent half of their wakeful hours in sedentary behavior and when active, walking was limited to short bursts followed by several minutes of rest.[24] This data suggests that individuals with IC likely adapt their activity patterns to minimize claudication symptoms without conscious awareness of compensatory behavioral changes. Patients with IC have a 12% higher mortality rate than age matched controls[25] and one in four patients with IC will have deterioration of symptoms.[26] It is estimated that for each symptomatic PAD patient, there are another three to four patients with PAD who do not meet the clinical criteria for intermittent claudication.[23]

Critical Limb Ischemia (CLI) represents the most severe clinical manifestation of PAD, and is the major cause of ischemic amputations.[27] In a recent review of insured patients within the United States, approximately 11% of patients with PAD had CLI.[27] Presentation patterns of CLI are not uniform. Longitudinal studies of patients with IC have shown that these individuals rarely progress to develop CLI. Conversely, patients can present with no recognized PAD symptoms as soon as six months prior to diagnosis of CLI,[28,29] and primary CLI is more common in patients with diabetes mellitus (DM).

Several risk factors are known to contribute to the development of PAD. Advancing age is a major underlying risk factor, and is reflected by the 1% prevalence of PAD in individuals at age 40 rising to 15-20% within individuals at age 70.[3,17,30] An individual's gender (male > female),[23] ethnicity (non-hispanic black > caucasian),[23,31] socioeconomic status, and access to health care,[32] contribute to risk of PAD. Family history of PAD is also an independent risk factor, likely due to a genetic component of PAD. Odds ratios of acquiring PAD are increased amongst monozygotic twins (OR: 17.7), dizygotic twins (OR: 5.7), and siblings (OR: ~2.0).[33,3435] Genetic factors may contribute to

the development of premature PAD, and candidate pathways include those involved in thrombosis, inflammation, and lipid and homocysteine metabolism.[35,36] Although causal variants could not be identified by genetic linkage studies, several candidate susceptibility genes were identified involving pathways of inflammation, coagulation, lipid metabolism, blood pressure regulation, and vascular matrix regulation.[37] Genome wide association studies have revealed several attractive single nucleotide polymorphisms, however, the odds ratios associated (1.13 – 1.31) are modest.[35]

Sedentary lifestyle is thought to be a significant avoidable risk factor. Additionally, tobacco use, poor dietary intake, obesity, and management of co-morbid conditions, particularly hypertension, diabetes, dyslipidemia, hyperhomocysteinemia, and renal insufficiency, contribute to avoidable risk. A clear dose-response relationship exists with tobacco use, with a strong increase in risk for PAD in heavy smokers, as well as a four-fold increase in risk of developing IC.[23,38] Smokers have a greater relative risk for developing PAD (RR: 2.71) than coronary artery disease (RR: 1.67),[39] and smokers are diagnosed approximately a decade earlier than non-smokers.[38] Fortunately, smoking cessation is associated with a decline in the incidence of IC.[23]

Diabetes and PAD are strongly linked. Insulin resistance raises the risk of PAD by approximately 40-50%, even in individuals without diabetes.[40] For every 1% increase in hemoglobin A1c, there is a corresponding 26% increased risk for PAD. Additionally, the natural course of PAD is worse in diabetics.[41,42] Amongst PAD patients, IC is approximately twice as common amongst diabetic versus non-diabetic patients.[43] Additionally, patients with both PAD and diabetes have a five to ten times higher lifetime risk of amputation compared to either disease alone.[23,44-47] It has been proposed that diabetes induces a state of inflammation and accelerates atherosclerosis by causing endovascular dysfunction of the microvascular and macrovascular circulation.[44,45,48] Insulin may increase total blood flow and stimulate glucose uptake within skeletal

muscle.[49,50] Interestingly, insulin recruitment of the microvasculature is normally rapid and occurs at a lower concentration of insulin than is required to increase total blood flow. Insulin may increase relaxation of terminal arterioles, thereby shunting blood flow from non-nutritive pathways towards nutritive capillary beds that are typically under perfused during rest, which greatly increases the surface area for nutrient exchange within skeletal muscle. [49,52] However, in patients with diabetes, microvascular recruitment is impaired.[51] Insulin resistance is accompanied by defects in skeletal muscle vasculature and includes loss of capillary density,[53] possibly resulting in a reduced ability of insulin and nutrients to reach myocytes.[54] In the skeletal muscle of type II diabetic patients, microvascular pathology was observed that included thickening of the microvascular basement membrane, endothelial and pericyte degeneration, and acellular capillaries.[55] Pericyte degeneration destabilizes microvessels and reduces angiogenesis in several organs of diabetic patients, and is best characterized in diabetic retinopathy. Advanced glycation end products and oxidative damage are prevalent features of diabetes, and may induce endothelial damage, thereby initiating the deleterious changes observed in the microvasculature of patients with DM.

The Limb Dysfunction in Peripheral Artery Disease

Arterial atherosclerotic occlusion is thought to impair blood flow to the lower extremities of PAD patients. However, the pathophysiology of PAD limb dysfunction is complex and is not fully explained by simple supply and demand mismatch of blood flow through the occluded arterial segments. A longstanding belief was that PAD limb dysfunction arose solely from IC. As individuals would begin walking, the metabolic demands of the tissues distal to the stenosis would rise, and blood flow across the

occlusion would be insufficient, generating brief periods of ischemia that would induce pain and impairment. For this model to be correct, the extent of arterial stenosis and collateral circulation would be the only mediators of PAD symptomology, and revascularization of occluded arterial segments should restore limb function. However, gait is improved but not restored after revascularization. Six months after bilateral revascularization, PAD patients with IC demonstrate improvements in quality of life, walking distances, plantar flexor strength, and gait biomechanics of the ankle and knee. However, there is a lack of improvement at the hip during pain-free gait as well as worsened gait at the ankle, knee, and hip after the onset of claudication pain which indicates that limb function does not resolve.[56] Additionally, advanced biomechanical gait analysis demonstrates that gait dysfunction precedes the onset of claudication. Although arterial stenosis is critical to the onset of PAD pathophysiology, it is likely that a subsequent myopathy develops which enhances limb dysfunction in PAD patients.

Studies comparing age-matched elderly patients with and without PAD have demonstrated that the effect of ageing on gait is not nearly as significant as the changes due to PAD.[57] Slower walking speeds and shorter strides are observed in older individuals with and without PAD. However, additional deficits are unique to PAD. Joint angle and torque analyses demonstrate that muscle weakness is present across ankle, knee, and hip joints of PAD patients with IC, and may be a fundamental source of PAD altered gait patterns.[57] Muscle weakness across plantar flexors, knee extensors, hip flexors, and hip extensors resulted in decreased plantar flexor torque, knee extensor torque, and hip extensor torque in early stance, as well as hip flexor torque during late stance in PAD patients.[57,58] Both kinetic and kinematic abnormalities are present before the onset of claudication pain, and occur rapidly after initiation of walking, often within the first 3-4 steps, and worsen during and after the onset of claudication.[58] The alterations of muscle

strength may contribute to the joint angle and torque changes observed in PAD gait, and are likely related to the extent of myopathy present.

The Myopathy of Peripheral Artery Disease

Skeletal muscle is the end organ most affected by PAD, leading to an ischemic myopathy that is characterized by altered myofiber morphology and degeneration, mitochondrial dysfunction, and impaired limb function.[59-66] Our group and others have demonstrated that myopathy is progressive as the severity of PAD advances.[64] In early stages of PAD myopathy, subtle changes in myocyte morphology arise and are heterogeneously distributed. Myofibers can become enlarged or conversely undergo degeneration and the polyhedral perimeter of myocytes can become rounded.[61] Whereas nuclei are normally found near the sarcolemma of myocytes, in PAD myopathy nuclei become centralized. Centralized myocyte nuclei are commonly encountered in regenerating myofibers, which suggests that myofibers may be attempting to repair tissue damage. Additionally, vacuolization within myofibers is commonly encountered and is thought to correspond to proteins with oxidative damage that have accumulated within the myocyte. As the myopathy progresses, myofiber pathology worsens, increases in frequency, and becomes more homogeneously distributed. Whereas fibrosis if relatively limited in early PAD myopathy, increased fibrotic deposition of collagen around myofibers, myofascicles, and microvessels occurs in later stages of PAD myopathy.[67]

Striking alterations are also observed within the vasculature of PAD limbs. Atherosclerosis induces medial hypertrophy of affected arteries, with a concomitant replacement of elastin with collagen.[68] These alterations result in a stiffening of PAD arteries, which may have deleterious effects on the transmission of mechanical force

across the vascular wall, with subsequent alterations of mechanically induced cell signaling, which ultimately may negatively impact blood flow regulation through myopathic tissues. Medial hypertrophy and hyperplasia are continuous across the arterial to arteriolar interface and aberrantly extend into the microvasculature of PAD muscle. Whereas VSMC are arranged to mediate vascular tone and contraction, the arrangement of pericytes around the microvessels (>50μm) may be integral in facilitating and integrating cellular communication[69] within the myopathic microenvironment. Consequently, small vessels in PAD leg muscles may sense ischemic hypoxia and induce VSMC hypertrophy and hyperplasia, and may lead to fibroblast accumulation, myofibroblast differentiation, and collagen deposition.[67] Thus, microvessels may be the initiators and drivers of fibrosis and PAD myopathy. However, the mechanism by which PAD microvessels influence vascular remodeling and blood flow regulation remains poorly characterized.

Mitochondropathy and Oxidative Damage Contribute to PAD Myopathy

Chronic cycles of ischemia-reperfusion may induce the myopathic changes observed in the lower limbs of PAD patients. Ischemia-reperfusion injury to skeletal muscle may lead to a decline in the integrity and function of myofibers, and as a consequence, sufficient myofiber degeneration may modify gait and ambulation. Initially, these cycles are related to the atherosclerotic occlusion of the arterial supply to the skeletal muscle of PAD patients. As patients begin to walk, the demand for oxygen and nutrients increases, but the stenosed vessels present hemodynamic restrictions which limit blood delivery to metabolically demanding tissues thereby producing a transient ischemia. As patients rest, metabolic demand decreases, and blood flow becomes sufficient to re-perfuse these tissues. Additionally, as patients become more sedentary,

venous and lymphatic clearance (*via* the muscle pump effect)[70] may be decreased. Stagnant blood may be populated with toxic metabolites that may be harmful to the skeletal muscle, which may contribute to PAD myopathy.

Cycling between hypoxia and normoxia has been shown to be highly damaging to end organs throughout the body.[71] With repeated incidents of transient hypoxia, reperfusion injury inflicts havoc on distal tissues indirectly through alterations in gene expression profiles [72,73] and directly through intracellular damage *via* reactive oxygen species (ROS).[65] Such damage can induce cellular necrosis, which leads to the local release of potent pro-inflammatory factors. Additionally, oxidative damage and mitochondrial dysfunction may play critical roles in the initiation and progression of PAD myopathy.

Mitochondrial function is abnormal in patients with PAD.[74] During exercise, skeletal muscle preferentially utilizes oxidative phosphorylation to supply the energy demands of the myocytes. Glucose and fatty acids are converted to acetyl-CoA and subsequently acetyl-CoA condensation with oxaloacetate generates citrate within the mitochondrial matrix. Citrate formation initiates the tricarboxylic acid cycle, the intermediates of which reduce electron carriers (NADH and $FADH_2$) and shuttle electrons to the electron transport chain of the inner mitochondrial membrane. A membrane potential is thus created by the resultant electro-chemical potential and is utilized by ATP synthase to phosphorylate adenosine diphosphate (ADP) into adenosine triphosphate (ATP).[75] PAD gastrocnemius biopsy specimens displayed an accumulation of metabolic intermediates, including acylcarnitine and lactate.[64,66,76,77] This data suggests that PAD muscle inefficiently utilizes glucose (anaerobic glucose oxidation), possibly due to a decreased capacity of mitochondria to complete the tricarboxylic acid cycle yielding incomplete oxidation of fuel substrates.

Mitochondria control ATP flux through several steps in oxidative phosphorylation. The electron transport chain capacity determines the pace of oxidation. Electron transport chain capacity decreases with age and likely contributes to declines in muscle power output and locomotor performance.[78] In advanced PAD, mitochondrial complexes I, III, and IV have significant reductions in respiratory capacity and enzymatic activity.[74,79] Decreased complex I activity has been observed in PAD muscle and suggests that a quantitative deficit in mitochondrial respiratory capacity in PAD.[80] Successful oxidative phosphorylation requires a terminal electron acceptor, which in mitochondria is molecular O_2. Mitochondrial coupling efficiency (the coupling of the cell's ATP supply from oxygen uptake) contributes to exercise efficiency and the capacity for sustained exercise.[78] Inhibition of adenine nucleotide translocase (*via* atractyloside titration) yields lower mitochondrial coupling control in PAD patients compared to control patients,[80] which suggests poorer quality of mitochondria in PAD myopathy. Lastly, ATP synthesis contributes to myocyte performance. ATP synthesis is dynamic, has several regulatory checkpoints, and can provide as much as a 50-fold range of ATP flux between resting muscle and exercise at the mitochondria's maximal capacity.[78] Studies using Phosphorus-31 nuclear resonance spectroscopy demonstrated phosphocreatine depletion and intracellular acidification were increased in PAD patients compared to healthy controls during exercise. These data suggest that PAD mitochondria have an impairment in oxidative ATP synthesis with a subsequent enhancement of non-oxidative ATP synthesis that is likely compounded by reduced proton efflux. Furthermore, acidification prevented an increase in ADP concentration, limiting compensation for the oxidative defect. Exercise induced changes in pH and phosphocreatine concentration necessitated approximately twice as much ATP turnover per given muscle power output in PAD patients relative to control patients.[81]

In a recent study by Baum and colleagues, ultrastructural assessment of vastus lateralus muscle biopsy samples demonstrated that capillary density, mitochondrial volume density, and peak power output during leg extension exercise were lower in PAD patients with IC than control. They also noted that the microvessels in these samples had thickened BM.[82] This suggests that alteration of the microvascular architecture may be associated with both limitations at the capillary to mitochondrial interface and muscle performance. Mitochondrial enzyme activity may be reduced in association with decreased mitochondrial density.[74,82] Paradoxically, an increased volume density has been observed in PAD gastrocnemius.[83,84] PAD pathology is often worse in the gastrocnemius than the vastus lateralis, and the elevated volume density of mitochondria in the gastrocnemius may represent a more robust compensatory effort in the face of limited oxygen delivery and poor mitochondrial function. The relationships between oxygen tension, mitochondrial function, muscle performance, microperfusion, and microvascular architecture are also poorly characterized, particularly within the gastrocnemius. Alterations of the microvascular architecture, such as BM thickening, may directly contribute to diffusion limitations, which may result in aberrant mitochondrial function and the generation of ROS, with consequent deleterious effects on muscle performance. Hence, understanding the relationship between microvascular structural alterations in PAD and oxidative stress is of particular interest and warrants further investigation.

Chronic cycles of ischemia/reperfusion injury occur and worsen with increasing atherosclerotic blockage of the arteries feeding the legs. During exercise when metabolic demands are heightened and myocytes are most vulnerable to hypoxia, the supply-demand mismatch of arterial blood flow likely enhances skeletal muscle ischemia and oxidative damage. Mitochondrial dysfunction contributes to the production of ROS and stagnant blood may carry toxic metabolites that may also contribute to oxidative stress

and tissue injury in PAD limbs. The capacity for PAD tissues to neutralize ROS is also diminished. Studies have demonstrated that manganese superoxide dismutase, a major antioxidant enzyme, is deficient in PAD skeletal muscle. Thus, the generation, accumulation, and inability to neutralize ROS collectively contribute to oxidative stress in PAD limbs. ROS may be involved in cell signaling during normal physiological function. Thus, elevated ROS may alter cellular functions, including promotion of cell survival, angiogenesis, differentiation, and proliferation. ROS signaling may become continuous and grow in intensity with advancing arterial flow limitations, and may contribute to pathological tissue remodeling, including microvascular structural alterations and fibrosis. Excessive ROS may also damage DNA and proteins, particularly within the mitochondria where ROS concentrations are likely the greatest within the cell.

Ultrastructural analysis of mitochondrial structure supports the conclusion that oxidative damage is greatest in mitochondria of PAD muscle. Mitochondria demonstrate hypertrophy, hyperplasia, and hypercristae. Mitochondria also acquire a transverse orientation and gain paracrystalline inclusions and lipid vacuolizations.[85,86] Mitochondrial ROS contributes to the oxidative damage and addition of adducts to proteins (carbonyl) and lipids (4-hydroxynonenal). Increases in carbonyl and 4-hydroxynonenal products have been observed in the myofibers of PAD patients and were associated with loss of myofibers and advancing PAD stage severity.[61] Additionally, PAD muscles had increased desmin and desmin gene transcripts, which corresponded to changes in myofiber morphology. Desminopathy was also associated with decreased mitochondrial respiration as well as decreased muscle strength and walking performance.[59] These data support that mitochondrial oxidative damage may directly contribute to myofiber degeneration, and likely declining limb performance.

Fibrosis is Progressive in PAD and Linked to Vascular TGF-β1 Expression

Fibrosis is defined by the stiffening and/or scarring of tissues which is attributed to excessive deposition of ECM components such as collagen. In skeletal muscle, myofibroblasts deposit collagen which subsequently compromises tissue architecture, myofiber contractility, and ultimately muscle force production.[58,61,64-66,80,85-92] Fibrosis is thought to occur as a generalized healing response after inflammation. Stimuli such as persistent infections, allergic reactions, autoimmunity, chemical or physical injury, and radiation can induce fibrosis.[93] However, in PAD patients, this fibrotic response arises from chronic intermittent hypoxia, becomes persistent, and leads to scarring associated with worsening myopathy and clinical symptoms. Our laboratory has shown that collagen deposition increases with advancing PAD disease stage[67]. One of the most striking pathological changes was the dense collagenous investment of the microvessels (5 -12 μm total diameter). In association with increased collagen deposition, we found a robust expression of transforming growth factor β1 (TGF-β1), a potent pro-fibrotic cytokine, in the VSMC of the small vessels (*ca.* 50 to 150 μm lumen diameter) of the affected gastrocnemius of PAD patients[67]. Increased TGF-β1 is a persistent feature of PAD myopathy[61,67,87,88,92,94-96] and is likely to be a predominant factor in propagating the fibrotic expansion of the ECM in the muscles of PAD limbs. Homogenates of gastrocnemius biopsies from PAD patients demonstrate, on average, a three-fold increase in TGF-β1[97] compared to age matched control patients. Furthermore, fibrosis occurs in PAD legs and leads to scarring that is associated with worsening myopathy and clinical symptoms which are the most severe in elderly subjects.[98]

Imaging Characteristics of PAD Skeletal Muscle

Various modalities have been used to assess arterial occlusion and skeletal muscle myopathy in PAD. Magnetic resonance imaging (MRI) is a powerful imaging modality for the visualization of tissue morphology. Work from our lab has recently focused on characterizing PAD myopathy by analyzing the distribution of pixel intensity across non-contrast enhanced T1 and T2 MRI-imaging sequences. Preliminary work from our lab shows that both T1 and T2 mean pixel intensity are associated with extent of macrovascular occlusion and muscle performance. Ankle brachial index (ABI), a surrogate measure for arterial occlusion, (**Figure 1**) and pain free peak plantarflexion (**Figure 2**) are positively correlated with T1 mean pixel intensity in the PAD muscle. T2 mean pixel intensity is inversely correlated with the time to recover from ischemia after exercise (**Figure 3**). Future studies are needed to characterize the relationship between MRI characteristics and histological features of myopathy, including collagen deposition and myocyte morphology, however, these data support that MRI may be able to non-invasively discriminate features that determine the extent and severity of PAD myopathy, which may allow correlational analysis of patient outcomes after standard interventions such as revascularization of supervised exercise therapy.

Figure 1: The Association Between ABI and T1 Mean Pixel Intensity

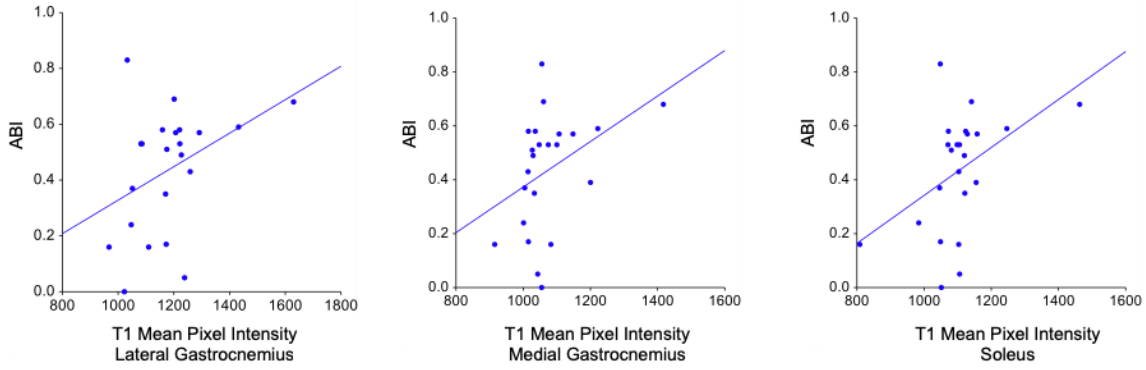

Figure 1: The association between ABI and T1 Mean Pixel Intensity
As ABI decreases, T1 mean pixel intensity decreases in the lateral gastrocnemius (n = 22; R = 0.37; p = 0.09), the medial gastrocnemius (n = 23; R = 0.45; p = 0.03), and the soleus (n = 23; R = 0.46; p = 0.03). Linear relationships were assessed by Spearman Rank Correlations.

Figure 2: Pain Free Peak Plantarflexion is Associated with T1 Mean Pixel Intensity

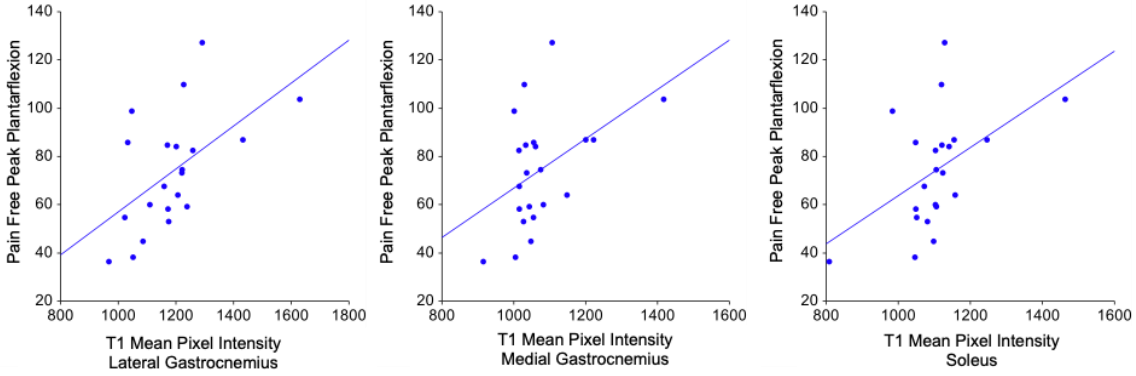

Figure 2: Pain Free Peak Plantarflexion is Associated with T1 Mean Pixel Intensity
Pain free peak plantarflexion increases in association with increasing T1 mean pixel intensity in the lateral gastrocnemius (n = 21; R = 0.55; p = 0.009), the medial gastrocnemius (n = 22; R = 0.43; p = 0.05), and the soleus (n = 22; R = 0.55; p = 0.008). Linear relationships were assessed by Spearman Rank Correlations.

Figure 3: Duration of Recovery from Ischemia is Associated with T2 Mean Pixel Intensity

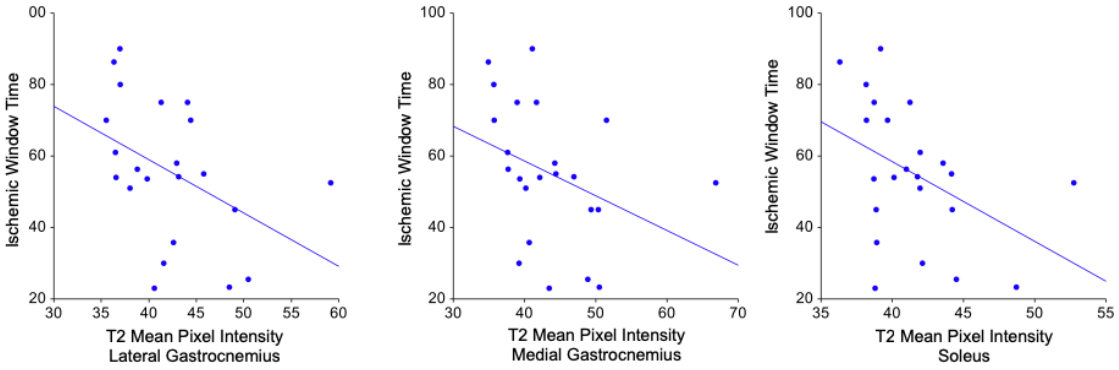

Figure 3: Duration of Recovery from Ischemia is Associated with T2 Mean Pixel Intensity.

The ischemic window measurement represents the severity of ischemic deficits present in the limb, whereas the ischemic window time measures the duration of time from the discontinuation of exercise to the recovery of pre-exercise ankle systolic pressure. An inverse relationship is present between ischemic window time and T2 mean pixel intensity in the lateral gastrocnemius (n = 22; R = -0.48; p = 0.03), the medial gastrocnemius (n = 23; R = -0.48; p = 0.03), and the soleus (n = 23; R = -0.46; p = 0.03). Linear relationships were assessed by Spearman Rank Correlations.

Traditional MRI offers superior spatial resolution for defining morphology, however, additional MRI sequences and techniques are available to quantify hemodynamic parameters, including perfusion. Magnetic resonance angiography (MRA) is frequently used to visualize blood vessels including areas of vascular occlusion or stenosis. MRA can be completed with or without contrast enhancement (gadolinium based). Although peak arterial flow can be visualized by contrast-enhanced MRA techniques, MRA does not offer good temporal resolution, particularly with regards to microvascular hemodynamics. Computed Tomography Angiography (CTA) utilizes similar principles to MRA and has also been used to visualize arterial pathology and flow.

Blood oxygenation level dependent (BOLD) MRI has recently been used to characterize the hyperemic response of PAD legs. BOLD MRI imaging works on the principle that deoxygenated hemoglobin is paramagnetic, and consequently conversion from oxygenated to deoxygenated hemoglobin can be detected as localized magnetic field distortions. Thus, ratios of oxygenated to deoxygenated hemoglobin can be quantified, which yields information about muscle oxygenation state, perfusion, and metabolic demand. BOLD signal is also dependent on blood volume, hemoglobin concentration, blood pH, and local metabolic products such as lactate and phosphate.[99] In addition to the multifactorial contribution to BOLD responses, BOLD MRI has limited reproducibility, with a coefficient of variation as high as 50.9%.[100] Ledermann and colleagues compared the BOLD response in calf muscles from PAD patients and healthy controls using a post-occlusive reactive hyperemia paradigm. The T2* time course (BOLD response) was reduced during reactive hyperemia in PAD patients compared to controls and the time to peak T2* signal was prolonged.[101] This suggests that muscle perfusion is delayed and decreased during reactive hyperemia in patients with PAD, however, the specific contribution of microvascular pathology could not be determined in this study.

Single photon emission computed tomography (SPECT) and positron emission tomography (PET) have also been used in studies addressing microvascular perfusion in PAD. Both SPECT and PET offer high sensitivity. However, these imaging modalities are riddled with disadvantages. PET imaging has limited access, is costly, and offers relatively modest spatial resolution. SPECT imaging also has modest spatial resolution and is difficult to quantify. PET and SPECT, like CT, also rely on the use of ionizing radiation. Thus, the use of these imaging modalities is of limited use in clinical evaluation of microvascular perfusion.

Although radiological standard modalities cannot accurately evaluate microperfusion[102], a relatively new imaging modality, contrast enhanced ultrasonography (CEU), may be able to evaluate microperfusion abnormalities in PAD legs. CEU offers the ability to visualize perfusion of large vessels as well as small vessels. CEU has excellent spatial and temporal resolution, which allows the visualization of flow redistribution (or lack thereof) between nutritive and non-nutritive circuits within PAD muscle during exercise.[103] CEU relies on the use of microbubble contrast agents which remain confined within the vascular system, and thus do not distribute to the interstitium of tissues.[99] CEU imaging has a resolution that can discriminate vessels as small as 100 μm,[104] making this imaging modality a potent means for evaluating microvascular hemodynamics.

The basic premise of CEU imaging begins with the composition and physical properties of microbubbles. Microbubbles are typically <5 μm in diameter, which allows them to pass unimpeded through capillary beds.[105] Microbubbles are encapsulated within lipid, protein, or biopolymer shells. Gas diffusion across the shell needs to remain limited, thus these shells must have sufficient barrier function and low surface tension.[105] Contemporary microbubble gases, such as octafluoropropane, sulfurhexafluoride, and

perfluorobutane, are less diffusible and less soluble in aqueous solutions (lower Ostwald coefficient) than first generation low molecular weight microbubbles.[105] These newer microbubble gaseous formulations have substantially greater longevity within the circulation, which enables more robust and accurate signal detection. Microbubble contrast agents also have unique physical properties that enhance the discriminatory capability between contrast and tissue signals. As the ultrasound transducer emits sound waves, rapid variations in acoustic pressure are propagated through the tissue. These sound waves induce resonant volumetric oscillations in the microbubbles, which produces asymmetric changes in microbubble diameter.[106] The degree of oscillation is dependent on the density of the gas core, microbubble shell components, ultrasound characteristics, and the surrounding medium.[105] Asymmetric changes in microbubble size lead to sound wave reflections that have strong non-linear components as well as harmonic overtones that are multiples of the transmitting frequency. Conversely, tissue and tissue motion reflect linear components back to the transducer.[105,106] Thus algorithms constructed around pulse correlation can detect and discriminate the non-linear microbubble signal from linear tissue signals. Microbubbles that oscillate without significant loss of microbubble integrity are in a state of stable cavitation. However, with increasing frequency or pressure amplitude, microbubbles can rupture and result in inertial cavitation.[105]

Low-power, real-time CEU utilizes signals are produced by microbubble stable cavitation. Two methodologies (bolus microbubble infusion kinetics and replenishment kinetics) have been used in the studies of human skeletal muscle in PAD muscle. Early CEU studies delivered a single bolus of microbubbles, thereby allowing the characterization of the wash in and wash out kinetics, the time to peak (TTP) contrast signal, the slope of the rise to maximal signal intensity, the maximum signal intensity, and the area under the curve (AUC) generated by contrast influx, which is an approximation

of blood volume. TTP likely reflects both macro- and microcirculation since achieving maximal contrast intensity requires microbubble delivery through both arterial and microvascular vessels.[107] Likewise, maximal signal intensity and AUC are influenced by arterial inflow and microvascular perfusion. The slope to maximal signal intensity, however, may be the most specific measurement of microcirculation.[102] However, dynamic CEU can be biased by several factors, including systemic flow and instability of contrast concentration in the blood pool, which limits the quantification and interpretation of microvascular hemodynamic performance.

In order to exclude the influence of macroperfusion and determine only microperfusion, replenishment kinetics must be assessed.[108] To assess these kinetics, contrast is continuously infused until a steady state is achieved. Subsequently, inertial cavitation is induced to destroy all microbubbles in the transducer's field. The replenishment of microbubbles from adjacent vessels into the field is recorded at each low power pulsing interval. Measurement of the rate of replenishment is thus directly proportional to the regional blood flow rate.[106] Quantification of replenishment kinetics is independent of systemic flow, and reflects microvascular flow.[109-113] Time intensity curves (TIC) are comprised of serial measurements of the signal intensity as a function of time after inertial cavitation, and when plotted as a non-linear equation can produce estimations of red blood cell velocity or blood flux rate, relative blood volume, and microvascular blood flow. The TIC reflects intravascular transit times.[106]

CEU has been used to assess the severity of PAD, as well as alterations of microperfusion. CEU has offered the opportunity to examine the influence of collateral perfusion on PAD, as well as large and small vessel physiologic effects on PAD limb perfusion.[110] In several studies, a relationship between CEU parameters and ABI was absent. This suggests that CEU provides information about PAD severity beyond what

ABI produces, and importantly CEU reveals information of hemodynamic relevance to myopathic areas, particularly microvascular dysfunction.[109,114]

Microperfusion is Altered in PAD Myopathic Skeletal Muscle

Increasing arterial stenosis contributes to flow limitations in PAD, particularly during exercise. Distal to the stenosis, vascular remodeling occurs throughout the vascular tree. This remodeling includes stiffening of the vessels, hypertrophy and hyperplasia of VSMC, perivascular collagen deposition, and microvascular structural alterations. Although arterial flow limitations are fairly well characterized, relatively few studies have addressed microvascular perfusion deficits in PAD patients. However, recent studies using CEU demonstrate that PAD pathology may have a microvascular component.

Several animal models have attempted to characterize microvascular perfusion deficits. In a porcine model of PAD, Bragadeesh and colleagues surgically created a gradient of stenosis across the femoral artery of pig hindlimbs. They observed that as the severity of stenosis increased, resting femoral blood flow decreased. Interestingly, skeletal muscle blood flow was preserved in moderate stenosis, and only became limited in severe stenosis.[110] This suggests that in moderate stenosis, collateral arteries may be able to compensate for the decreased flow across the stenosed artery and that the contribution of collateral circulation is inadequate in severe stenosis. Diminished resting microvascular blood flow was attributed to decreased microvascular blood flux rate. During adenosine induced hyperemia, blood flux rate increased, but was blunted with increasing stenosis. With exercise, microvascular blood volume decreased more than blood flux rate in association with increasing stenosis severity.[110] It is possible that the

decline in blood volume reflects the muscle pump effect, in which contracting muscles squeeze venous blood and encourage venous return to the heart. Conversely, reduction in microvascular blood volume during exercise may reflect active de-recruitment of capillary circuits, possibly *via* constriction at pre-capillary sphincters, as a means to preserve precapillary pressure and maintain blood flux through a subset of capillary beds.[110,115,116] Microvascular flow reserve is calculated as the ratio of microvascular blood flow during hyperemia to microvascular blood flow at rest. Flow reserve was nearly completely lost in animals with severe stenosis. As stenosis severity increased flow reserve decreased after both adenosine-induced hyperemia and exercise in association with stenotic pressure gradients.[110]

In a rodent hindlimb ischemia model, Pascotto and colleagues used CEU to assess specific components of perfusion alongside histological analysis. They segregated blood flow into three categories: 1) arterial; 2) non-capillary microvessels (arterioles); and 3) capillaries. On completion of the surgical ligation, capillary blood flow decreased by approximately 30% relative to the intact contralateral limb. Capillary blood flux rate was affected to a greater extent than blood volume. Over the following two weeks, large collateral vessels expanded and reorganized, and changes in perfusion, predominantly non-capillary blood volume, were temporally related to arteriogenesis and expansion of the collateral network. Histological review revealed an increase in the number of microvessels (20 – 40 μm) within myofibers, as well as enlargement of larger arterioles that bridged myofascicles. Thus, it was suggested that large collateral circuits are the most rapidly effective means of restoring tissue perfusion after ligation, but only if remodeling of more distal arterioles has occurred. These alterations may allow reductions in distal resistance in the presence of persistently low perfusion pressures. Interestingly, changes in capillary flow did not occur until after remodeling of non-capillary microvessels. The greatest changes observed in capillary flow were attributable to microvascular blood

flux rate, possibly as a result of pressure correction at the precapillary level.[117] Taken together, these data suggest that as arterial stenosis worsens, a distal remodeling of non-capillary microvessels occurs to optimize collateral network conductance and connections. As these networks become enhanced, terminal microvascular beds begin to augment flow patterns, likely to reduce the total network resistance and improve blood distribution across microvascular beds.

One of the greatest limitations of animal models of PAD includes the temporal aspects of arterial occlusion. Arterial stenosis is induced surgically in animals, and as a result, induction of ischemia is immediate. In humans, the perfusion limiting stenosis is gained gradually over the course of several years. Thus, human alterations in collateral vessel formation and microvascular pathology may not mirror the adaptations observed in animals. Furthermore, several important risk factors such as chronic smoking, alcohol consumption, and poor dietary intake cannot be readily duplicated in animals, and these factors may be strong contributors to the formation of microvascular pathology in PAD. For example, insulin resistance and smoking are associated with detrimental alterations in microvascular blood flow through skeletal muscle.

Microvascular physiology during exercise in humans is complex. Blood velocity decreases as it travels distally, and the slowest flow is observed within the terminal microvascular beds, which have the greatest surface area. However, blood volume is largest within the veins.[109] At rest, approximately 25 – 40% of capillaries are actively perfused within skeletal muscle. Increases in blood flow result in increased blood flux through capillaries, typically with a concomitant increase in number of perfused capillaries. Thus, a high capacity for microvascular blood flow is present in healthy skeletal muscle, which when coupled with a low basal flow rate potentiates a high flow reserve.[118-120] Muscle metabolism influences blood flow regulation, likely at the level of the capillaries and arterioles.[107,121,122] As muscle begins to contract and muscle metabolism increases,

blood flow rapidly increases and stabilizes.[123] Using CEU and venous occlusion plethysmography (VOP), Krix and colleagues quantified several components of hemodyanamic responses to exercise. They observed that with higher levels of exercise, global flow, as assessed by VOP, increased as CEU blood volume decreased. The decrease in blood volume correlated to spent muscle work. They postulated that the decrease in blood flow was a result of diameter reduction of the veins *via* increased intramuscular pressure during muscle contraction. As participants discontinued exercise, blood volume increased rapidly in proportion to the performed muscle force.[107] The role of venous blood flow during muscle training may be of particular interest in PAD patients. A combination of muscle blood flow restriction and slow walking training (Kaatsu walking) have been shown to induce muscle hypertrophy and strength gain without measurable muscle damage.[124] Thus, Kaatsu walking may be of utility in improving walking function for patients with severe walking limitations.

Healthy aging is associated with several functional alterations that may alter skeletal muscle hyperemic responses. Endothelium-dependent dilation may be limited in response to increased shear stress within medium and small vessels, and changes of nitric oxide-mediated signaling may occur within elderly patients.[125-129] Additionally, elevations in resting sympathetic outflow and sensitivity to acute sympathetic stimulation may contribute to increased vasoconstriction, especially during exercise.[130,131] These functional modifications may account for the longer TTP and dampened reperfusion responses observed in elderly patients.[132]

A handful of studies have been conducted using CEU that compared control and PAD patients microperfusion. When compared to controls, PAD patients have similar resting microvascular blood flow.[133] Conflicting results have been obtained for several CEU parameters, including TTP and AUC. The majority of studies have observed a delayed TTP in PAD patients relative to controls after exercise and post-occlusive reactive

hyperemia,[99,102,108,109,133-136] however, other studies did not observe a significant difference.[137,138] Duerschmied and colleagues analyzed both angiographic and CEU images and determined that PAD patients that were classified as “poorly” collateralized had prolonged TTP, which did not correspond with a decreased ABI. Additionally, patients in more advanced stages of PAD had a prolonged TTP.[109] Post-occlusive reactive hyperemia TTP was inversely correlated with ABI, whereas post-exercise TTP was not significantly correlated to ABI.[108,135] The slope to maximum intensity after post-occlusive reactive hyperemia was decreased in PAD patients relative to controls as was the AUC.[102,108] Surprisingly, maximum intensity and AUC were larger in PAD patients relative to elderly control patients, which may reflect an expanded network of arterioles and capillaries secondary to hypoxia-induced angiogenesis.[132] Revascularization surgery shortened TTP in PAD patients immediately after surgery, and TTP was further shortened 3 – 5 months post operatively.[102,139] Additionally, the slope to maximum intensity after post-occlusive reactive hyperemia was increased after revascularization, as was the maximum intensity.[102]

Smoking may have an impact on microvascular perfusion and is likely a confounder in studies of PAD microcirculation. Mancini and colleagues demonstrated that in a cohort of patients with diabetes, TTP was delayed in current versus never smokers. Furthermore, the transit time of contrast agent to reach the tissue was delayed, as was the duration of time required for microbubbles to traverse through the gastrocnemius in smokers versus non-smokers. Each patient enrolled in this study was assessed for the presence of PAD, and approximately half of both smokers and non-smokers had a history of IC. In a sub-analysis, they observed that there was no difference in TTP between non-PAD and PAD patients in all Fontaine stages.[137] This data suggests that when stratified by smoking status, the relationship between TTP prolongation and PAD is lost. However, the cohort of patients assessed in this study was small (11 PAD versus 15 non-PAD), and

the severity of PAD was poorly characterized. Additionally, all of the participants had diabetes and it remains unclear if the remaining comorbidities were equally distributed between groups. Smokers experience a complex alteration in regulation of microperfusion.[137] Studies have reported impaired endothelium-dependent dilation, inappropriate resting dilation, and reduction in VSMC relaxation of the microcirculation, as well as declines in arterial elasticity in the vasculature of smokers.[140-143] Additional studies are merited to determine the contribution of smoking status (never, former, current) on PAD microcirculatory performance in patients with and without diabetes.

Ultrasonography has the capability to discriminate and quantify blood flow through arteries, veins, and the microcirculation. By using color coded duplex mode, ROIs can be selected that represent arterial and venous vessels. Switching to B mode enables the quantification of the flow. Contrast transit velocity (CTV) can then be estimated based on the distance between the selected ROIs. Duerschmied and colleagues utilized this strategy and assessed the contrast transit time (CTT) to the artery, the microcirculation, and the vein within the gastrocnemius of control, PAD, and DM patients. The greatest differences between groups were observed when comparing the composite transit times between the artery and the vein, and the CTVs. Blood traversed the muscle more rapidly in the controls (CTT artery to vein = 11 s; CTV = 2.0 – 3.3 mm/s) compared to PAD (CTT artery to vein = 22 s; CTV = 0.7 – 1.9 mm/s), and was substantially slower in late diabetic syndrome (CTT artery to vein = 43 s; CTV = 0.3 – 0.9 mm/s).[136] The delays in CTT arose predominantly from slower progression through the microvascular compartment. These data support that CEU can discriminate microcirculation from small arteries and veins. Additionally, the results of this study suggest that significant alterations of microperfusion are present in PAD, and are exaggerated in DM. However, the microvasculature was not characterized at the tissue level, so it remains unclear if these findings reflect functional changes, structural alterations of microvessels, or the number of microvessels.

A handful of studies have assessed the replenishment kinetics within PAD legs. Surprisingly, resting microvascular blood flow (MBF) did not differ between controls and PAD patients in multiple studies.[133,144] It has been postulated that healthy individuals have greater metabolic efficiency and thus a lower resting tissue demand. Conversely, PAD patients have lower arterial flow which limits perfusion and subsequently induces muscle atrophy and loss, effectively normalizing muscle mass to perfusion.[133] Post-occlusive reactive hyperemia is also altered in PAD microcirculation. Whereas control and PAD patients do not differ in the peak microvascular blood volume obtained on cuff release, PAD patients achieve this peak much more slowly. This may be due in part to the diminished increase in microvascular blood velocity that was observed during reactive hyperemia. Post-occlusion whole leg blood flow was associated with reperfusion MBF, and both whole leg blood flow and MBF were decreased in PAD patients relative to controls.[138] Vasodilator stress can be induced by administering dipyridamole. In PAD patients, dipyridamole was observed to increase the blood transit rate in large vessels and modestly increase the microvascular flux rate without significant augmentation of microvascular flow at rest. The response to dipyridamole did not differ significantly between control and PAD subjects.[144]

In comparison, the hyperemic response after contractile exercise is more robust in control versus PAD patients.[103,144] During moderate contractile exercise, microvascular blood volume was slightly lower than controls, whereas microvascular blood velocity was substantially diminished in PAD patients. [144] Similarly, in coronary artery disease, MBF augmentation in response to stress or metabolic demand is also limited.[114] In PAD patients, the diminished increase in MBF in response to exercise resulted in decreased flow reserve in PAD patients.[103] After adjusting for diabetes, exercise MBF (OR: 0.67) and flow reserve (OR: 0.46) could predict severity of disease defined by the claudication threshold.[103] In a subset of patients who were evaluated both before and after

revascularization surgery, exercise MBF increased substantially post-operatively.[144] Furthermore, the hyperemic response during exercise, but not during dipyridamole, is associated with the degree of flow impairment in PAD and potentially the degree of improvement with revascularization.[144] However, substantial variation in flow reserve has been observed from fairly homogeneous cohorts of both control and PAD patients.[114] Since resting MBF is typically very low, small absolute differences in hyperemic flow can create deceptively large flow reserves. Thus, the degree of hyperemic MBF may be a more reliable parameter by which to determine the presence or severity of PAD.[114] Additionally, the spatial heterogeneity of MBF distribution likely represents microdomains of severe ischemia in PAD patients,[114] however, this has yet to be confirmed by histological analysis. In a study of the relationship between total leg and microvascular flow in response to exercise, Meneses and colleagues demonstrated that during submaximal leg exercise, both total leg flow and MBF did not differ between PAD and control patients. However, after the conclusion of exercise, PAD patients had a higher microvascular blood volume than control.[138]

Alteration of microperfusion likely reflects both disease severity and compensatory mechanisms. It has been speculated that enhancing blood volume is compensatory for declining microvascular blood velocity, potentially by reducing microvascular resistance and increasing oxygen and nutrient delivery to a greater area.[138] It is also possible that increased blood volumes reflect an increase in angiogenesis and microvascular density. Conversely, elevations in microvascular blood volume may reflect weakened muscle contraction and reduced venous clearance (muscle pump effect). Although these studies illuminate that microvascular flow limitations exist in PAD patients, additional studies are necessary to determine the mechanisms by which MBF is altered during exercise, as well as the contribution of large vessel stenosis to microperfusion deficits. In particular, histological analysis of microvascular architecture and density in parallel with

microperfusion assessment may clarify the etiology of microcirculatory deficits, as well as the significance of microvascular pathology in PAD.

In addition to visualizing perfusion in PAD limbs, CEU may have future applications as a therapy for PAD. Studies have shown that under the right ultrasound settings, microbubbles may stimulate improvements in MBF. Microbubbles are capable of convective motion, or microstreaming, which can encourage shear-mediated endothelial production of nitric oxide. In a model of PAD, delivery of microbubbles at high acoustic powers have been shown to reverse moderate tissue ischemia.[145] Although still in the early experimental stages, CEU may be a powerful clinical tool in the diagnosis and treatment of PAD.

Endothelial Dysfunction Contributes to PAD Pathophysiology

Atherosclerotic blockage of arteries leading to the lower limbs leads to hemodynamic changes and consequently macrovascular and microvascular adaptations. It is believed that as the arterial occlusion worsens, inflammation and ischemia/reperfusion become more frequent, which initiates vascular remodeling including arteriogenesis and angiogenesis. Arterial occlusion leads to inefficient delivery of oxygen and toxic metabolite clearance, which results in the accumulation of ROS, tissue necrosis, and microcirculatory damage, ultimately resulting in irreversible deterioration and injury to the endothelium.[146-148]

Endothelial dysfunction is a feature of many chronic diseases, including hypertension, DM, renal disease, and obesity.[149-151] The pathophysiology of endothelial dysfunction likely arises from the imbalance of ROS signaling to nitric oxide (NO), as well as overexpression of pro-inflammatory mediators. Inflammatory signals, such as tumor

necrosis factor-α (TNF-α), are produced by atherosclerotic plaques and may travel distally to microvascular beds. TNF-α has been shown to stimulate endothelial expression of selectin and adhesion molecules which enable the interaction of endothelial cells with leukocytes and platelets, thus creating a localized pro-inflammatory and pro-thrombotic microenvironment.[152] Activated endothelial cells express cell surface adhesion molecules such as intracellular adhesion molecule-1 (ICAM-1) and vascular cell adhesion molecule-1 (VCAM-1), which are both elevated in PAD patients and are associated with poorer lower extremity performance.[153-155]

Several studies have shown that the production of NO, an important component in the regulation of vascular resistance and blood flow distribution,[156] is decreased in PAD patients.[157,158] In the microcirculation, endothelial dysfunction may also be related to the ratio of endothelin-1 to NO.[159] Sedentary lifestyle and obesity may exacerbate the deficits in NO production. Excess body fat is linked to elevated production of inflammatory cytokines and adipokines that reduce NO and other vascular signaling substances.[159] Declines in blood flow yield lower flow-mediated shear stress, and consequently shear-mediated production of NO. During periods of reperfusion, surplus oxygen may overwhelm the endothelial antioxidant capacity, leading to oxidative stress and peroxynitrite formation. Consequently, endothelial nitric oxide synthase (eNOS) is inhibited and the production of NO is decreased, which further limits endothelial function.[160] The capacity for vasodilation declines as NO production decreases, which may lead to increased vasoconstriction and limited delivery of blood to terminal microvascular beds.

In a recent study by Baum and colleagues, patients with IC had more capillary walls composed of swollen endothelial cells compared to controls.[82] Endothelial swelling has been shown to be aggravated by clamp-induced ischemia before femorodistal bypass

surgery in the muscles of patients with CLI,[161] which suggests that endothelial cell swelling also occurs in acute muscle ischemia in conjunction with reperfusion.[162-164] Ischemic muscles have a low pH and addition of muscle activity may create a local acidosis. In the setting of shock, acidosis is associated with both endothelial swelling, possibly mediated by the influx of sodium into the endothelial cell, and with the addition of hypovolemia, narrowing of the capillary lumen is also observed.[165,166] In rodent models of hindlimb ischemia, two weeks of intermittent hindlimb muscle stimulation demonstrated a significant increase in the percentage of swollen capillary endothelial cells, both locally, and systemically.[167] Swollen endothelial cells are also observed in the skeletal muscle of humans after application of a tourniquet for 1 – 3 hours.[164] It has been proposed that endothelial swelling is in part mediated by Ca^{2+} influx, likely arising from the accumulation of adenosine in ischemic muscles.[162] ROS may also be involved in endothelial swelling.[162] In ischemic muscles, the breakdown of high-energy phosphates during muscle contraction results in the production of hypoxanthine. Xanthine oxidase converts hypoxanthine to xanthine and oxygen free radicals when oxygen becomes available during reperfusion. In studies of prolonged muscle stimulation, endothelial swelling has been shown to decrease the volume of the capillary lumen, which is thought to increase the duration of red blood cell transit through the capillaries, thereby improving oxygen extraction.[168] Thus endothelial swelling in PAD may initially be a physiologic response to ischemia, but in the setting of chronic intermittent ischemia may reflect endothelial damage and dysfunction.

Damage to endothelial cells may have a significant impact in PAD muscle. Endothelial cell death may have a detrimental effect on angiogenesis. Constant loss of endothelial cells or ineffective communication with pericytes may challenge the ability of pericytes to stabilize vulnerable endothelial sprouts.[169] Furthermore, lack of pericyte coverage likely leads to leaky microvessels that may further enhance inflammation. Endothelial dysfunction and death may thus lead to both mature and immature vessel

instability, microvascular regression, and deleterious alterations in microvascular flow, which may further contribute to PAD tissue ischemia. Importantly, chronic loss and repair of endothelial cells may contribute to the pathological remodeling of microvascular BM[55,170] observed in PAD muscles.[82,171-174]

Microvascular Remodeling in PAD Myopathy

Structural changes occur within the microvascular basement membrane (BM) of skeletal muscle with age, physical activity, and diseases such as hypertension, DM, and congestive heart failure.[172,175,176] In a recent study, Bigler and colleagues demonstrated that the BM thickness increases with age and may differ by gender. No relationship was observed between thickening BM and pericyte coverage.[175] However, with age the connectivity between endothelial cells and pericytes becomes altered. A higher proportion of empty sockets is present in both endothelial cells and pericytes, and the filopodia that bridge these cells are shorter. This suggests that there is a regression of pegs from sockets. These alterations may lead to decreased mechanical coupling between the endothelium and pericytes, as well as a decline in the stability of the microvessel and impairment of pericyte-mediated vasoconstriction. As a result, a compensatory thickening of the BM may occur in the elderly.[175] BM thickness increases, likely in relationship to the orthostatic blood pressure, in a distal-proximal gradient.[55,175] In other words, BM thickening of microvessels is greatest at the feet and becomes progressively thinner as microvessels ascend towards the head. There is considerable variability in the BM of microvessels, even within the same muscle, and often between adjacent capillaries.[175]

Physical activity can reduce the thickness of the BM, including the microvessels of the elderly.[172,175] Baum and colleagues demonstrated that strenuous endurance exercise

can both thin the microvascular BM and stimulate angiogenesis with subsequent increases in capillary density. With strenuous endurance exercise, increases in the thickness of endothelial cells and pericytes were observed and pericyte coverage was increased. Interestingly, these microvascular changes occurred without a change in myofiber size. In a separate cohort undergoing moderate endurance training, endothelial cell thickness was enhanced, but the BM thickness, pericyte thickness, pericyte coverage, and capillary density did not change.[177]

Alterations of microvascular ultrastructure have been observed in PAD skeletal muscle. Although some level of debate remains whether microvascular BM thickening is progressive in PAD, studies have demonstrated that the microvascular BM is thickened in patients with IC and CLI.[82,85,171,173,178] Comparisons of the gastrocnemius and rectus femoris between patients with Fontaine Stage II & III PAD and young controls (mean of 37 years) revealed no significant difference between total capillary area (combination of BM, pericytes, endothelial cells, and lumen areas). However, the BM was thicker and the lumen was smaller in PAD patients, and appeared to worsen with PAD symptom severity.[85] Relative to an age-matched cohort of controls, PAD patients had significantly increased BM thickness.[82,171,173,178] In a comparison of the tibialis anterior muscles of age-matched controls (n = 4), PAD patients with IC (n = 4), and PAD patients with CLI (n = 10), significant differences were observed between PAD (IC combined with CLI) compared to control, but a marginally significant difference was observed between PAD patients with IC versus CLI, suggesting that this analysis was statistically underpowered. Comparison across groups suggested that a relationship existed between BM thickness, DM, and age.[171] PAD patients with CLI have been shown to have up to a 50-fold thicker microvascular BM than controls.[173]

In a recent study, Baum and colleagues executed a detailed analysis of the ultrastructure of skeletal muscle in patients with IC (n = 14) and controls (n = 10). They

observed a 24% increase in the volume density of BM in PAD capillaries, as well as a 23% increase in arithmetic thickness, which corresponded to a 24% decrease in the mitochondria of adjacent myofibers. Peak power output diminished by 45% in PAD patients. There was no alteration in pericyte coverage. Linear associations were observed between several parameters when compared across control and PAD, however all of these associations were lost when analyzed in the PAD cohort alone.[82]

The number of capillaries present in PAD muscle may be associated with microvascular architecture. The capillary to fiber ratio is elevated in the gastrocnemius, but not the rectus femoris, of PAD patients and increased with symptom severity in PAD patients with IC.[174] Likewise, in the vastus lateralis, capillary density is decreased and capillary to fiber ratios are unchanged in patients with IC relative to controls.[82] Ho and colleagues demonstrated that the capillary density was enhanced in the gastrocnemius of CLI patients relative to controls, although a non-significant increase in αSMA+ capillaries was observed.[173] Conversely, Baum and colleagues demonstrated that the proportion of αSMA+ capillaries was increased in PAD relative to control patients. When encountered, the αSMA immunoreactivity formed dense rings around microvessels and coincided with gaps within Collagen IV, suggesting an “arteriolization” of the capillary beds of PAD patients.[171] The measurement of the number and proportion of αSMA+ capillaries deserves further characterization, as it remains unclear if the number of αSMA+ cells around individual capillaries is increased, as well as the cell type expressing the αSMA (*i.e.* pericytes, myofibroblasts, fibroblasts, VSMC, endothelial cells).

Several abnormalities have been observed in PAD microvascular endothelial cells, including increased presence of large vacuoles, increased number of protrusions into the lumen, and numerous pinocytotic vesicles, and nuclear abnormalities such as substantial reduction in chromatin content.[173,174] Necrosis of endothelial cells as well as endothelial

swelling are observed in PAD microvessels.[82,171,174] Slit like capillaries are also more frequently encountered in PAD muscle.[82] This suggests that endothelial necrosis is occurring within PAD capillaries or conversely that these capillaries are not perfused. Interestingly, the endothelial cells from CLI patients no longer demonstrated features suggestive of angiogenesis.[173] In support of this finding, PAD endothelium did not express vascular endothelial growth factor (VEGF), but rather expressed fibroblast growth factor 2 (FGF-2).[171]

Increases in BM thickness of microvessels in PAD may be significant to the pathogenesis of PAD. In addition to limiting diffusion (Fick's principle), altering microvascular blood flow, and hindering angiogenesis, the presence of additional ECM around microvessels may modulate local regenerative and pathological responses. Alteration of perivascular extracellular matrix (ECM) may have a direct deleterious effect on endothelial function. In DM, non-enzymatic glycosylation (glycation) of the ECM alters endothelial cell function and is implicated with atherosclerotic plaque development. Endothelial cell cultures grown on native collagen versus glycated collagen responded differently to shear stress. Furthermore, endothelial cells grown on glycated collagen released half as much NO than those grown on native collagen, and this decrease correlated with decreased eNOS phosphorylation. Alteration of the endothelial integrin interactions with the collagen matrix likely mediated the diminished response to shear stress mechanotransduction, possibly through attenuated focal adhesion kinase (FAK) activation.[179]

Pericyte Mediated Modulation of Microenvironments, from Pro-Regenerative to Pro-Fibrotic

The Role of Pericytes in Angiogenesis and Microvascular Vasomotion

Pericytes are closely associated with endothelial cells and are contained within a common BM which is continuous around the microvessel.[180] Pericytes are considered to be ubiquitous in higher order vessels, including pre-capillary arterioles, post-capillary venules, and veins, and absent in lymphatic vasculature[181-183] and the reported range of pericyte to endothelial cell ratios within skeletal muscle is broad (1:10 - 1: 100).[180,184 185,186] Morphologically pericytes appear to be fibroblast-like with a prominent nucleus, meager cytoplasm, and multiple projections.[187] Pericytes can be identified by their location and the positive expression of several markers including α-smooth muscle actin (αSMA), platelet derived growth factor receptor-β (PDGFR-β), neuro/glial antigen-2 (NG2), regulator of G-protein signaling-5 (RGS-5), CD146, as well as the mesenchymal stem cell markers CD44, CD73, CD90, and CD105.[181] However, pericyte identification using these markers alone is challenging as marker expression can vary greatly between pericytes, even within the same tissue bed. No single marker has been discovered that can definitively and specifically identify pericytes. Of note, pericytes express neither the endothelial and hematopoietic markers CD31, CD34, and von Willebrand factor nor the neural cell and myogenic marker CD56.[181]

Pericytes have a crucial role in vascular homeostasis and angiogenesis. During angiogenesis, pericytes stabilize the sprouting endothelial tubes and are responsible for microvessel maturation.[54,187,188] Endothelial cells are stimulated to sprout by pro-angiogenic factors such as VEGF. Subsequently, they secrete proteases to degrade the ECM, proliferate, and migrate to form new, but unstable, vessels. To encourage migration of pericytes to the vascular sprout, endothelial cells secrete platelet derived growth factor-β (PDGF-β) (a structural homolog of VEGF), S1P-1, and angiopoietins.[49,187,189,190]

Endothelial cells and pericytes have substantial crosstalk during angiogenesis. TGF-β and activin-like kinase receptor-5 (ALK5) stimulate proliferation and differentiation of both endothelial cells and pericytes,[187] which not only contributes to vessel sprouting and stabilization, but are also critical in vessel maturation. Pericyte density and coverage are in part organ specific, but also directly correlate with endothelial barrier properties and orthostatic (gravitational) blood pressure and inversely correlate with endothelial cell turnover.[55,181,191-193] Taken together, these observations point to the central role of pericytes in the regulation of endothelial proliferation, microvascular barriers, and microvessel diameter.[191] Pericytes are also thought to have a role in immunological defense, coagulation, repair processes, and VSMC contractility and tone.[187]

Pericytes maintain close communication with endothelial cells and signal directly through peg-and-socket contacts as well as indirectly through paracrine signaling.[194,195] The peg-and-socket contacts consist of several components including tight junctions, adherence junctions (both β-catenin and N-cadherin), and gap junctions.[194] Adhesion plaques support the transmission of contractile and shear stress forces and stabilize gap junctions.[192,196-198] Additionally, gap junctions may be further stabilized by fibronectin in the ECM.[198] Connexin 43, a gap junction protein, is rich in contact sites between pericytes and endothelial cells as well as between pericytes. [192,197,199] Dye transfer studies have shown that dye is rapidly transferred to endothelial cells and adjacent pericytes,[200] likely *via* gap junctions. The direct gap junction exchange of small molecules and ions between cells may reinforce cell-cell signals. The parallel arrangement of pericytes to the endothelial axis thus appears to be related to the facilitation and integration of endothelial-pericyte communication.[69] Integrin signaling also communicates the mechanical forces present between the ECM, endothelial cells, and pericytes. Multiple types of signaling interactions, including gap junctions and integrins communication, suggests that these

cells compose a functional intercommunicating unit in the vasculature that is capable of integrating and coordinating neighboring endothelial cell responses as well as regulating the distribution of the mechanical contractile forces generated by VSMC.[181,188,194,198,201] The arrangement of VSMC around vessels differs from pericytes. The perpendicular arrangement of VSMC to the endothelial axis facilitates contraction and the mediation of vascular tone.[69] Interestingly, functional coupling is absent between pericytes and VSMC,[181] which suggests that pericyte-mediated regulation of the vasculature is either indirect or independent of VSMC.[181]

VSMC are important in vasoconstriction and vasodilation in larger vessels, however, pericytes may be influential in regulation of microvascular vasomotion. Pericytes have several actin-like sub-structural proteins located near the endothelial side of the cell. These proteins include αSMA, desmin, and vimentin, and may contribute to vessel constriction, thus potentially regulating microvessel diameter.[196,202] The pre-capillary arteriolar pericytes express a high concentration of contractile proteins, suggesting that they may act as pre-capillary sphincters.[203] Recent studies utilizing *in vitro* microfluidics and *in vivo* intravital microscopy demonstrated the presence of pericyte-dependent capillary constriction.[204-206] Notably, capillary-mediated functional hyperemia was absent, which supports arterioles as the mediators of functional hyperemia.[204] αSMA is expressed in both VSMC and pericytes and is associated with vasomotion and blood pressure control.[207] It has been proposed that the pericyte response to vasomotion may contribute to increased vessel wall stiffness, possibly as a compensatory mechanism to counteract elevated blood pressure. This process may be partially mediated by calpain-induced remodeling of cytoskeletal proteins which in turn increases the stiffness of pericyte subcellular contractile structures.[196,208]

In the setting of traumatic brain injury, increased αSMA expression was induced by endothelin-1 (ET-1) through endothelin receptor A (ET_A) and B (ET_B), and inhibition of

ET_A signaling resulted in decreased pericyte αSMA expression. αSMA expression was positively associated with constriction of both arterioles and capillaries,[209] which supports that $αSMA^+$ pericytes are contractile. Brain pericytes can adjust capillary diameter and blood flow in response to chemical and electrical stimuli.[192] Studies have shown that hyperoxic conditions trigger pericyte contraction whereas increased levels of carbon dioxide induce pericyte relaxation.[210,211] Activation of pericyte cell-surface receptors by vasoactive agents such as ET-1, angiotensin-2 (ANG2), serotonin, and histamine induce vasoconstriction whereas NO and cholinergic agonists induce vasodilation.[196,212] Pericytes, including those that express αSMA, can also secrete vasoactive agents and express α2- and β2-adrenergic receptors, [187,212] which also supports the role of pericytes in microvascular blood flow regulation. Importantly, pericyte-mediated vasoconstriction has been implicated in the "no reflow" phenomenon that occurs as a complication of reperfusion after acute organ/limb (*e.g.* brain, heart, leg) ischemia. Strikingly, pericyte vasoconstriction persisted even after restoration of flow through the occluded vessels.[213,214] Oxidative and nitrative stress may also induce pericyte-mediated vasoconstriction and contributes to ischemia/reperfusion injury.[202,215,216] Understanding the contribution of pericytes to vasomotion, particularly in the setting of chronic intermittent hypoxia, may yield novel insights into the pathogenesis of PAD myopathy.

Skeletal muscle pericytes have been shown to have therapeutic potential in post-ischemic neovascularization in mouse limb ischemia models.[41,217-221] Ten days post induction of limb ischemia, $nestin^+/NG2^+$ pericytes improved recovery by incorporating into the murine neovasculature.[217] Skeletal muscle pericyte therapy also improved blood flow recovery via collateral artery enlargement, but did not improve angiogenesis in wild type mice. Formation of collateral circulation in PAD contributes to better limb perfusion and may have subsequent positive effects on terminal microvascular beds. However, Type 2

diabetic mice displayed neither improvements in blood flow nor collateral artery enlargement, likely as a result of limited pericyte incorporation into the newly formed collateral arteries.[41] Localization of pericytes to forming collateral arteries may be mediated by Notch signaling. Notch signaling has been shown to autonomously and independently specify arterial characteristics in both endothelial cells and pericytes.[69] Furthermore, Notch signaling can stimulate pericytes to differentiate to VSMC,[222] and may contribute to the expansion of VSMC in PAD skeletal muscle. It is also possible that the "arteriolization" observed in PAD microvessels[171] reflects arteriolar enlargement as a means to expand collateral networks. However, microvascular alterations in PAD remain poorly characterized, as do the mechanisms by which they arise.

The Myogenic Potential of Pericytes After Muscle Injury

The role of pericytes in skeletal muscle is not limited to vascular development and homeostasis. There is increasing evidence that pericytes may be a possible reservoir of stem or progenitor cells in adult skeletal muscle.[191] Purified and cultured pericytes from multiple adult tissues retained perivascular markers (NG2, CD146, and PDGFR-β) but also expressed several mesenchymal stem cell (MSC) markers.[223-225] These pericytes did not express hematopoietic, endothelial, or myogenic cell markers. Crisan and colleagues demonstrated that pericytes isolated from adult skeletal muscle were myogenic *in vitro* and *in vivo* and retained myogenicity when long-term cultured. Skeletal muscle pericytes at the clonal level had chondrogenic, osteogenic, and adipogenic potential. MSC markers were expressed in both cultured and native cells, which suggests that pericytes have multi-lineage long term differentiation capacity.[223] Moreover, it has been suggested that pericytes from skeletal muscle present a broader range of differentiation abilities than

MSCs.[198] During acute muscle injury, pericytes contribute to a regenerative microenvironment by coordinating neovascularization, modulating local immune responses, releasing trophic factors, and differentiating into myofibers.[181,226] Additionally, pericytes may sense hypoxia and hypoglycemia, and thereby mediate adaptive tissue protective responses.[69] Several potent cytokines, growth factors, and chemokines are implicated in pericyte injury response including VEGF, TGF-β1, PDGF-β, angiopoietin 1 and 2, basic FGF, epidermal growth factor, thrombopoietin, stem cell factor, and stromal cell-derived factor-1α.[181,227-229]

The myogenic potential of pericytes obtained from human skeletal muscle is strikingly high. It has been shown that 20 – 40% of cultured patient-derived pericytes exposed to muscle-differentiation medium spontaneously differentiate and form myosin$^+$ multinucleated myotubes.[230] These myogenic precursor pericytes are distinct from satellite cells, both by location and marker expression. Unlike pericytes that are located within the BM of microvessels, satellite cells reside within the BM of myocytes. Satellite cells express MyoD, Pax7, Myf5, MEF2C, CD56, and M-cadherin whereas pericytes do not. Myogenic precursor pericytes uniquely express NG2 and alkaline phosphatase (ALP). NG2$^+$ pericytes are progressively associated with post-natal muscle stem cells. Only on terminal differentiation do pericytes express MyoD and Myf5, which suggests that the kinetics of myogenic differentiation are different between satellite cells and pericytes.[230] Furthermore, pericytes likely coordinate the myogenic response by promoting myogenic cell differentiation through insulin-like growth factor 1 and satellite cell quiescence through angiopoietin 1. In support of this, it has been observed that pericyte ablation in growing mice yields myofiber hypotrophy and impairs the transition of satellite cells into quiescence.[231] In human skeletal muscle, the number of pericytes declines in response to resistance exercise in association with increases in

$CD90^+$/PDGFR-α^+ MSC pools and $Pax7^+$ satellite pools.[232] Taken together, these studies suggest that pericytes may regulate the expansion of the muscle progenitor pool during exercise and possibly after acute injury by increasing pericyte myogenic differentiation and regulating satellite cell quiescence. Interestingly, the regenerative capacity of pericytes differs in aging microenvironments. Pericytes have a lower regenerative capacity when transplanted into older mice. Bribrair and colleagues demonstrated that with age, Type 2 pro-myogenic pericytes (Nestin-GFP^+/NG2-$DsRed^+$) are more quiescent and Type 1 pro-fibrotic pericytes (Nestin-GFP^-/NG2-$DsRed^+$) are more active.[233] Additionally, a subset of skeletal muscle pericytes have several similarities to Schwann cells and may be neural progenitor cells.[234] It is speculated that these pericytes may be involved in coordinating muscle reinnervation after injury.[181,234] The contribution of pericytes to muscle repair in PAD remains mostly unknown. However, given the propensity for pericytes to favor fibrosis at the expense of myogenesis with age, pericytes are a promising target for therapies that may be able to coax pericytes into a pro-regenerative role.

Pericytes and Inflammation

Pericytes are implicated in the inflammatory response that follows injury in several organs. In brain, pericytes are thought to have a bidirectional and modulatory effect of neuroinflammation and neurodegeneration.[235,236] Furthermore, pericytes are a key mediator of the inflammatory response during skeletal muscle regeneration.[186] A subset of pericytes (lacking expression of Collagen I and Foxd1) express several immune surveillance and effector genes, which suggests that they may act as sentinels of the innate immune response.[237-243] Pericytes may coordinate leukocyte and macrophage

trafficking to inflamed tissues by expressing ICAM-1 and secreting chemoattractants such as macrophage migration-inhibitory factor (MIF) and monocyte chemoattractant protein-1 (MCP-1).[244-246] Pericytes may also alter the responsiveness of these immune cells after migration into the interstitial tissue.[245] Muscle pericytes highly express several other immunoregulatory cytokines and chemokines including COX2, heme oxygenase 1, leukemia inhibitory factor, hypoxia inducible factor-1α (HIF-1α), and IL6.[246] Inflammatory signals, such as MCP-1, are linked to angiogenesis.[186,247] In a C2C12 coculture model of muscle injury, pericytes secreted MCP-1. Knockdown of the transcription factor CCAAT enhance binding protein-δ (C/EBPδ) in culture lead to enhanced pericyte-mediated inflammation by increasing MCP-1 production. C/EBPδ regulates activation of macrophages and expression of genes involved in both immune and inflammatory responses. Knockdown of C/EBPδ in pericytes also lead to increased ICAM1, IL8, and IL-1β expression and reduced superoxide dismutase-2 (SOD2) and COX2 production,[248] which suggests that pericyte C/EBPδ expression is involved with switching between pro- and anti-inflammatory programs.

Pericyte gene expression patterns also suggest that pericytes may also function similarly to macrophages.[243,249-251] Pericytes express several macrophage markers (CR3 compliment receptor, CD4, and class I & II major histocompatibility complex).[252] Pericytes also have phagocytic activity and can perform antibody-dependent phagocytosis *via* Fc receptors.[187,252,253] Pericyte pinocytosis has been shown to have an important role in cleaning cerebrospinal fluid[254] and exchange of metabolites in liver.[187] Thus, pericyte pinocytosis allows sampling of the local microenvironment for toxins and metabolites, which may induce pro-inflammatory responses in pericytes.

Activation of the nuclear factor-κB (NF-κB) transcription family plays a central role in inflammation by its ability to induce transcription of pro-inflammatory genes after

stimulation by signals related to pathogens or stress.[255,256] NF-κB activation regulates myogenesis during skeletal muscle injury and disease.[186,257,258] Within 3 hours of muscle damage induced by eccentric exercise in human quadriceps, NF-κB is activated.[186,259] Pericyte NF-κB enhances not only inflammation but also angiogenic crosstalk by increasing translation and secretion of GM-CSF, MCP-1, and IL-8, which has potential downstream effects on vascular growth, endothelial proliferation, and angiogenesis.[186,260]

Several pro-inflammatory cytokines stimulate pericytes. IL-1β activates pericytes and increases pericyte matrix production, whereas IL-1β decreases fibroblast matrix deposition.[261,262] Locally administered IL-1β or TNFα can induce a morphological change in pericytes that yields transient gaps between pericytes that allow the migration of neutrophils into the interstitium.[243] Interestingly, pericyte matrix deposition alters endothelial ICAM-1 expression and sensitizes endothelial cells to IL-1β activation which encourages neutrophil transmigration. Endothelial cells cultured on collagen I responded to IL-1β differently than endothelial cells cultured on fibronectin. Collagen I cultured endothelial cells had significantly less neutrophil transmigration than fibronectin cultured endothelial cells. This suggests that pro-inflammatory activation of pericytes induces deposition of compositionally distinct ECM that may promote local inflammation impacting surrounding cell functions.[261] Endothelial cells present integrins at their cell surface that interact with this remodeled ECM and induce a pro-angiogenic state. Consequently, endothelial cells display increases in migration, cell survival, and sensitivity to circulating cytokines.[261] Taken together, this data suggests that alterations of the ECM can be highly influential in promoting inflammation.[261,263] Although pericytes are stimulated by several pro-inflammatory cytokines, they have minimal expression of IL-1alpha, TNFα, and interferon-γ, even under hypoxic conditions.[246]

The pro-inflammatory cytokine IL-6 may also be of great importance in muscle damage and repair. IL-6 is produced during inflammation. Depending on the muscle mass and intensity and duration exercise, mechanical load increases IL-6 production which may impact metabolism. Addition of recombinant IL-6 enhances insulin-stimulated fatty acid oxidation and glucose disposal in myotubes in culture.[264] Interestingly, muscle derived IL-6 may dampen the effects of other inflammatory cytokines, such as TNFα, [264] suggesting that muscle derived IL-6 may induce muscle repair after exercise without inflammation, or may trigger inflammation past an unknown threshold. In samples acquired from lungs of patients with pulmonary arterial hypertension (PAH), IL-6 levels were markedly elevated.[54] Addition of IL-6 to cultured pulmonary pericytes induced pericyte migration whereas anti-IL-6 neutralizing antibodies substantially attenuated pericyte migration.[54] Delivery of exogenous IL-6 to rodents induces pulmonary vascular remodeling, which is exaggerated in response to hypoxia.[265,266] Exogenous delivery of IL-6 to murine retinas increased αSMA^+ pericyte coverage. Strikingly, in neonatal mice, pericyte coverage increased by approximately 35-40% in response to recombinant IL-6 and increased pericyte coverage was abolished with addition of anti-IL-6 neutralizing antibodies.[54]

It has been suggested that with chronic inflammation, pericytes escape the microvascular BM and differentiate into myofibroblasts that contribute to the deposition of collagen during wound healing and fibrosis.[69] Depending on the pro-inflammatory or pro-fibrotic signaling milieu, pericytes can modulate the ratio of fibronectin to collagen I within the microvascular ECM.[261] Pericytes and myofibroblasts have similar responses to pro-inflammatory signals, which supports the notion that pericytes may indirectly regulate inflammation, possibly through ECM deposition,[261] and are likely candidates to respond to chronic inflammatory signals and initiate microvascular remodeling in PAD myopathy.

Pericytes and Microvascular Remodeling

Microvascular remodeling, particularly BM thickening of the smallest microvessels, has been observed in the pathology of a diverse set of organs. Microvascular BM thickening is a common feature amongst immune-based diseases. In delayed type hypersensitivity reactions, several epithelial abnormalities are present in conjunction with thickened microvessels.[267-269] Infectious disease initiates an immune response, and in patients with Chagas disease, several skeletal muscle microvascular abnormalities were observed. The most prominent feature was microvascular BM thickening, however capillary reduplication and occlusion were also noted. During immune responses, pericytes and endothelial cells also demonstrate abnormalities at the ultrastructural level.[270] Alterations of microvascular structure, particularly BM thickening, have been observed in autoimmune diseases and inflammatory myopathies such as scleroderma, rheumatoid myositis, polymyositis, and dermatomyositis.[270-273] Interestingly, in patients with autoimmunity of the nervous system associated with muscloskeletal pathology (*i.e.*Guillain-Barre Syndrome, multiple sclerosis, amyotrophic lateral sclerosis, and carcinomatous neuromyopathy), skeletal muscle also had microvascular alterations and increases in BM thickness.[270,274] In patients with systemic lupus erythematosus (SLE) and mixed connective tissue disease (MCTD), microvascular BM thickness was associated with the level of plasma complement protein C3dg, suggesting that auto-antibodies or immune complex deposition damages endothelial cells or pericytes. Microvascular BM thickening had an inverse relationship with steroid treatment,[275] suggesting that reduction of immune responses may limit microvascular remodeling. Circulating cytokines are thought to also contribute to the BM thickening of SLE microvessels by activating endothelial cells, subsequently inducing expression of adhesion molecules such as E-selectin, ICAM-1 and VCAM-1.[275,276] In SLE and MCTD skeletal muscle, increased

pericyte coverage was associated to ANA titer[275], supporting that both endothelial cells and pericytes are activated in the auto-immune response.

Microvascular and airway remodeling of the lung are also thought to arise from a chronic inflammatory process.[249,277] In chronic asthma, myofibroblast accumulation and vascular remodeling are considered key mediators of asthma complications.[277] Chronic asthma is characterized by thickening of the VSMC layer of arterioles, endothelial cell proliferation, and perivascular fibrosis.[249] It is thought that pericytes may have an integral role in microvascular remodeling in asthma.[277] In PAH, excessive pericyte coverage is seen in the distal pulmonary microvasculature and is directly linked to endothelial dysfunction.[54] Like asthma, PAH arterioles experience VSMC hypertrophy and hyperplasia, with increased muscularization by αSMA^{+} cells in the distal microvasculartur e. Both *in situ* and *in vivo* studies revealed that increased pericyte coverage contributes to pulmonary vascular remodeling, and is likely the source of these contractile αSMA^{+} cells.[54]

A classic finding in diabetic microvascular pathology is altered microvascular architecture. Pericyte changes are associated with diabetes, particularly with regards to microvascular complications.[49] Diabetic neuropathy is characterized by thickened microvessels, pericyte degeneration, and reduced blood flow.[278] Pericyte degeneration is a hallmark finding of diabetic retinopathy, with loss of pericyte coverage leading to microvascular instability and microhemorrhages. The skeletal muscle microvasculature is also altered in patients with DM. Tilton and colleagues demonstrated that skeletal muscle microvascular BM thickness was greater in diabetics versus non-diabetics. Cellular debris were commonly encountered within the thickened BM, with approximately 35% more debris incorporation in diabetic versus healthy microvascular BM.[279] Degenerating pericytes were the likely culprit for the debris generated and collected within the BM. Orthostatic and venous pressure are thought to contribute to these microvascular

alterations, as BM thickness, pericyte degeneration, and acellular capillaries increased progressively from the head to the foot in diabetic patients, with the gastrocnemius paradoxically having greater microvascular alteration than the foot.[55,180] Pericytes in diabetes show ultrastructural alterations and gain a differentiation bias towards adipogenesis, likely at the expense of myogenesis and angiogenesis.[220] This is consistent with the observations that capillary density is decreased in the skeletal muscle of patients with DM. Thus, insulin resistance and vascular defects are likely linked within skeletal muscle, with insulin resistance encouraging a shift towards a vasoconstrictive state.[49] In support of this, studies utilizing CEU and 1-methylxanthine metabolism (capillaries contain xanthine oxidase which metabolizes 1-methylxanthine and provides an estimate of the extent of perfusion[280]) demonstrated that insulin can induce capillary recruitment *via* increasing muscle microvascular blood volume without alteration of the total blood flow.[281-283] Furthermore, it has been proposed that loss of VSMC and pericytes may increase vessel dilation, and thus muscle perfusion, with a beneficial increase of capillary surface area for nutrient delivery and exchange.[49]

PDGFR-β^+ pericytes may regulate microvascular remodeling and BM deposition. PDGFR-β^+ pericytes express several fibroblast-associated markers and contribute to scar formation during wound healing.[244] In addition to displaying several fibroblast surface proteins, PDGFR-β^+ pericytes also produce collagen I, collagen IV, and fibonectin.[284] Rgs5, a regulator of G-protein signaling, is normally expressed in relatively few pericytes, however, Rgs5 expression is up-regulated transiently as angiogenic sprouts become covered with pericytes, suggesting that Rgs5 is a key mediator of vessel stabilization and maturation.[285] In line with these findings, Rgs5 pericytes are associated with pathological vascular remodeling, including microvascular regression, rarefaction, and altered vasomotion.[284] Rgs5 can potentiate PDGFR signaling, and thus may enhance the activity

of PDGFR-β^+ pericytes.[285,286] Goritz and colleagues demonstrated that after spinal cord injury, a subset of PDGFR-β^+ pericytes increased three fold in number, migrated from the vessel wall, produced fibronectin, and expressed αSMA. Within the spinal lesion, pericytes also deposited abundant ECM within their basal lamina encasement and likely differentiated into myofibroblasts.[287] In the kidney, pericytes that underwent a pericyte to myofibroblast transition increased the expression of the disintegrin ADAMTS1 and decreased expression of the metalloproteinase TIMP3.[288] ADAMST1 is involved with BM degradation and may be a key mediator of pericyte detachment from the microvessel and migration into the interstitium. Inhibition of ADAMTS1 abolished pericyte detachment with a resultant decrease in fibrosis. In mice deficient in TIMP3, kidney pericytes were susceptible to injury-induced microvascular rarefaction and fibrosis.[288] In kidney fibrosis, Ren and colleagues demonstrated that pericyte activation, detachment, and transition to myofibroblasts were inhibited by Dickkopf-related protein 1 (DKK-1). This resulted in improvements of capillary rarefaction, inflammation, and attenuated fibrogenesis. DKK-1 also blocked pericyte proliferation in response to PDGFR-β, pericyte migration, gene activation, and TGF-β1-induced cytoskeletal rearrangement.[289] The predominant mechanism of action of DKK-1 was on the inhibition of PDGF- and TGF-β- signaling cascades, [289] which may be critical in stimulating pericyte BM deposition. Taken together, these studies support the notion that pericytes are mediators of the creation and degradation of BM.

BM thickness is altered as a response to mechanical stress and injury. In the skeletal muscle of patients with hypertension, BM becomes thickened and reduplicated as concentric layers of BM, the flow lumen becomes constricted, and total diameter remains unchanged.[290] Decreased flow lumen likely reflects microvessel occlusion, degeneration, and the increased incidence of endothelial in-folding into the lumen.[290] Tissue injury

induces wound healing programs within tissues, with chronic injury yielding fibrosis. In several organs, pericytes have been implicated as initiators of fibrosis, which suggests that fibrosis is a disease that is originated and coordinated by microvessels. It is possible that fibrosis is initially localized to microvessels and is manifested only as alterations of microvascular BM. Pericytes and endothelial cells are the sole occupants within the microvascular BM. Fibroblasts and other perivascular cells are not found within microvascular BM,[180] which strongly supports the role of pericytes in the initiation and propagation of BM thickening. With increasing changes of the microenvironment, pericytes undergo differentiation,[54] suggesting that architectural remodeling of the BM occurs primarily via pericyte BM deposition and secondarily by differentiation into pro-fibrotic progenitors which may expand ECM deposition around and beyond the microvasculature. Cross talk with endothelial cells is likely critical in microvascular remodeling, as studies have shown that the presence of both endothelial cells and pericytes is required for the formation of the BM. Endothelial cells have the machinery to synthesize many of the BM components, however, pericytes are required for BM assembly and regulation of synthesis.[191,196,291,292] In co-cultures of endothelial cells and pericytes, ECM binding integrins are upregulated, a finding that is absent when endothelial cells are cultured alone. Mechanical injury of these co-cultured cells induces to shifts of ECM component concentrations, including the ratio of collagen I and fibronectin, with deleterious effects on endothelial function.[261]

A wealth of structural components are located within the microvascular BM. Both pharmacological and genetic studies have shown that loss of nearly any ECM component can lead to a myopathy that often includes fibrosis and fatty degeneration.[264] Collagen IV, laminin, fibronectin, perlecans, and nidogens are the best characterized BM components in health and disease states. Collagen IV is involved in membrane stability and is crucial in providing the structural integrity of the vessel.[196,293] Laminin is an essential scaffold

protein and is important in the organization of the BM.[196] Working in parallel, collagen IV and laminin produce the three dimensional network of the BM. Perlecan and nidogen act as bridges between the collagen IV-laminin network, thus stabilizing the BM.[211] IL-1β activates pericyte deposition of collagen IV and fibronectin, whereas TGF-β1 upregulates the deposition of laminin.[261] Deposition of ECM components, including microvascular BM, provides structural scaffolding to regenerating muscle, which supports satellite cell migration and myogenesis.[294.] Thus, differential deposition of ECM components by pericytes may alter the microenvironment and deter myogenesis in favor of fibrosis.

In addition to providing structure to tissues, the BM is also capable of supplying signals to vessels and surrounding cells. BM is highly glycosylated, which yields a high binding capacity and affinity for secreted growth factors.[295] These factors are potent directors of cell proliferation and activation. Proteolytic cleavage can release growth factors such as FGF-2, TGF-β, VEGF, and PDGF.[54] TGF-β1 signaling can then induce additional deposition of ECM components, including Collagen I and IV, fibronectin, and laminin.[296] BM also provides a depot of chemotactic factors that likely contribute to immune surveillance.[295]

Considering the similarities present in microvascular remodeling across diverse tissues (*e.g.* heart, lung, brain, muscle, eye, kidney) and pathologies (*i.e.* injury, ischemia, auto-immunity), it appears that a common mechanism may be present that induces microvascular architectural remodeling. It is likely that injury to endothelial cells and activation of pericytes initiate the deleterious process of BM remodeling. With chronic inflammation and insult, death of pericytes and endothelial cells becomes common and induces repair paradigms, including angiogenesis, thus actively participating in a cycle of degeneration and regeneration.[55,69,290,297] When damage and inflammation become recurrent and frequent (like during the episodes of ischemia and reperfusion that occur

each time a PAD patient walks) they may lead to an advanced stage of vascular regeneration[170,271,298,299] that becomes "frustrated". As endothelial cells and pericytes perish, the BM remains intact as a scaffold and regenerating endothelial cells and pericytes may add new inner layers of BM,[170] which results in pathological modifications in the injured microvessels and subsequently promotion of a fibrotic response. Although the initiation and progression of microvascular changes in PAD remains largely unknown, such a mechanism may occur in the genesis of microvascular pathology in PAD myopathy.

Pericytes, Myofibroblasts, and Fibrosis

In acute muscle injury, pericytes coordinate a regenerative response by creating a favorable microenvironment for muscle repair. However, in the face of chronic injury (*i.e.* inflammation, hypoxia, mechanical trauma), normal pericyte processes become deregulated and pericytes coordinate the development of pathological fibrosis, heterotopic ossification, and calcification.[181,191] Fibrosis of skeletal muscle leads to significant functional impairment and predisposes the muscle to additional injury.[96,181,300] As patients become older, the capacity for muscle repair is lowered, and may be related to the transition of pericytes differentiation programs from pro-regenerative to pro-fibrotic.[233]

PDGFR-β^+ pericytes are implicated in fibrosis. PDGFR-β^+ pericytes have the ability to transition to αSMA^+, collagen producing myofibroblasts in injured skeletal muscle. Ablation of these cells abrogates collagen deposition and the generation of pro-fibrotic cells after muscle injury.[301] Additionally, PDGFR-β^+ pericytes express fibroblast-associated markers, including fibroblast surface proteins, fibronectin, and collagen IV.[244] Blockade of PDGF-β signaling attenuated kidney fibrosis and capillary rarefaction after unilateral ureteral obstruction.[302] In isolated lung cell cultures, PDGF-β treatment

enhanced proliferation and migration of fibroblasts, but not pericytes.[237] Additionally, in allergic airway disease, PDGF-β has been shown to work synergistically with TGF-β to stimulate VSMC cell migration.[277,303] Thus, PDGFR-β$^+$ pericytes may contribute to the regulation of fibroblast and VSMC migration and proliferation.

TGF-β1 is strongly implicated in fibrogenesis.[243] Early fibrosis is associated with a substantial increase in pro-fibrotic TGF-β1 and pro-inflammatory IL-1β.[261] TGF-β1 stimulates differentiation and proliferation of both endothelial cells and pericytes.[69] Integrins are likely regulators of TGF-β1 activation perhaps through directing conformational changes of latent TGF-β1 to the active form,[304] possibly *via* cell constriction-mediated tensile force,[305] or indirectly directing MMP activation of latent TGF-β1.[306] Production of TGF-β1 may require connexin 43 gap junction-mediated communication between endothelial cells and pericytes.[69,191,307] Not surprisingly, TGF-β1 receptors are located on both endothelial cells and pericytes. [243] Juxtaposition and collaboration of endothelial cells and pericytes are required to activate latent TGF-β1.[308] [309] Deficiencies in TGF-β signaling lead to loss of pericyte coverage.[243] Additionally, inhibition of TGF-β release by endothelial cells limits the differentiation of PDGFR-β$^+$ pericytes into αSMA$^+$ pericytes. Pericyte secretion of TGF-β1 suppresses endothelial cell growth and migration. These data suggest that normally TGF-β is involved in pericyte and vessel maturation, as well as endothelial barrier function.[196]

TGF-β can stimulate pericyte production of contractile, ECM, and BM proteins, [197,296] which may, alternatively, contribute to fibrosis. TGF-β pathway overactivation is observed in PAH and is associated with PAH progression. Strikingly, phosphorylated Smad2 immunofluorescence was prominent across pericytes of PAH lung specimens, with approximately 45% of pericytes demonstrating TGF-β1-mediated activation of Smad2 signaling compared to approximately 6% of pericytes in healthy lung tissue.[54] TGF-β1

may have a more powerful effect on a select subset of pericytes, particularly pericytes that may be involved in fibrotic responses and myofibroblast differentiation. In a recent study, Hung and colleagues demonstrated that Foxd1 progenitor-derived pulmonary pericytes are enriched in genes related to angiogenesis, immune regulation, and migration. Within this lineage, a subset of these pericytes expressed PDGFR-β and NG2, and had a transcriptionally distinct signature which resembled fibroblasts.[237] Interestingly, in co-cultures of Foxd1 progenitor-derived pericytes and fibroblasts, pericytes activated high levels of collagen I production. When co-cultures were stimulated with TGF-β, PDGF-β, and PDGF-α, fibroblasts increased migratory activity. Additionally, TGF-β activated pericyte αSMA protein expression and stress fiber formation.[237]

TGF-β1 has context-dependent effects. TGF-β1 stimulation of ALK on endothelial cells can induce signaling *via* ALK1/Smad1/5 which is promoted by endoglin and incites proliferation.[310] TGF-β1 may also activate ALK5/Smad2/3 pathways which leads to differentiation of both endothelial cells and pericytes.[311] ALK1 and ALK5 receptors are also located on pericytes. Disruption of endothelial TGF-β1 signaling impacts pericytes, possibly by impairing TGF-β/ALK5 signaling, and inhibits pericyte-mediated stabilization of endothelial sprouts and differentiation into VSMC.[311] In addition to mediating differentiation to VSMC, activation of pericyte ALK5/Smad2/3 pathways promotes mitotic and migratory quiescence.[312,313] Pericyte activation of ALK1/Smad1/5 also stimulates proliferation and migration while limiting differentiation to VSMC.[312,313] Taken together, these studies suggest that ALK1/Smad1/5 pathway activation promotes vascular sprouting, whereas ALK5/Smad2/3 pathways promote vessel maturation.[191] Undoubtedly, the net effect of TGF-β1 depends on relative levels of ALK1/5 signaling.[191] However, TGF-β1 signal strength and duration are likely critical in the progression towards fibrosis.

TGF-β1 strongly induces pericytes to express αSMA.[54] In one study of PAH, 68% of αSMA$^+$ cells were pericyte derived.[237] In lung cell culture, TGF-β1 stimulated pericytes to become contractile and express αSMA, calponin, and SM22.[54] Lung pericytes that have been stimulated with TGF-β1 also increase expression of NG2, snail, and collagens, and undergo myofibroblast transition.[284] It is important to note that these αSMA$^+$ pericytes show great heterogeneity and may be representative of select subsets of pericytes. Regardless, the phenotypic changes observed in these pericytes suggests that they are contributing to collagen production, myofibroblast pools, and potentially increased vasoconstriction across affected microvascular beds.

It is well established that a critical step in fibrogenesis is the activation of myofibroblasts. Myofibroblasts express αSMA, generate contractile force, remodel and deposit excessive ECM, and are directly linked to the extent of fibrosis.[191,243] The origin of myofibroblasts remains elusive, although there is increasing evidence to suggest that pericytes differentiate into myofibroblasts during fibrogenesis, and are a significant source of the myofibroblast pool. Bleomycin treatment induced lung Foxd1 progenitor-derived pericytes expansion, expression of αSMA and collagen I that was limited to fibrotic foci, suggesting that in response to injury these pericytes become a myofibroblast precursor population.[237] In line with this finding, pericytes expressed fibroblast specific protein-1 (FSP1) and the number of NG2$^+$/FSP1$^+$ pericytes significantly increased in remodeled pulmonary vessels.[314] Moreover, lineage tracing experiments have demonstrated that pericytes and resident fibroblasts are the predominant source of pulmonary myofibroblasts during development, normal state, and after injury.[69,237,315,316] In the setting of spinal cord injury, pericytes have been shown to proliferate, migrate, differentiate, and contribute to fibrotic repair.[235,287] Analysis of the lesion demonstrated that a subset of pericytes expressed fibronectin, PDGFR-β, and αSMA, and were attributed as the cells responsible

for deposition of ECM components into vessel BM and scar connective tissues,[287] likely *via* differentiation into myofibroblasts. These pericytes were particularly proliferative within the first few days after injury.[287] Pericytes have been implicated as a major source of collagen producing myofibroblasts in several other organs, including skeletal muscle, kidney, and liver, as well as in systemic sclerosis.[191,249,289,302,317-320]

The transition from pericyte to myofibroblast includes detachment from the endothelium and likely contributes to loss of vascular homeostasis.[191,243,284] Pericyte departure may result in leaky vessels, ineffective angiogenesis, and ultimately vessel destruction.[237] In a model of cardiac fibrosis induced by ANGII infusion, αSMA^+ pericytes that adopted myofibroblast fates expressed Gli1. Collagen rich areas of the myocardium displayed an abundance of Gli1-labeled cells following acute MI and analysis of the infarcted myocardium revealed that approximately 60% of myofibroblasts were derived from $Gli1^+$cells.[321] As stated previously, TGF-β1 signaling is likely critical in the differentiation of pericytes to myofibroblasts.[284] Gene analysis suggests that pericytes that become myofibroblasts have the greatest gene expression profile changes in immunity, inflammation, wound healing, and cytokine response.[289] Intriguingly, evidence is arising that as pericytes become myofibroblasts, they become insensitive to hypoxia.[289]

Pericytes in the Setting of Ischemia

Ischemia exacerbates the fibrotic response of several organs, such as skeletal muscle, lung, and kidney. Microvessel pathology may contribute to ischemia, particularly in the non-proliferative phases of microvascular remodeling. The hypoxia produced by loss of microvessels may then drive the excessive growth response in capillary density seen in late vascular remodeling.[196,197,289,322,323] Furthermore, during the proliferative stage

of vascular remodeling pericytes detach from the endothelium and differentiate into myofibroblasts, leaving the poorly supported endothelium vulnerable to regression.[196] Thus, pericytes contribute to fibrosis by several mechanisms: 1) mediation of inflammation; 2) ECM deposition, including BM thickening that limits diffusion; 3) differentiation into myofibroblasts; 3) contribution to microvessel regression and subsequent hypoxia.

Ischemia-reperfusion injury triggers oxidative stress in affected tissues, and likely contributes to pathological pericyte activity. Skeletal muscle pericytes demonstrated increased oxidant stress when harvested from diabetic PAD patients with CLI versus control.[41,220] Pericytes from diabetic PAD patients had weakened anti-oxidative protection and increased levels of ROS, and the resultant oxidative stress negatively affected pericyte and endothelial function.[41,220] The redox imbalance reflects decreased SOD1 and catalase production as well as activation of mitochondrial adaptor proteins and redox enzymes that are involved in promoting mitochondrial apoptosis.[220] In pericytes obtained from fibrotic kidneys, gene expression analysis shows that several processes that are involved in mitochondrial function are downregulated.[289] Likewise, PAH lung pericytes demonstrate significant enrichment of genes involved in metabolic processes.[324] Pyruvate dehydrogenase Kinase 4 (PDK4) is particularly upregulated.[324] The PDK4 gene gives rise to an enzyme involved with suppressing mitochondrial activity in favor of glycolysis. This decoupling of glycolysis and glucose oxidation leads to inefficient cellular metabolism. Hypoxia may increase expression of PDK4 as it is regulated by various transcription factors, including HIF-1α.[325] Yuan and colleagues demonstrated that in PAH, PDK4 expression was associated with higher rates of pericyte glycolysis, proliferation, and survival. Reduction of PDK4 levels restored mitochondrial metabolism, decreased pericyte proliferation, and improved pericyte-endothelial interactions. Thus, hypoxia likely

induces changes in pericyte gene expression that limit mitochondrial function and alter pericyte metabolism with negative consequences on pericyte and endothelial functions.

Undoubtedly, hypoxia is a key mediator in vascular remodeling. In PAH, the HIF-α hydroxylase system is associated with pathological alterations of the microvasculature. HIF-1α is degraded when it is complexed with von Hippel-Lindau protein and oxygen-sensing prolyl hydroxylase domain proteins (PHD). HIF-2α activation induced vascular remodeling and loss of HIF-2α regulation by PHD2 in endothelial cells was associated with hyperplasia of arterial medial layers, perivascular fibrosis, and pericyte expression of FSP-1. Loss of PHD2 expression also increased pericyte coverage induced by TGF-β1 and Notch-3 signaling.[314] Pericyte expression of αSMA is greatly enhanced in response to chronic hypoxia[54] which may augment vasomotion towards preferential vasoconstriction of microvascular beds.

Pericyte damage may directly contribute to microvascular perfusion deficits with consequent ischemic tissue damage. Recent studies have shown that following traumatic brain injury, ET-1 is upregulated, which resulted in increased αSMA expression in pericytes, reduction of vessel diameter due to pericyte contraction, and hypoperfusion.[209,326] It is useful to note that vasoactive compounds converge onto signaling pathways that transiently raise intracellular calcium.[196] Dysfunctional pericyte contractility has also been shown in response to ischemic events. In both cerebral stroke and myocardial infarction (MI) models, ischemia evoked pericyte-mediated microvascular constriction. Subsequently, pericytes perished in rigor, irreversibly constricting capillaries. Elevated ROS interaction with ion transport molecules may allow increased influx of calcium into the intracellular space where contractile proteins become activated by calcium-activated phosphorylation thereby initiating rigor. Despite restoration of flow through occluded vessels, pericytes remained contracted, effectively obstructing

microvascular blood flow, which may account for the “no-reflow” phenomenon observed in cerebral ischemia and MI.[213,214] It remains unknown if intermittent hypoxia can induce similar consequences in the legs of PAD patients.

Pericytes in PAD Myopathy

Surprisingly little is known about pericytes in PAD myopathy. Very few studies have directly assessed the contribution of pericytes to initiation or progression of PAD myopathy. Augmenting pericyte function may have a considerable therapeutic potential in PAD skeletal muscle. With age, pericytes lose regenerative capacity, predisposing the aging and ischemic muscle of PAD patients to aberrant wound healing and fibrosis. However, understanding the signaling pathways and micro-environmental cues that predispose pericytes towards this shift could potentially yield novel approaches decreasing muscle degeneration or limiting fibrosis, thereby improving microperfusion and nutrient delivery to ischemic muscle and improving leg performance in PAD patients. A better understanding of microvascular pathology can therefore be critical to the development of better diagnostic strategies, treatment efficacy, and prediction of favorable responses to standard therapies for PAD such as revascularization surgery and exercise therapy.

Current Management Strategies for the Treatment of PAD

Early detection and diagnosis of PAD may allow for maximal preventative intervention. By managing risk and controlling comorbidities, it may be possible to prevent or limit the progression of atherosclerotic occlusion. Additional benefit may be seen at the

level of the affected skeletal muscle, particularly through limiting the ischemia/reperfusion injury to the legs. Several modalities are available to detect PAD. The most readily available, cost effective, and widely used test is the measurement of the ABI. Hemodynamically significant arterial stenosis is indicative of an ABI $\leq$0.90, and is often considered a hemodynamic definition of PAD.[23] **Table 1** summarizes characteristics of the utility of ABI in PAD diagnosis and research. Medical management is the mainstay of PAD treatment, and is typically centered around minimizing risk factors, smoking cessation, exercise training, and improving diet. Structured walking exercise protocols are effective in relieving claudication,[327] however, our laboratory has data that suggest that structured exercise protocols may exacerbate the progression of myopathy in PAD legs in a subset of patients.

Table 1: Overview of the Ankle Brachial Index (ABI)

	ABI
Practicality	Very practical. Easily performed at any clinic visit.
Reliability	High[328]
Validity	High, ABI is a component in establishing diagnosis[4] Using multivariate logistic regression, odds ratios for the false negative result of ABI were 4.36 in patients with diabetes mellitus (DM), 3.41 in patients with distal lesions, 3.02 in elderly patients, and 1.13 in patients with mild stenosis[329]
Specificity	Highly specific (also increases with decreasing ABI) 99% at ABI >0.8[328,330]
Responsiveness	MCID= 0.15 mmHG

Table 1: Overview of the Ankle Brachial Index (ABI).
MCID: Minimal Clinically Important Difference

Furthermore, the quality of life reported by patients who complete the structured exercise protocol is reduced compared to patients undergoing revascularization surgery.[331] Medications are typically given to manage hypertension, hypercholesterolemia, inflammation, and diabetes. Both cilostazol and pentoxifylline can be prescribed to alleviate claudication pain, and are thought to work by dilating arteries, decreasing platelet aggregation, and decreasing blood viscosity- all of which can improve blood flow. Currently, there is no pharmacological intervention available to treat either atherosclerosis or PAD myopathy directly. All therapies are targeting symptom reduction or alleviation.

For patients with CLI or PAD symptoms that significantly interfere with their ability to execute activities of daily living, revascularization becomes an option for therapy. Revascularization of PAD limbs can be achieved by either open bypass surgery (veins grafted proximally and distally to the atherosclerotic occlusion) or endovascular surgery (percutaneous balloon angioplasty and/or stenting). Revascularization surgery is known to improve both walking function and quality of life in patients, however, endovascular and especially open revascularizations are invasive and include significant risks to the patient. Additionally, it remains unclear to what extent the myopathy of PAD limbs is improved after revascularization.

Several tests and surveys have been developed to help assess PAD severity, as well as the efficacy of interventions. The Walking Impairment Questionnaire (WIQ) was formulated to assess ambulation deficits and is more PAD specific than the Short Form-36 (SF-36), which is general Quality of Life Instrument. The WIQ has been validated in patients with IC as a physical function quality of life survey.[330,332] The WIQ is scored on a scale from 0 to 100, with lower scores representing greater functional limitations within that category. The subcategory of pain describes the amount of difficulty the patient has with walking that is due to pain in the lower limbs. The distance category describes the amount of difficulty a patient experiences when walking specific distances, with the range

of distances covering 50 – 1500 feet. The speed subcategory captures the difficulty the patient experiences in traveling one block at various speeds, which span from a slow walk to a run or jog. The final subcategory, stair climbing, assesses the difficulty patients experience in climbing 1-3 flights of stairs. **Table 2** provides an overview of the utility of the WIQ in a clinical and research setting. The WIQ pain, speed, and distance subscales are the measures that correlated the best with the ambulatory limitation of patients with symptomatic peripheral arterial disease. Thus, the WIQ is the most specific questionnaire for documenting the qualitative walking deficits of patients with IC while concurrently providing strong relationships with the quantitative measures of arterial disease.[10]

Table 2: Overview of the Walking Impairment Questionnaire (WIQ)

WIQ	
Practicality	Highly practical. Easily administered and scored.
Reliability	High. Cronbach α of 0.82-0.9 when compared to initial claudication distance and absolute claudication distance.[333]
Validity	The Pearson coefficient between the WIQ and absolute claudication distance was 0.58. WIQ may not be as accurate for patients with variable/ highly atypical claudication.[334]
Specificity	Area under the curve analysis using cutoffs for overall WIQ scores had a sensitivity of 0.90 and specificity of 0.73 for low performers. For high performers, a combined subscale score of distance and stairs above a specified threshold had a sensitivity of 0.41 and specificity of 0.90.[335]
Responsiveness	The WIQ can detect improvement or deterioration and has a history of use in clinical trials.[334,336]

Table 2: Overview of the Walking Impairment Questionnaire (WIQ).

Quantitative measures of walking performance have also been developed and include the six minute walk test, initial claudication distance and absolute claudication distance (**Table 3**). The six minute walking test requires the patient to walk at sub-maximal exertion along a corridor of at least 100 ft in length. At six minutes after the initiation of walking, the test is concluded, and the total distance traversed by the patient is recorded. This paradigm allows patients to rest, although time continues to elapse. Although the six minute walk test replicates normal walking ability in PAD patients, it is susceptible to environmental factors, particularly since this test is done under submaximal exercise. The Gardner protocol is typically used in the assessment of PAD patient walking performance and is considered the gold standard in assessment of claudication pain onset and maximal walking duration. The Gardner protocol consists of patients walking on a treadmill beginning at a zero degree incline and 2 mph velocity which is incrementally increased by a 2% grade every 2 minutes.[337] The onset of this protocol is typically tolerated very well by PAD patients, and the incline and speed are thought to replicate low-intensity activities encountered in normal daily routines. As the grade (incline and velocity) increase, patients have increasing difficulty and begin to experience pain, which marks both the claudication onset time and initial claudication distance. Over time, PAD patients have pain that limits further participation, and they must discontinue the treadmill walking task to rest, which marks the absolute claudication distance corresponding peak walking time.

Table 3: Comparison of Quantitative Measures of PAD Walking Performance

	Six Minute Walk Test	Initial Claudication Distance	Absolute Claudication Distance
Reliability *	94%[338,339]	73.7%[340]	87.6%[340]
Validity	High[338,341] ICC= 0.94-0.97[338]	High, considered the gold standard ICC= 0.90[341]	
Specificity	Literature unclear	High when used with ABI[339]	
Practicality	Practicality is limited by the patient's ability and time to travel to conduct the tests. Usually, walking tests can be coordinated to the same visit as the clinical evaluation or prior to biopsy acquisition. The six minute walk test can be done on any level surface, however the initial and absolute claudication times utilize the Gardner Protocol which requires a treadmill.		
Responsiveness	The MCID is not established for walking performance measures in PAD.[341] In frail elderly, a small MCID is 20 meters and a substantial MCID is 50 meters for the six minute walk test. In non-elderly, non-PAD patients, a 52 meter increase is the smallest detected clinical difference *via* self-report.[338]		

Table 3: Comparison of Quantitative Measures of PAD Walking Performance.
ICC: Interclass Correlation Coefficient
MCID: Minimal Clinically Important Difference
* Obtained *via* test-retest comparisons

Inhibitors of the angiotensin system including ACE inhibitors and Angiotensin Receptor Blockers are promising candidates for the medical management of PAD and have been shown to reduce fibrosis in multiple organ systems.[342-344] Ramipril, an ACE inhibitor, reduces coronary fibrosis and improves arterial compliance in patients with cardiovascular disease. In PAD patients, six months of treatment with Ramipril produces improvements in walking distances comparable to those produced by supervised exercise therapy and revascularization,[344] however, the mechanism(s) by which Ramipril improves walking performance in PAD patients is unknown. Preliminary data from our laboratory suggests that ACE inhibitors slow progression and improve PAD myopathy in association with improved walking performance. The ACE inhibitor Ramipril has shown efficacy in ameliorating PAD symptoms in several recent randomized trials.[7,23,344-348]

Although Ramipril is a promising therapeutic option,[349] the mechanism(s) by which it improves PAD myopathy remains unclear. The benefit of ACE inhibitors may occur at the macrovascular level.[344,349-351] Treatment with ACE inhibitors increase arterial compliance[351] and may be expected to reduce arterial stiffness in PAD patients.[344] Additionally, ACE inhibitors may stabilize atherosclerotic plaques and promote plaque regression.[350] However, treatment of PAD patients with six months of Ramipril produced no significant change in the ankle brachial index (ABI), suggesting that the most beneficial effects of Ramipril may not be at the macrovascular level. ACE inhibitors prevent the cleavage of angiotensin I to angiotensin II (ANGII). Stimulation of ANGII sensitive receptors on endothelial cells generates a significant pro-inflammatory effect, as well as reactive oxygen species production at the endothelial cell membrane.[352,353] Chronic inflammation and oxidative damage may induce reactive changes in microvascular structure,[353] such as thickening of the BM which may result in loss of flexibility of microvascular beds. ANGII also promotes migration, proliferation, and hypertrophy of the

vascular smooth muscle cells (VSMC) surrounding the arterioles,[353,29] potentially altering arteriolar compliance and vasomotion. Inhibition of ANGII stimulation is associated with reduced secretion of endothelin-1[349], which promotes increased blood flow and improves the maintenance of collateral circulation.[354-356] Currently it is unknown whether ANGII inhibition impacts the microperfusion of capillary beds in PAD legs.

It is predicted that Ramipril may exert its beneficial effects in PAD limbs partially *via* immunomodulation. ANGII is known to increase the expression of pro-inflammatory cytokines in arterial VSMC in the setting of atherosclerosis.[357-359] Inflammation has been implicated in PAD pathogenesis, and is suspected to play a critical role in the initiation and progression of PAD.[360] In particular, the microvascular response to inflammatory signals may be crucial in the development of PAD myopathic changes and the microvasculature may be amenable to early therapeutic intervention. Of note, inflammation in PAD significantly predisposes an individual to developing Coronary Artery Disease (CAD), which greatly increases the risk of cardiovascular death and total mortality.[361] Therefore, it would be of tremendous value to understand the interaction of the renin-angiotensin system with the inflammation that occurs within PAD legs, particularly when considering subsets of patients who would be ideal candidates for ACE-Inhibitor therapies. We anticipate that microvascular pathology is progressive in PAD, and that the microvasculature may act as a nidus of the fibrosis present in PAD. Inhibition of ANGII activation with a therapeutic intervention such as Ramipril is most likely to impact the microvasculature, and if so, we anticipate seeing stabilization or regression of microvascular pathology that is concordant with improvements in fibrosis (**Figure 4**).

Figure 4: Conceptual Framework of Microvascular Pathology and Fibrosis with Advancing PAD Severity

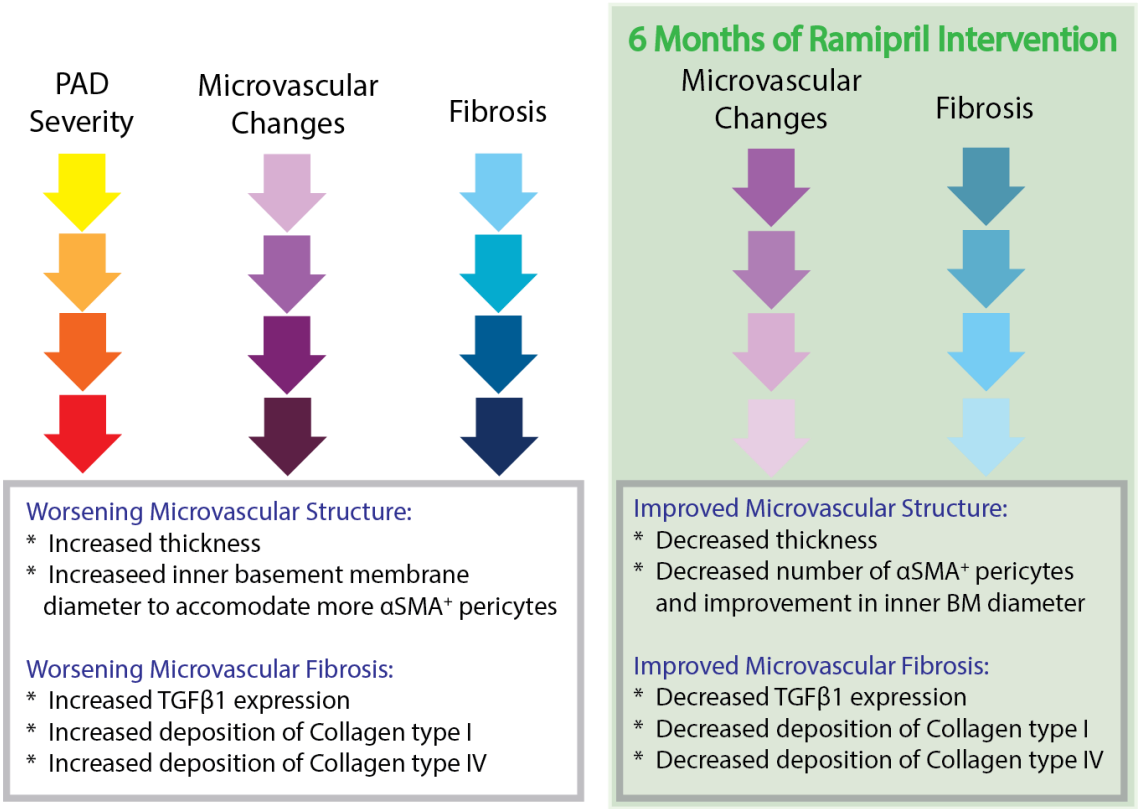

Figure 4: Conceptual Framework of Microvascular Pathology and Fibrosis with Advancing PAD Severity.

A relationship likely exists between microvascular pathology and fibrosis. As microvascular architecture worsens, fibrosis increases. Targeted treatment of microvascular pathology may improve microvascular structure, performance, and fibrosis. It is anticipated that six months of Ramipril treatment will improve microvascular structure and fibrosis.

Hypothesis and Specific Aims

Review of the literature suggests that PAD myopathy is progressive, and has detrimental impact to patient walking performance, quality of life, morbidity, and mortality. Thus, understanding the mechanisms by which PAD myopathy develops and progresses is of utmost importance for the development of more effective treatment strategies. Microvascular pathology may be essential in the induction and propagation of the myopathic changes observed in PAD skeletal muscle. Ultrastructural studies suggest that microvascular architecture is altered in PAD patients. Increases in BM thickness, in particular, are striking features of PAD pathology. However, the mechanism by which microvascular remodeling occurs remains exceptionally poorly characterized in PAD muscle. Currently no direct comparisons of microvascular architecture across PAD have been conducted. Furthermore, the relationship between microvascular architecture and oxygen delivery, hemodynamics, and walking performance are unknown. The present studies are designed to investigate the microvascular architectural alterations that are present across stages of PAD myopathy. We will characterize pericyte phenotypes that may be contributory to microvascular remodeling. Furthermore, we will demonstrate the relationship between microvascular architecture and macrovascular occlusion, muscle oxygenation, microperfusion, and walking performance in patients with IC. Finally, we will examine the effect of Ramipril on microvascular architecture and microperfusion. **Our overall hypothesis is that microvascular pathology is present in PAD muscle, worsens with increasing macrovascular hemodynamic restrictions, and advances with PAD severity in association with increasing αSMA^{+} pericytes and fibrosis and decreasing microperfusion, muscle oxygenation, and walking performance.** We will test our hypothesis by evaluating macrovascular hemodynamic restriction, microvascular architecture, pericyte characteristics, microvascular density, and fibrosis in patients from

control, Stage II, and Stage IV PAD patient groups. The parameters will be expanded in the Stage II PAD cohort to quantify 1) microvascular architecture; 2) fibrosis; 3) microvascular density; 4) microperfusion; 5) muscle oxygenation; and 6) walking performance and 7) macrovascular occlusion. We will implement the following Specific Aims.

Specific Aim #1: *To determine if microvascular pathology is progressive across stages of PAD.* We will measure microvascular BM thickness, inner BM diameter, and microvascular total diameter, quantify microvascular density and collagen I and IV deposition, total collagen, and characterize pericyte phenotype in the gastrocnemious biopsy specimens of control, Stage II and Stage IV PAD. We hypothesize that microvascular pathology worsens with advancing stage in association with increasing fibrosis.

Specific Aim #2: *To determine if microvascular pathology is influenced by macrovascular occlusion and characterize the relationship between microvascular architecture and microperfusion in patients with IC.* We will quantify microvascular architecture, as in Specific Aim 1, and determine if microvascular architecture is associated with arterial occlusion as assessed by ABI at rest and after post-occlusive reactive hyperemia, and microperfusion as assessed by flow reserve and microvascular blood velocity, volume, and blood flow before and after an ischemic stress. We hypothesize that microvascular pathology is associated with macrovascular hemodynamic limitations, and that microvascular architecture is associated with microperfusion deficits.

Specific Aim #3: *To determine if microvascular pathology influences muscle oxygenation and walking performance in patients with IC.* We will quantify microvascular architecture,

as in Specific Aim 1 and 2, and determine if microvascular architecture is associated with qualitative (WIQ) and quantitative measures (COT and PWT) of walking performance and muscle oxygen saturation. We hypothesize that as microvascular architecture worsens, the time to reach the minimum oxygen saturation shortens and patient walking performance deteriorates.

If our overall hypothesis is correct, we will have demonstrated that microvascular pathology is progressive in PAD, independent of macrovascular hemodynamic restriction, and associated with microperfusion deficits. We will have shown that pericyte phenotype is altered in association with increasing microvascular pathology. Additionally, we will have demonstrated that microvascular architectural alterations are linked to limitations in muscle oxygen delivery and patient walking performance.

Chapter II: Microvascular Pathology is Progressive Across Stages of PAD

Introduction

Peripheral Artery Disease (PAD) is a progressive disease that begins with the atherosclerotic narrowing of arteries supplying the lower extremities leading to failure of the vascular system to deliver adequate levels of oxygenated blood to the peripheral tissues.[4] PAD is estimated to affect approximately 202 million individuals globally, including 8.5 million Americans,[5,6] and the prevalence of PAD is anticipated to rise as populations age.[3] The Fontaine schema clinically classifies PAD into four stages. Asymptomatic patients with blocked arteries are classified as Fontaine Stage I.[4,19] Most symptomatic PAD patients suffer from claudication, presenting as walking-induced, ischemic pain of the affected legs (Fontaine Stage II). [19,20] In later stages, PAD patients experience severe pain at rest (Fontaine Stage III) [19,21,22] and progress to develop variable degrees of tissue loss and gangrene (Fontaine Stage IV).[19,21]

Poor perfusion affects all tissues of PAD legs, however, skeletal muscle is the most extensively studied due to its functional significance for walking. Studies of the muscles from PAD legs by our group and others demonstrate an ischemic myopathy that is characterized by a number of histological abnormalities, most importantly myofiber degeneration and fibrosis.[59-66,362] In a recent examination of fibrosis in PAD, our group demonstrated that collagen deposition occurs initially

around abnormally thickened microvessels and subsequently expands into the extracellular matrix (ECM) between myofibers and around myofascicles.[67] These thickened microvessels are surrounded by increased layers of proliferative and synthetic vascular smooth muscle cells (VSMC) that express large amounts of the pro-fibrotic cytokine TGF-β1. Microvessels with diameters around 50 - 150 μm were the primary focus of that study, but our findings suggested the possibility of pathological changes in the smallest vessels with diameters less than 15 μm, which includes capillaries. Structural alterations have been observed in the capillaries of PAD muscle. Transmission electron microscopy studies revealed that the BM of capillaries is thickened in PAD muscle.[82,171-173] Currently, the observation that BM thickening is progressive across stages of PAD remains mostly qualitative, and debate remains on whether additional BM thickening occurs in CLI relative to patients with claudication. Likewise, quantification of αSMA$^+$ capillary numbers between control and PAD muscle has yielded conflicting results.[127,171] Furthermore, it remains unclear if the αSMA immunoreactivity around PAD microvessels represents VSMC, pericytes, or myofibroblasts. These cell types have differing functions in normal physiology and may have unique contributions to PAD pathology, particularly fibrosis. The relationship between microvascular architectural alterations, microperfusion, and fibrosis remains unknown. Thus, characterization of the cells involved in expanding αSMA+ reactivity around PAD microvessels may provide insight into the mechanism of microvascular pathogenesis by determining if myofibroblast accumulation occurs

around microvessels or if inappropriate muscularization is occurring within terminal microvascular beds.

We hypothesized that microvascular pathology is present in the calf muscle of PAD patients compared to controls and that the microvessels are more diseased in Fontaine Stage IV patients compared to Stage II patients. This hypothesis was tested by investigating (1) microvessel architecture, including BM thickness, inner BM diameter, and total microvessel diameter; (2) deposition of Collagen I and Collagen IV around the microvasculature; (3) αSMA^{+} pericyte abundance and pericyte expression of the profibrotic cytokine TGF-β1 in microvessels and (4) fibrotic burden within the skeletal muscle specimens; in gastrocnemius samples from age matched control patients, Fontaine Stage II and Stage IV PAD patients.

Methods

Human Subjects

The experimental protocol was approved by the University of Nebraska Medical Center and the Veterans Affairs Nebraska-Western Iowa Institutional Review Boards. All subjects gave informed consent.

Control Group

We recruited 14 control patients who were undergoing vascular operations for abdominal aortic aneurysm repair. Control patients led sedentary lifestyles and had no history of

PAD symptoms. Control patients had normal blood flow to their lower limbs as indicated by normal lower extremity pulses at examination and normal ABI at rest and after stress.

PAD Groups

We recruited 15 patients with claudication (Fontaine Stage II) and 16 patients presenting with tissue loss (Fontaine Stage IV) who were undergoing lower extremity operations for symptomatic PAD. Medical history, physical examination, decreased ankle brachial index (ABI< 0.9), and computerized or standard arteriography that revealed stenotic and/or occluded arteries supplying the lower extremity were evaluated to establish the diagnosis for each PAD patient. Stage II PAD patients presented with intermittent claudication, but no rest pain or tissue loss. Stage IV PAD patients presented with non-healing ulcers and/or gangrene.

Biopsy

Gastrocnemius samples weighing approximately 250 mg were obtained from the anteromedial aspect of the muscle belly, 10 cm distal to the tibial tuberosity. All biopsies were obtained with a 6 mm Bergstrom needle. Samples were immediately placed into cold methacarn and fixed for 48 hours. Specimens were transferred to cold 50% ethanol, and subsequently embedded in paraffin.

Fluorescence Microscopy

Specimen Labeling

General

Paraffin-embedded biopsies were sectioned at 4 μm. Slide specimens were deparaffinized with xylene and rehydrated via a series of ethanol washes and distilled water. The rehydrated slide specimens were heated at 85 °C in either 10 mM citrate buffer (pH 6.0) or 10 mM tris with EDTA buffer (pH 9.0) for 15 minutes and then allowed to cool for 20 minutes. Subsequently, slide specimens were washed in Super-Sensitive Wash buffer (BioGenex Laboratories, Freemont, CA) for 30 minutes, followed by a 10 minute was in Dulbecco's Phosphate Buffered Saline. A programmable autostainer (BioGenex i6000, BioGenex Laboratories) was used to label specimens. Washes with super sensitive wash buffer were done prior to blocking and after treatment with primary and secondary antibodies (Abs). Washes in Dulbecco's Phosphate Buffered Saline were done prior to application of Prolong Diamond Mounting Media with the nuclear label 4',6-diamidino-2-phenylindole (Invitrogen, Carlsbad, CA). Specimens were treated with primary Ab or isotype control overnight, at 4 °C and with secondary Ab for 1 hour, at room temperature. All labeling protocols included duplicate slides with corresponding isotype controls.

Collagen I and Collagen IV

Specimens were blocked with 10% goat serum (cat# 500622, Life Technologies, Carlsbad, CA) and were treated with a mixture of mouse monoclonal anti-collagen IV (10 μg/mL, clone M3F7, Developmental Studies Hybridoma Bank, Iowa City, Iowa) and rabbit monoclonal anti-collagen I (2 μg/mL, cat# ab138492) Abcam, Cambridge, MA) Abs. Isotype control specimens were treated with a mixture of mouse IgG1κ (10 μg/mL, ref#

14-4714-85 Ebioscience, San Diego, CA) and rabbit monoclonal IgG (2 µg/mL, cat#ab172730, Abcam, Cambridge, MA) . Subsequently, the specimens were treated with a mixture of goat anti-mouse IgG-Alexa Fluor 647 (2 µg/mL, cat# A21236, Molecular Probes, Eugene, OR) and goat anti-rabbit IgG-Alexa Fluor 555 (2 µg/mL, cat# A21429, Molecular Probes, Eugene OR) Abs.

Collagen IV, αSMA, CD31

Specimens were blocked with 10% donkey serum (cat# ab7475, Abcam, Cambridge, MA) and were treated with a mixture of mouse monoclonal anti-collagen IV, rabbit polyclonal anti-αSMA (1 µg/mL, cat# ab5694, Abcam, Cambridge, MA), and sheep polyclonal anti-CD31 (3.5 µg/mL, cat# AF806-SP, R&D Systems, Minneapolis, MN) Abs. Isotype control specimens were treated with a mixture of mouse IgG1κ, normal rabbit polyclonal IgG (1 µg/mL, cat# AB-105-C, R&D System, Minneapolis, MN), and normal sheep polyclonal IgG (3.5 µg/mL, cat# 5-001-A, R&D Systems, Minneapolis, MN) . Subsequently, the slides were treated with a mixture of donkey anti-mouse IgG-Alexa Fluor 488 (2 µg/mL, cat# A21202, Molecular Probes, Eugene, OR), donkey anti-rabbit IgG-Alexa Fluor 555 (2 µg/mL, cat# A31572, Molecular Probes, Eugene, OR), and donkey anti-sheep IgG-Alexa Fluor 647 (2 µg/mL, cat# A21448, Molecular Probes, Eugene, OR) Abs.

Collagen IV, TGF-β1, CD31

Specimens were blocked with 10% donkey serum and were treated with a mixture of mouse monoclonal anti-collagen IV, rabbit polyclonal anti-TGF-β1 (5 µg/mL, cat# ab92486, Abcam, Cambridge, MA), and sheep polyclonal anti-CD31 antibodies. Isotype control specimens were treated with a mixture of mouse IgG1κ, normal rabbit polyclonal

IgG, and sheep polyclonal IgG. Subsequently, the slides were treated with a mixture of donkey anti-mouse IgG-Alexa Fluor 488, donkey anti-rabbit IgG-Alexa Fluor 555, and donkey anti-sheep IgG-Alexa Fluor 647 Abs.

Image Acquisition

General

Gray-scale (12-bit) fluorescence images (1344 x 1044) were captured with a wide-field, epifluorescence microscope (Leica DMRXA2; North Central Instruments, Plymouth, MN) (x10 objective; 0.5128 μm/pixel, 40x objective; 0.129 um/pixel), a B/W CCD camera (Orca ER C4742-95; Hamamatsu Photonics, Bridgewater, NJ) and HCImage Hamamatsu software (64-bit version, 4.2.5; Hamamatsu Photonics).

Microvascular Collagen I and Collagen IV

An acquisition matrix was programmed into HCImage to cover the whole muscle specimen area using the 10x objective, acquiring 70-150 microscopic frames per field for the collagen IV fluorophore channel. The frames were montaged in one large image to represent the given (whole) specimen. Subsequently, 12 representative regions of interest (ROI) were selected per biopsy specimen for microvascular architecture measurements with a 40x objective. Three ROIs were selected for acquisition from the isotype controls. An acquisition matrix was programmed into HCImage to collect 4 microscopic frames per ROI. At each ROI location, images were collected and montaged in fluorescence channels corresponding to each fluorophore; 1) 4',6-diamidino-2-phenylindole (DAPI, a nuclear stain) with an excitation maximum at 358 nm and emission

maximum at 461 nm, 2) Alexa Fluor 555 (collagen I) with an excitation maximum at 553 and emission maximum at 568 nm, 3) Alexa Fluor 647 (collagen IV) with an excitation maximum 650 nm and emission maximum at 668 nm.

Collagen IV, CD31, αSMA, and TGF-β1

Serial sections were labeled in duplicate to characterize pericyte phenotype. The following combinations of antibodies were used: (1) Collagen IV, αSMA, and CD31; (2) Collagen IV, TGF-β1, and CD31. Using the 40x objective, 5 ROIs were captured per muscle specimen. At each ROI location, images were collected in fluorescence channels corresponding to each fluorophore; 1) DAPI, a nuclear stain, 2) Alexa Fluor 488 (Collagen IV) with an excitation maximum at 495 nm and emission maximum at 519 nm, 3) Alexa Fluor 555 (αSMA or TGF-β1), 4) Alexa Fluor 647 (CD31). Corresponding ROIs were collected from the isotype control specimens.

Multi-Spectral Imaging

Specimen Labeling

Paraffin-embedded biopsies were sectioned at 4 microns. Slides were stained in duplicate with the Thermo Scientific Richard-Allan Scientific Chromaview Masson Trichrome staining kit (Fisher catalog number 22-110-648). The standard staining protocol was used with the following modifications. Slides were in Biebrich Scarlet-Acid Fuchsin Solution for 3 to 3 ½ minutes. After 3 minutes, slides were moved in pairs to deionized water at 10 second intervals. After 30 seconds in water, the first pair moved to phosphotungstic-phosphomolybdic solution with subsequent pairs moving every 10 seconds. After 5

minutes, the first pair moved to aniline blue stain solution and remained there for 10 ½ minutes. The remaining pairs moved into the stain solution at 10 second intervals with the last pair staining for 10 minutes. Remaining steps follow the standard protocol. After the last xylene bath, the cover slip was attached using paramount (Fisher Catalog Number Sp15-500).

Image Acquisition

Slides were viewed using a Leica DM RXA2 microscope, with a 20X objective. Image Cubes were generated from five different Regions of Interest (ROI) per slide using the Nuance Multispectral Imaging System 3.0.2 (PerkinElmer N-MSI-EX Model, Waltham, MA) that incorporates a CCD camera and liquid crystal tunable filter. Muscle tissue completely filled each selected field. The Nuance system generates an absorbance spectrum (450 nm to 700 nm) at each pixel of a two-dimensional spatial image of the specimen. Extracted images were acquired for each of the three colors produced by Masson trichrome stain: collagen(blue) and the muscle tissue (red) and nuclei (black). Thereafter, a specific collagen spectrum is generated with the Nuance software which quantitatively extracts the collagen spectrum at each pixel, producing a grey scale image of the deposited collagen.

Image Analysis and Quantification

All image analysis and quantification was performed blinded from group status.

Microvascular Architecture; Basement Membrane Thickness, Inner Basement Membrane Diameter, and Total Microvessel Diameter

Grey scale images of Collagen IV labeled basement membranes were obtained and transferred into the Image Pro® Plus image analysis environment (Media Cybernetics, Warrendale, PA). Background pixel intensity was determined and subtracted from the image. Images were then transferred into AutoQuant deconvolution software (Media Cybernetics, Warrendale, PA)(**Figure 5**). Deconvolution improves the point spread function that is inherent to light microscopy, thereby greatly improving both the image resolution and contrast. Each image underwent 4 iterations of 2D deconvolution. Image segmentation and microvessel architecture measurement was done with a custom-made Matlab algorithm (R2012a; MathWorks Inc, Natick, MA). Briefly, two perpendicular lines are drawn through each microvessel wall, with the initial line being placed across the longest microvessel axis, and corresponding intensity profiles are extracted (**Figure 5**). Automated capture of the microvascular wall and inner basement membrane diameter utilized a Gaussian Mixture Model alongside the Expectation Maximization algorithm. A ratio of the total microvessel diameter from each line was calculated to determine circularity of the microvessel. To avoid artificially biasing architecture measurements, microvessels with ratios below 0.75 were excluded from analysis. For each microvessel wall thickness, a 95% confidence interval of basement membrane thickness was obtained. Inner basement membrane diameter was calculated as the distance between the two luminal boundaries of the microvessel basement membrane. Means of four thickness values and two inner basement membrane diameter were calculated for each individual vessel. Total microvessel diameter was calculated as the inner basement membrane diameter plus twice the basement membrane thickness (**Figure 6**). Approximately 50-250

microvessels were assessed per biopsy specimen, with variability in the number of microvessels quantified per ROI reflecting the microvascular density present in the specimen. The mean of individual microvessel basement membrane thickness, inner basement membrane diameter, and total microvessel diameter were calculated for each patient.

Figure 5: Image Acquisition, Preparation, and Quantification for Measurement of Microvascular Architecture

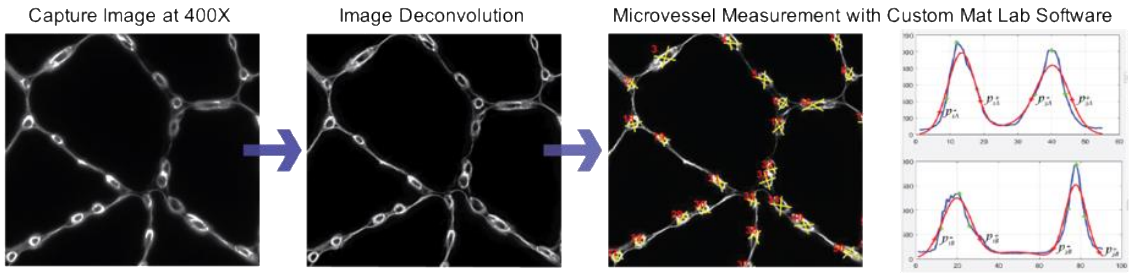

Figure 5: Acquisition of Microvascular Measurements.
Collagen IV-labelled specimens are imaged with a 40x objective. Image preparation includes image deconvolution to reduce light scatter and better delineate microvessel architecture. Subsequently, images are imported into custom MatLab software for quantification. For each vessel, two line profiles are generated which represent the pixel intensity across the distance of the line. Gaussian distributions (red) are fit to the actual pixel intensities (blue), with individual thickness measurements consisting of the distance contained with the 95% confidence interval of the approximated distribution. Means of four thicknesses are acquired per each vessel. Inner BM diameter is calculated as the distance between the two inner boundaries of the vessel thickness curves, with the mean of two measurements being acquired for each individual vessel.

Figure 6: Schematic Representation of Microvascular Architectural Measurements

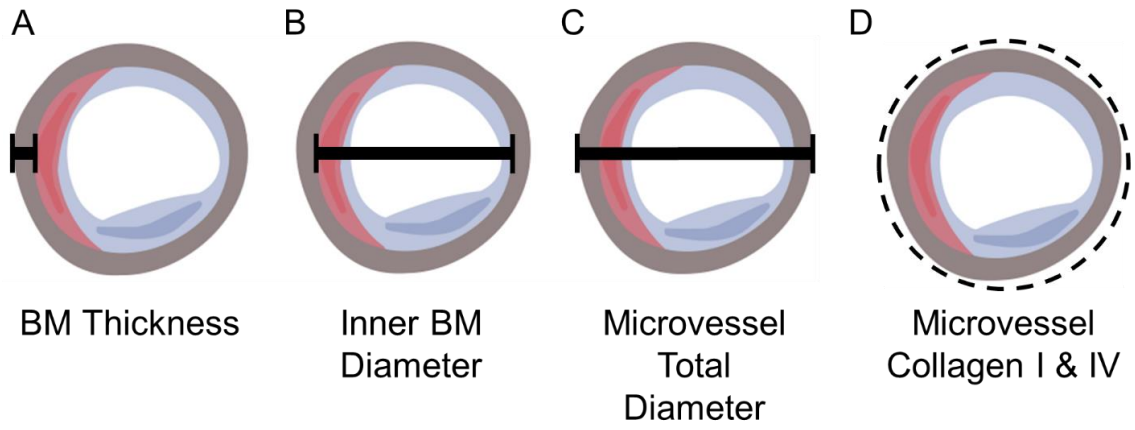

Figure 6: Schematic Representation of Microvascular Architectural and Collagen I & IV Measurements.

Cartoon depictions of microvessels are depicted. The red represents pericytes, the blue represents endothelial cells, and the grey represents basement membrane. The black bars denote the measurements made to determine BM thickness (A), inner BM diameter (B), and microvessel total diameter (C). The density of Collagen I and abundance of Collagen IV are measured around each microvessel. The area within the dashed circle represents the area analyzed for microvascular collagen deposition (D).

Microvascular Collagen IV Abundance and Collagen I Density

Specimens of gastrocnemius biopsies were labelled with Collagen I and Collagen IV. The 12 ROIs generated for the microvascular architectural analysis were analyzed for microvascular Collagen I & IV. Three ROIs were analyzed from the isotype controls. Grey scale montages (12 bit) were acquired for both Collagen I and Collagen IV and transferred to the Image Pro® Plus environment. A circular Area of Interest (AOI) was placed around each microvessel (**Figure 6**). Subsequently the AOIs were partitioned and both event area and mean pixel intensity were determined. For each ROI, an average of the mean pixel intensities and event areas of individual vessels was obtained. The Collagen IV abundance was calculated as the product of microvessel event area and mean Collagen IV pixel intensity (gsu•μm^2). Collagen IV abundance measurements from 12 ROIs were averaged to determine the mean patient Collagen IV abundance. Identical AOIs were used to determine Collagen I area weighted mean density, which was calculated as the sum of the products of microvessel event area and mean Collagen I pixel intensity of all positive events per microscopic field divided by the sum of the event areas (gsu).

Total Extracellular Matrix Collagen

Grey scale images obtained from the multi-spectral imaging of duplicate Masson trichrome stained slides were imported into the Image Pro® Premiere 9.3 (Media Cybernetics, Warrendale, PA) environment for quantification of collagen area and intensity mean values (12-bit grey scale). Total collagen abundance was determined as area multiplied by intensity (gsu•μm2) for each ROI generated.

Microvascular Density

Grey scale images obtained from Collagen I & IV labeling were transferred into the Image Pro® Plus environment. Collagen IV label uniformly identified microvessel structure and was used to create partitions that yielded accurate vessel identification. The number of microvessels and total tissue area were determined. A ratio of microvessels per total tissue area was calculated to determine microvascular density per ROI.

Pericyte Identification and Characterization

Slides labeled with Collagen IV, αSMA, and CD31 were qualitatively reviewed. αSMA has been shown to be variably expressed in pericytes of various tissues, including skeletal muscle. Candidate cells were considered pericytes if they were abluminal to the endothelium (CD31 label) and within the microvascular basement membrane (Collagen IV label). Grey scale images were transferred into Image Pro® Plus software, and the abundance of microvascular αSMA^{+} pericytes was calculated as the product of event area by mean pixel intensity ($gsu \bullet \mu m^2$). Microvessels greater than 15 μm in diameter were excluded from the analysis of αSMA^{+} pericyte abundance. Adjacent slides were labeled with Collagen IV, TGF-β1, and CD31 to qualitatively determine the presence and location of TGF-β1 expression within the microvessel structure.

Statistical Analysis

To assess how balanced the three PAD groups (Control, Stage II, and Stage IV) are, they were compared using the nonparametric Kruskal-Wallis test for continuous predictor variables, and the Chi-square test for categorical predictor variables, All biological parameters were assessed for normality, and transformed if nonnormal. When two groups had to be compared, the two-sided independent t-test was performed for normally distributed parameters, whereas the non-parametric Mann-Whitney U test was used when nonnormality was encountered. In order to avoid confounding, the three PAD groups (Control, Stage II, and Stage IV) were compared with respect to each of the response variables using by a multivariable general linear model while controlling for the rest of the predictor covariates. Parametric simple linear regressions were performed to assess the relationship between variables. The overall level of statistical significance was kept at alpha 0.05 in all analyses. The basic statistical analyses were performed with NCSS 12 Statistical Software, whereas the multivariable analyses were performed using SAS 9.4 (SAS Inst, Cary, NC).

Results

Patient Demographics

Limited cohorts of control (n = 14), Stage II PAD (n = 15), and Stage IV PAD patients (n = 16) were analyzed due to the detailed and extensive nature of characterizing microvascular features. Previous studies of microvascular structure were able to detect differences between microvessels from PAD patients versus control with cohorts of 8 – 14 patients.(20-23) Thus, we utilized a minimum of 14 patients per group. Demographic data for Control, Stage II, and Stage IV PAD are presented in **Table 4**. ABI differed between control and Stage II PAD patients ($p < 0.0001$), between control and Stage IV PAD patients ($p < 0.0001$), and Stage II PAD and Stage IV PAD patients ($p = 0.0002$). The Stage IV

PAD cohort had a greater percentage of diabetes mellitus than control ($p = 0.04$) and Stage II PAD ($p = 0.03$). The Stage IV PAD cohort also had a greater percentage of rental insufficiency than control ($p = 0.03$) and Stage II PAD ($p < 0.005$). Family history of cardiovascular disease was greater in Stage IV PAD patients than control ($p = 0.05$) and Stage II PAD ($p = 0.01$). Age, gender, smoking status, hypertension, coronary and cerebrovascular disease, obesity (body mass index >30), dyslipidemia, Chronic Obstructive Pulmonary Disease, and statin use did not differ between groups ($p > 0.05$). Significant variables were treated as covariates in all subsequent analyses.

Table 4: Patient Demographics; Control, Stage II, and Stage IV PAD

	Control	Stage II PAD	Stage IV PAD
Number of subjects	14	15	16
Mean age (years)	67.29 ± 1.34	64.27 ± 1.22	69.40 ± 1.01
Ankle Brachial Index	1.089 ± 0.027 ‡	0.604 ± 0.033 **	0.184 ± 0.058 **‡
Gender (male / female)	100	100	94
Smoking (never / current / former)	14/ 43 / 43	0 / 40 / 60	13 /56 / 31
Coronary artery disease	29	20	50
Cerebrovascular disease (none / TIA [A] / stroke)	93 / 7 / 0	87 / 0 /13	75 / 6/ 19
Obesity [B]	43	20	25
Dyslipidemia	71	53	44
Diabetes Mellitus	14	13	50 *†
Chronic Obstructive Pulmonary Disease	0	20	6
Renal insufficiency [C]	7	0	44 *‡
Statins	64	80	56
Family history of cardiovascular disease	36	47	88 *†
Hypertension	57	60	88

Table 4: Patient Demographics.

Note: Continuous variables were analyzed by Kruskal-Wallis test and are presented as mean ± S.E.M. Categorical variables were analyzed by Chi-square test and are presented as percentages.

* Significant difference from control ($p < 0.05$)

** Significant difference from control ($p < 0.005$)

† Significant difference from Stage II PAD ($p < 0.05$)

‡ Significant difference from Stage II PAD ($p < 0.005$)

A Transient Ischemic Attack

B Body Mass Index > 30

C Creatinine clearance < 60ml/min.1.73m^2

Altered microvascular architecture is an early feature of PAD myopathy and worsens with PAD severity

To investigate the structural changes in PAD microvessels, we measured microvessel BM thickness, inner BM diameter, and total microvessel diameter. We observed that a progressive thickening is present between control (1.408 ± 0.025 μm) and Stage II PAD (1.577 ± 0.030 μm; p=0.0002), as well as, Stage II PAD and Stage IV PAD (1.747 ± 0.060 μm; p=0.02). Whereas BM thickening appeared to be an early feature in PAD myopathy, inner BM diameter increases were found in advanced PAD. Microvessel inner BM diameter was similar between control (3.243 ± 0.094 μm) and Stage II PAD (3.295 ± 0.064 μm). Interestingly, we observed a significant increase in Stage IV PAD inner BM diameter (3.972 ± 0.124 μm) compared to control (p=0.00007) and Stage II PAD (p=0.00007). Total microvessel diameter was significantly greater in Stage IV PAD (7.466 ± 0.224 μm) compared to control (6.058 ± 0.111 μm; p=0.00001) and Stage II PAD (6.448 ± 0.112 μm; p =0.0005) (**Table 5**). Multivariate analysis revealed that the stage of PAD was the predominant predictor of BM thickness ($p = 0.0005$), inner BM diameter ($p = 0.0048$), and microvascular total diameter ($p < 0.0001$). The presence of cerebrovascular disease influenced BM thickness ($p = 0.046$), and inner BM diameter ($p = 0.008$), and marginally influenced microvascular total diameter ($p = 0.057$). Hypertension ($p = 0.035$) contributed to inner BM diameter. The contribution of diabetes to inner BM diameter was marginally significant ($p = 0.082$).

Table 5: Microvascular Architecture Measurements Across Stages of Peripheral Artery Disease

	Control	Stage II PAD	Stage IV PAD
Microvascular BM Thickness	1.408 ± 0.025	1.577 ± 0.030 *	1.747 ± 0.060 *†
Microvascular Inner BM Diameter	3.243 ± 0.094	3.295 ± 0.064	3.972 ± 0.124 *#
Microvascular Total Diameter	6.058 ± 0.111	6.448 ± 0.112	7.466 ± 0.224 *#

Table 5: Microvascular Architecture Measurements Across Stages of Peripheral Artery Disease.

Gastronemius biopsy specimens were labeled with Collagen IV and microvascular architectural features were measured. Measurements were obtained for approximately 50 - 200 microvessels per each biopsy specimen. Control (n = 14), PAD Stage II (n = 15), and PAD Stage IV (n = 16). Measurements are presented as mean ± S.E.M.

* : significant difference from Control ($p < 0.001$)

† : significant difference from Stage II PAD ($p = 0.02$)

\# : significant difference from Stage II PAD ($p > 0.001$)

Collagen IV deposition is increased around PAD microvessels

Quantitative fluorescence microscopy (QFM) revealed increased Collagen IV deposition in PAD gastrocnemius. Collagen IV labeling was most intense around the microvessels and was also observed around individual myocytes. Qualitative review of specimens demonstrated an increased deposition of Collagen IV around microvessels, but not myocytes, in PAD microvessels (**Figure 7A-C**). PAD microvessels appeared to be thickened by Collagen IV, with greater thickening around microvessels in advanced PAD (**Figure 7D-F**). Interestingly, microvascular thickening was not homogeneous in Stage II PAD muscle and instead demonstrated a skip lesion phenomenon. However, thickened microvasculature appeared ubiquitous across Stage IV PAD muscle. To characterize the extent of Collagen IV deposition around the microvasculature we measured microvessel Collagen IV abundance. We observed a trend for increase in Collagen IV deposition from control (16,670 gsu•μm^2, IQR = 12,778) to Stage II PAD (22,378 gsu•μm^2, IQR = 14,860) to Stage IV PAD (29,165 gsu•μm^2, IQR = 27,286). Microvascular Collagen IV abundance was significantly greater in Stage IV than control (p=0.029), but did not reach significance between control and Stage II (p=0.59), or Stage II and Stage IV (p= 0.15) (**Figure 7G**). When adjusted for covariates, Collagen IV abundance was marginally significant (p = 0.056).

Figure 7: Collagen IV is Increased Around PAD Microvessels

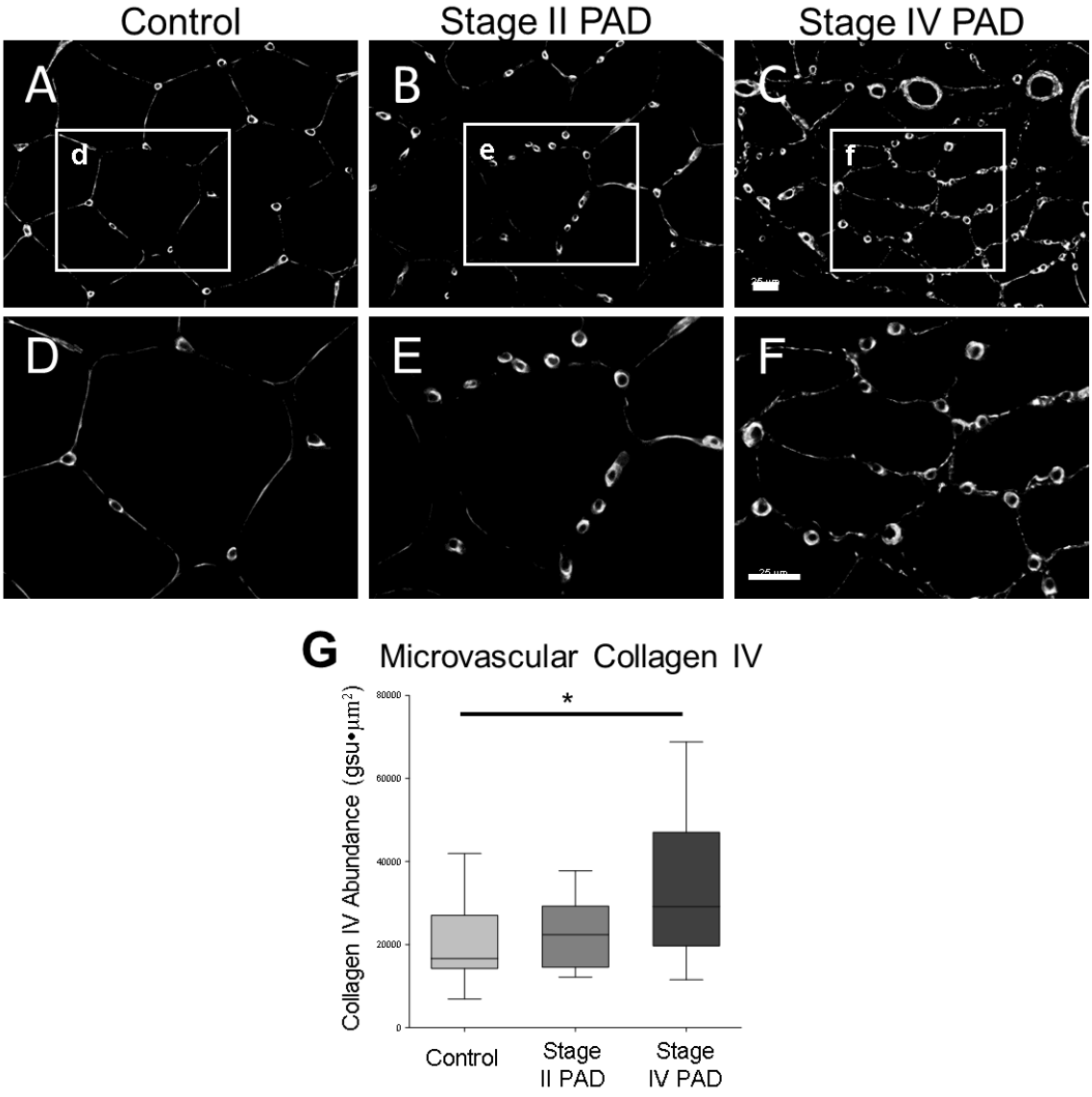

Figure 7: Collagen IV deposition is enhanced around PAD microvessels.

Gastrocnemius biopsy specimens were labelled with Collagen IV. Qualitative review shows progressive increases in deposition of collagen IV between control (A), Stage II PAD (B), and Stage IV PAD (C). Callout boxes in A-C are enlarged in D-F, respectively. Collagen IV abundance was significantly elevated in Stage IV PAD compared to control ($p = 0.029$) (F).

Next, we explored the relationship between early and late microvascular architectural alterations. A positive linear relationship is present between microvascular BM thickness and inner BM diameter ($R= 0.72$, $R^2= 0.52$; $p>0.0001$), suggesting that changes in microvascular architecture may be continuous with PAD progression (**Figure 8A**). To determine if microvascular architectural changes limited the formation of additional microvessels, we quantified microvascular density. Compared to control (4.8 ± 0.7 microvessels per 10^3 μm^2), both Stage II PAD (5.6 ± 0.7 microvessels per 10^3 μm^2; $p> 0.00001$) and Stage IV PAD (6.1 ± 0.9 microvessels per 10^3 μm^2; $p>0.00001$) had elevated microvascular density. Stage IV PAD microvascular density was larger than Stage II PAD, however, the difference between these groups was marginally significant ($p=0.053$) (**Figure 8B**). Covariate analysis yielded no significant influence of DM, FH, renal insufficiency, or age on microvascular architecture or microvascular density.

Figure 8: Relationships Between Microvascular Architectural Parameters and Microvascular Density with PAD Severity

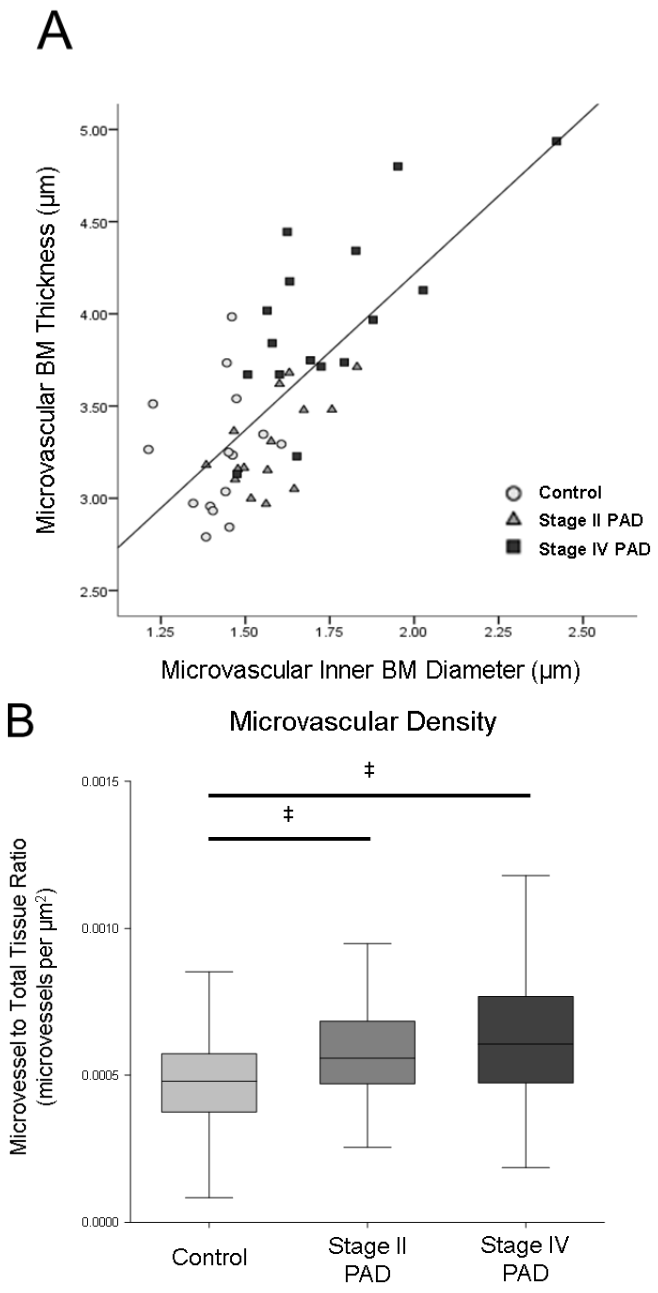

Figure 8: Microvascular Thickness is Associated with Inner BM Diameter and Microvascular Density Increases Across Stages of PAD.

Microvascular BM thickness is positively associated with inner BM diameter across stages of PAD ($R^2 = 0.52$; $p < 0.0001$) (A). Microvascular density is progressively increased with stage severity. Stage IV PAD microvascular density was greater than Stage II PAD ($p = 0.053$), which was greater than control ($p < 0.00001$) (B). Data presented as mean ± S.E.M.

Collagen I is preferentially deposited around PAD microvessels

Collagen I is present within healthy skeletal muscle and provides tensile support to these tissues. Aberrant Collagen I deposition has been implicated in the fibrosis of various organs, including PAD skeletal muscle. [58,61,64-66,80,85-92] We assessed the distribution of Collagen I deposition within control and PAD gastrocnemius. A subset of thickened PAD microvessels gained a secondary investment of Collagen I around and within the microvascular BM (**Figure 9A-B**). Collagen I deposition varied in PAD specimens and included interstitial deposition between myocytes. In areas with limited fibrosis, Collagen I was found mainly around microvessels (triangles), while in areas with pronounced fibrosis Collagen I was found around microvessels and extended into the interstitial space (arrows), suggesting that collagen I deposition may arise from the microvasculature (**Figure 9C**).

Quantitative fluorescence microvscopy revealed that Collagen I is discretely present around myofibers and microvessels of control gastrocnemius (**Figure 9D**). In Stage II PAD, fibrosis was increased but modest. Isolated areas of increased Collagen I deposition were encountered and were preferentially deposited around Stage II PAD microvessels (**Figure 9E**). In Stage IV PAD, fibrosis was pronounced and Collagen I deposition was present diffusely with Stage IV PAD microvessels being frequently encapsulated by Collagen I (**Figure 9F**). Quantification of microvascular Collagen I density demonstrated similar medians between control (132.6 gsu, IQR = 316.9) and Stage II PAD (159.7 gsu, IQR = 302.0). Microvascular collagen I deposition was increased in Stage IV PAD (427.9 gsu, IQR = 914.6) compared to Stage II PAD ($p=0.023$) and control ($p=0.044$). Adjustment for covariates revealed that PAD stage was the predominant predictor of Collagen I density ($p = 0.027$).

Figure 9: Collagen I is Preferentially Depositied Around Microvessels

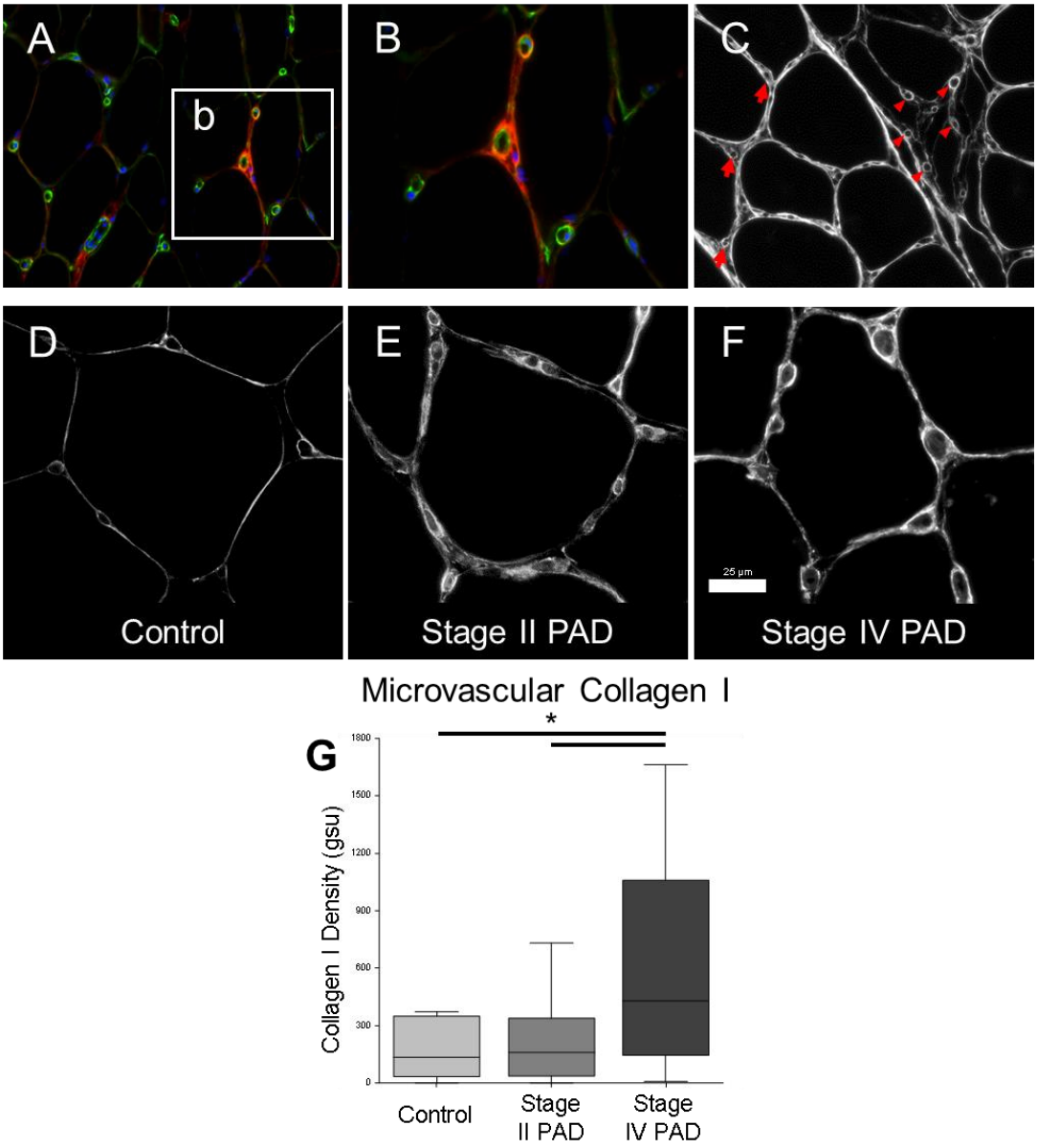

Figure 9: Collagen I is Preferentially Deposited Around PAD Microvessels.
Collagen I (red) is heterogeneously deposited in Stage II PAD muscle and is preferentially deposited around collagen IV-thickened microvessels (green) in areas of limited fibrosis (A). Enlargement of the callout box (b) reveals that collagen I is deposited as a second annulus around and within the microvascular basement membrane (B). Fibrotic areas of Stage II muscle show that collagen I deposition is prominent around microvessels (triangles) which appears to extend from the microvessels into the surrounding interstitium (arrows)(C). Microvascular Collagen I deposition is restricted and uniform in control (D), enhanced in select areas of Stage II PAD (E), and prominent in Stage IV PAD (F). Microvascular Collagen I density is greater in Stage IV PAD relative to Stage II PAD ($p = 0.023$) and control ($p = 0.044$)(G).

Fibrotic burden is increased in PAD

To determine the fibrotic burden present within the gastrocnemius, we utilized Masson trichrome stain to determine the abundance of total collagen present within the biopsy specimens. We observed uniform collagen distribution in control (**Figure 10A,D**), areas of increased collagen deposition in Stage II PAD (**Figure 10B,E**) and areas of overt fibrosis in Stage IV PAD (**Figure 10C,F**). Dense collagenous investment of microvessels was observed. Collagen label was extracted from Masson trichrome stained sections (**Figure 10D-F**) and quantified by spectral analysis. Total collagen abundance was increased in Stage IV PAD (1066 gsu•μm^2, IQR = 734) compared to Stage II PAD (358 gsu•μm^2, IQR = 256; p=0.0001) and control (287 gsu•μm^2, IQR = 168; p=0.00003). Total collagen abundance was increased in Stage II PAD compared to control, although this difference was marginally significant (p=0.055). Multivariate analysis revealed that PAD stage was the predominant predictor of total collagen abundance (p <0.0001).

Figure 10: Fibrotic Burden is Increased in PAD

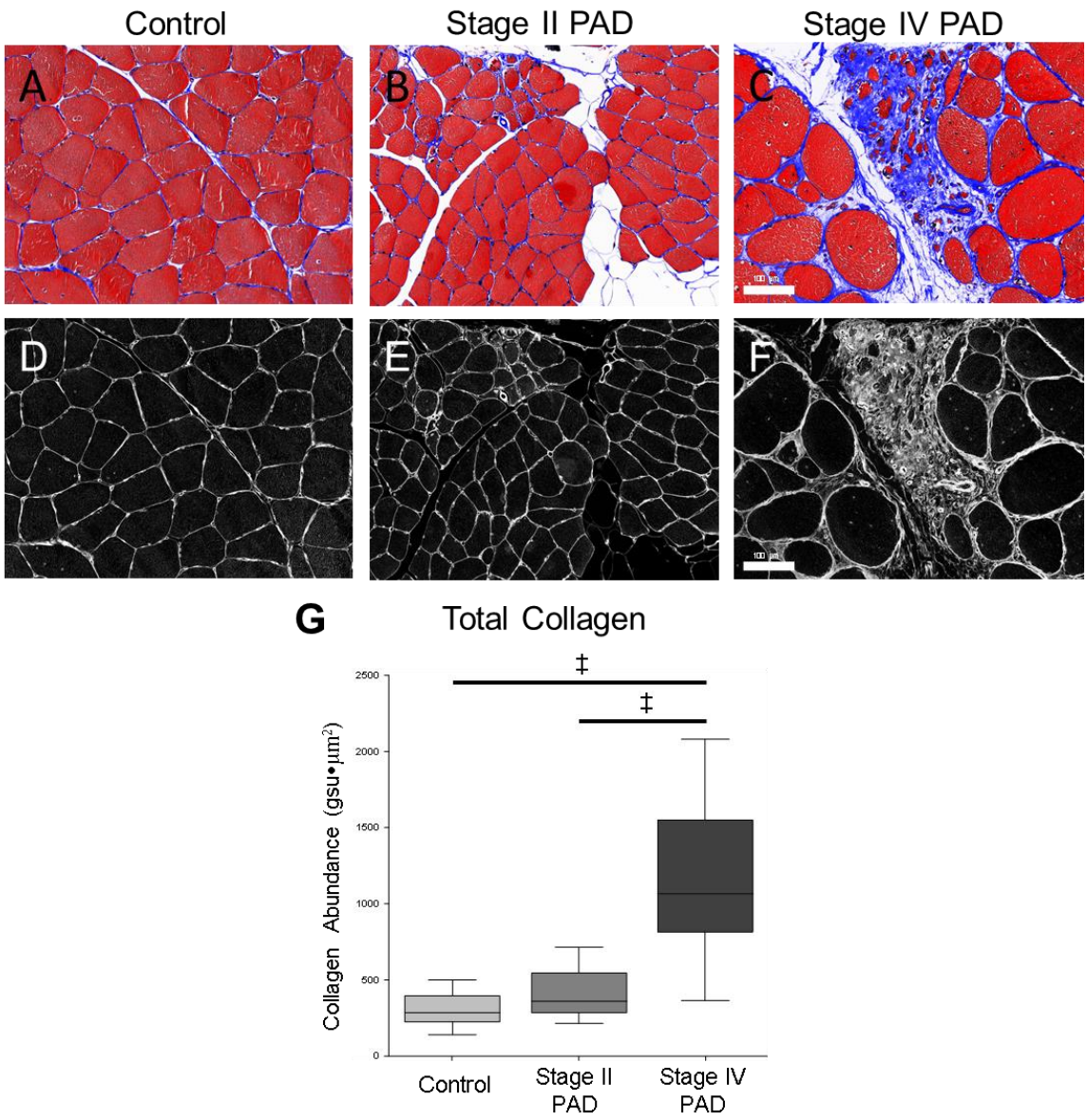

Figure 10: Fibrotic burden is increased in PAD.
Masson Trichrome stained sections reveal that collagen deposition is limited in control muscle (A), heterogeneously increased in select regions of Stage II PAD (B), and extensive in Stage IV PAD (C). Corresponding collagen extractions are presented from A-C and show dense collagenous deposition around microvessels in areas of fibrosis (D-F, respectively). Collagen quantification revealed increased total collagen abundance in Stage IV compared to Stage II ($p = 0.0001$) and control ($p= 0.00003$)(G).

PAD pericytes acquire an αSMA$^+$ phenotype, increase in abundance with PAD severity, and express TGF-β1

Our assessment of microvascular architecture focused on the structure of microvascular matrix proteins, Collagen I & IV. The finding that the microvascular inner BM diameter expanded with advancing disease prompted exploration of cellular changes within the collagenous annulus. CD31$^+$ endothelial cells were encountered within the Collagen IV annulus; however qualitative review of the endothelial lumen diameter did not yield luminal enlargement between control and Stage II or Stage IV PAD. Instead, endothelial swelling was frequently encountered in advanced PAD. Pericytes can express αSMA and reside within a shared basement membrane with endothelial cells with which they maintain close contact with through gap junctions, adhesion junctions, and peg and socket contacts.[180,194]

Quantitative fluorescence microscopy labeling of specimens with CD31, αSMA, and Collagen IV revealed increased numbers of αSMA$^+$ pericytes in and around PAD microvessels which were most prominent within thickened microvessels. Control microvessels (5-15μm) demonstrated rare αSMA$^+$ pericyte cell bodies, but αSMA$^+$ puncta, likely representing pericyte processes, were present (**Figure 11A**). Stage II PAD microvessels demonstrated αSMA$^+$ puncta as well as frequent αSMA$^+$ cell bodies (**Figure 11B**). Stage IV PAD microvessels had a striking increase in αSMA$^+$ cell bodies, with multiple αSMA$^+$ pericytes being present around individual microvessels. In slightly larger microvessels (15-30μm), multiple layers of αSMA$^+$ pericytes were present within the thickened Collagen IV network (arrow). Additionally, acellular microvessels were encountered (arrowheads) (**Figure 11C**). Quantification of αSMA abundance was restricted to pericytes from microvessels with a total diameter of <15μm. As PAD severity

advanced, αSMA$^+$ pericyte abundance increased. Stage IV PAD (32957 gsu•μm^2, IQR = 69876) had a greater αSMA$^+$ pericyte abundance than Stage II PAD (20308 gsu•μm^2, IQR = 13771; p=0.00027), and Stage II PAD had a greater αSMA$^+$ pericyte abundance than control (7156 gsu•μm^2, IQR = 7035; p<0.00001)(**Figure 11D**). After adjusting for covariates, PAD stage remained the predominant predictor of sum of αSMA$^+$ pericyte area (p = 0.0003). BMI had a marginal contribution to the sum of αSMA$^+$ pericyte area (p = 0.081). Adjacent sections were labeled with CD31, TGF-β1, and Collagen IV. The αSMA$^+$ pericytes encased in thickened PAD microvessels (5-15μm) (**Figure 12A**) also express TGF-β1 (**Figure 12B**).

Increasing αSMA$^+$ pericyte abundance and expression of TGF-β1 point to a potential relationship between pericytes, microvascular architectural alteration, and peri-microvascular fibrosis. We observed that αSMA$^+$ pericyte abundance increased in association with increasing BM thickness (R = 0.69, p = 0.004), inner BM diameter (R = 0.53, p = 0.04), and total diameter (R = 0.76, p = 0.001). There was a strong positive linear relationship between αSMA$^+$ pericyte abundance and peri-microvascular Collagen IV abundance (R = 0.74, p = 0.002). Additionally, we observed a strong relationship with increasing αSMA$^+$ pericyte abundance and increasing peri-microvascular Collagen I density (R = 0.65, p = 0.008).

Figure 11: αSMA Positive Pericyte Abundance Increases with PAD Severity

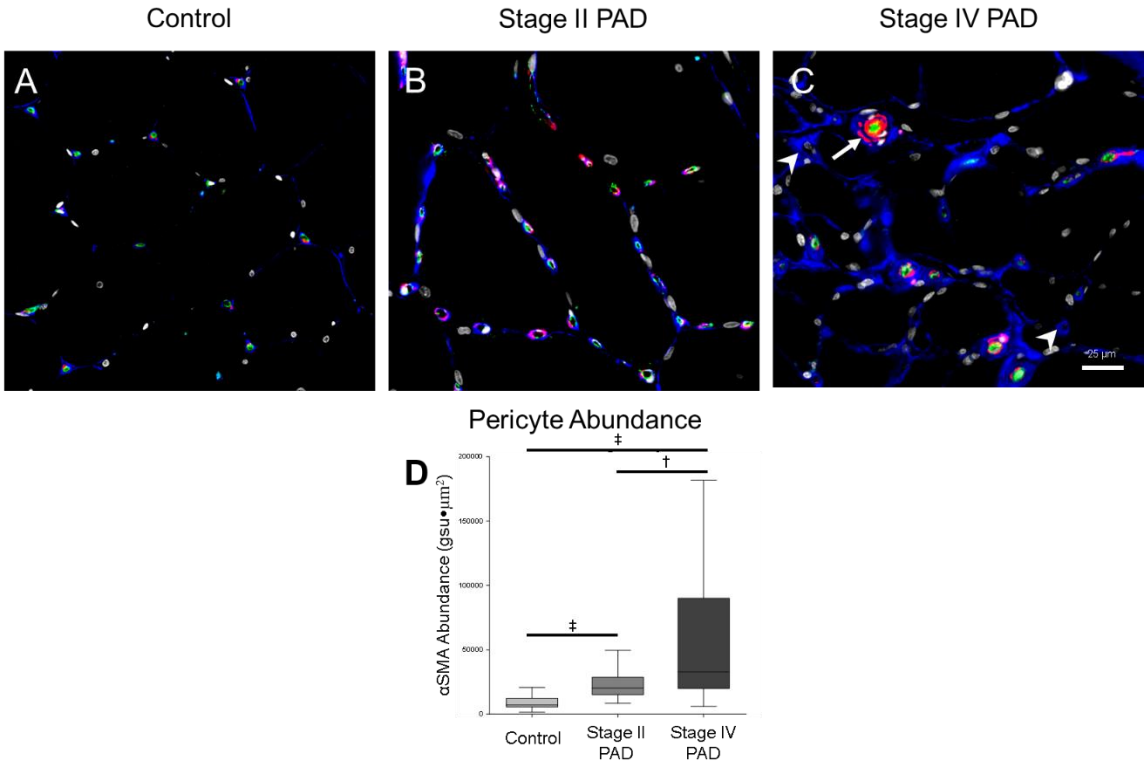

Figure 11: αSMA⁺ Pericyte Abundance Increases with PAD Severity.
Specimens were labeled for collagen IV (blue), αSMA (red), CD-31 (green), and DAPI (grey). Control microvessels had few αSMA⁺ pericytes (A). Thickened microvessels had increased αSMA⁺ pericyte coverage in Stage II PAD (B). The number of αSMA⁺ pericytes was substantially increased in Stage IV PAD. Multiple αSMA⁺ pericytes were present on terminal microvessels which appeared "arteriolarized" (arrow). Acellular microvessels were also commonly encountered (arrowheads) (C). αSMA⁺ pericyte abundance progressively increased with PAD severity. Stage IV PAD had a greater abundance of αSMA⁺ pericytes than Stage II PAD ($p = 0.0003$), and Stage II PAD was greater than control ($p < 0.00001$)(D).

Figure 12: In PAD Microvessels, αSMA+ Pericytes Express TGF-β1

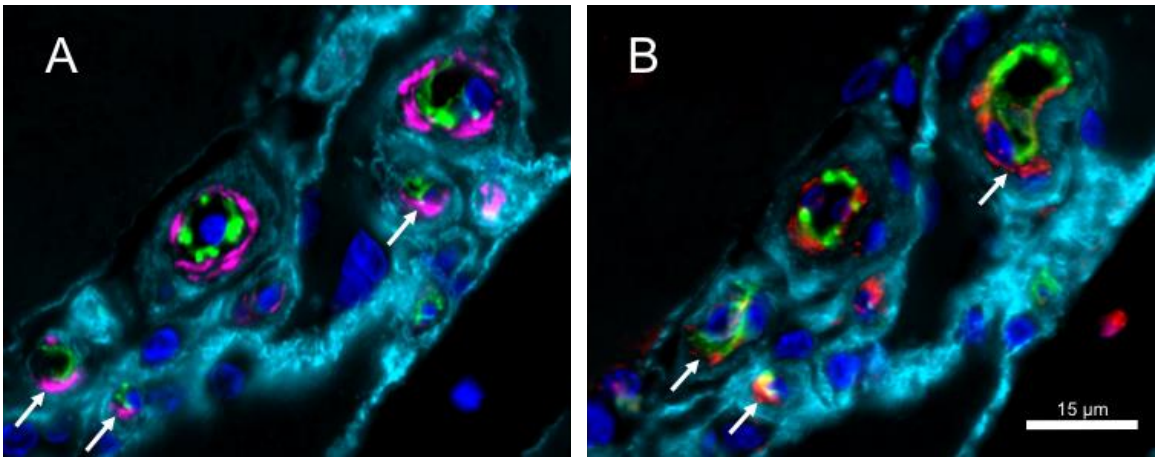

Figure 12: αSMA^{+} Pericytes Express TGF-β1 in PAD Microvasculature.

Serial sections were labeled for Collagen IV (teal), CD-31 (green), DAPI (blue) and either αSMA (magenta)(A) or TGF-β1 (red)(B). αSMA and TGF-β1 labeling was present on pericytes from the same microvessels (arrows).

Discussion

PAD starts as atherosclerotic occlusive disease of the named inflow arteries (macrovascular disease) supplying the legs, most commonly affecting the aortic bifurcation, the superficial femoral artery at Hunter's hiatus and the popliteal trifurcation. Our study established that the vascular pathology of PAD extends beyond macrovascular atherosclerosis and produces a microvascular disease in the ischemic muscles of PAD limbs. We have previously shown that small vessels (diameters of 50 – 150 μm) are diseased in PAD limbs,[67] and in the current study we extend these findings to demonstrate that the smallest microvessels (<15 μm) are also affected by PAD. Microvascular pathology is present in the calf muscle of claudicating patients and is substantially more advanced in patients with CLI. Using quantitative methods, we have shown that in PAD muscle, pathological changes are present in microvessels less than 15 μm in diameter and include thickening of the BM, mainly due to deposition of Collagen I and IV, diameter enlargement of the BM ring, and a rise in the abundance of αSMA^+ pericytes. All of these microvascular alterations increase in parallel with advancing disease severity. As PAD severity advanced from Stage II to Stage IV, the fibrotic burden increased alongside microvascular architectural alterations. Substantial thickening of the Collagen IV annulus was observed in advanced PAD, and the microvascular annulus was further thickened by a secondary layer of Collagen I. The abundance of αSMA^+ pericytes was also substantially increased around these thickened microvessels. Furthermore, late stage PAD patients had a significantly enlarged inner BM diameter, which does not appear to represent an increase the luminal flow diameter, but rather represented the accommodation of the more numerous pericytes within the thickened BM (**Figure 13**). BM thickness positively correlated with inner BM diameter, which supports that pericyte

proliferation and excessive BM synthesis are progressive in PAD myopathy. Moreover, the abnormally increased αSMA$^+$ pericytes expressed TGF-β1 (**Figure 12**), which likely induces pericyte secretion and peri-microvascular deposition of Collagen I and IV. In support of this, we observed strong associations between increasing αSMA$^+$ pericyte abundance, and increasing microvascular BM thickness, inner BM diameter, total microvessel diameter, Collagen IV abundance and Collagen I density. Collagen I deposition circumscribed microvessels and extended around the myofibers and myofascicles. Taken together, these data suggest that microvascular pathology may be central to PAD myopathy. Microvascular disease may have a substantial deleterious effect of muscle perfusion and is a likely source of myofibrosis within ischemic PAD muscle.

Figure 13: Schematic Representation of Microvascular Remodeling in PAD

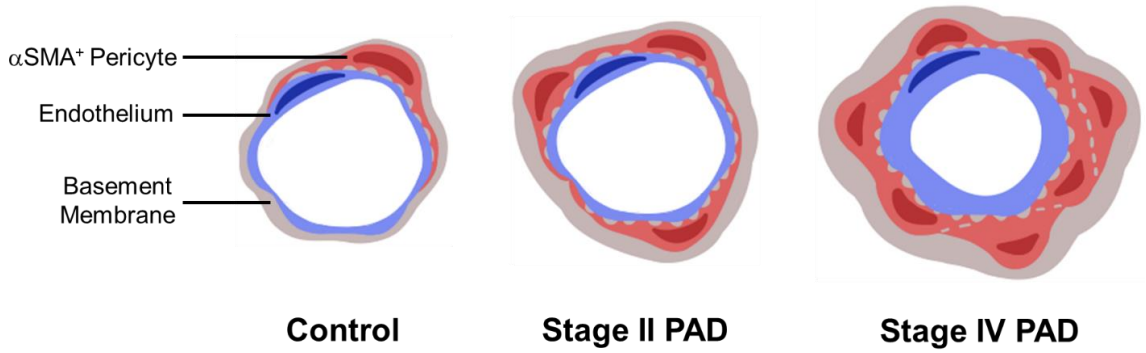

Figure 13: Schematic Representation of Microvascular Remodeling in PAD. Microvascular architectural alterations across stages of PAD are depicted in the cartoon. The number of αSMA^+ pericytes (red cells) increases with PAD severity around the endothelium (blue cells) of microvessels less than 15 μm in diameter. The BM (grey) is thickened in the microvessels of PAD patients. As the abundance of αSMA^+ pericytes increases, the BM becomes thicker and the diameter of the BM annulus expands to accommodate more pericytes. However, the endothelial diameter does not expand.

The results of this study expand upon previous ultrastructural studies of BM thickening in PAD capillaries. Our results are in agreement with previous reports that BM thickness is increased around PAD microvessels,[171] particularly in CLI patients.[173] Baum and colleagues compared BM thickness across controls (n = 4), PAD patients with intermittent claudication (n = 4), and PAD patients with CLI (n = 10). Although BM thickness was significantly greater in PAD patients relative to controls, they did not observe differences between PAD cohorts.[171] The absence of a significant difference between PAD patients with claudication and CLI may reflect the methodology used to identify and quantify BM thickness or insufficient statistical power due to the limited cohort size. In the current study, we developed a methodology to produce highly reliable and reproducible identification and quantification of microvascular BM thickness and inner BM diameter. In comparing microvascular architecture across advancing stages of PAD severity, we observed qualitative and quantitative increases in BM thickness between controls, patients with claudication, and patients with CLI, which suggests that microvascular pathology is progressive in PAD.

Cross talk between pericytes and endothelial cells is likely critical in the process of microvascular remodeling. Studies have shown that the presence of both endothelial cells and pericytes are required for the formation of the BM. Pericytes are closely associated with endothelial cells and are ensheathed by a common basement membrane which is continuous around the microvessel.[363] Endothelial cells have the machinery to synthesize many of the BM components, however, pericytes are required for BM assembly and regulation of synthesis.[191,196,291,292] In PAD muscle, inflammation and hypoxia lead to endothelial cell injury and subsequently the activation of pericytes, which likely initiates the deleterious process of BM remodeling. Elaboration of cytokines from the atherosclerotic plaques bath the distal microvessels and may be the initiating cause of the pathological endothelial and pericyte responses seen in PAD microcirculation, which are

further worsened by the reperfusion/ischemia injury that arises with arterial stenosis. Microvascular remodeling likely begins with endothelial death and a preliminary regression of microvessels. The hypoxia produced by loss of microvessels may then drive the excessive growth response seen, particularly in the late phases of microvascular remodeling.[196,197,289,322,323] With chronic inflammation, ischemia, and injury, death of pericytes and endothelial cells becomes common and may induce repair paradigms, including angiogenesis, thus beginning a cycle of degeneration and regeneration.[55,69,290,297] In line with this putative mechanism, we observed that microvascular density is elevated in PAD muscles and increases with microvascular disease severity. Continuous damage and inflammation may lead to an advanced stage of vascular regeneration[170,271,298,299] that becomes exhausted in PAD muscles. As endothelial cells and pericytes perish, the BM remains intact and regenerating endothelial cells and pericytes synthesize a new inner layer of BM,[170] which likely results in the cumulative thickening of the microvascular BM and the increased prevalence of acellular microvessels observed in our analysis. Furthermore, during the proliferative stage of vascular remodeling, pericytes can detach from the endothelium and differentiate into myofibroblasts, leaving the denuded endothelium vulnerable to regression,[196] which subsequently propagates both fibrosis and additional deleterious microvascular remodeling. It is possible that PAD myopathy starts as an adaptation of the affected skeletal muscles to the low flow state and the abnormal metabolic, hemodynamic, and inflammatory milieu produced by the atherosclerotic obstruction of the main feeding arteries. However, over time the myopathy becomes independently pathogenic and self-perpetuating. In this sense, the myopathy of PAD appears to have substantial similarities to the myocardial remodeling seen in patients with chronic coronary artery disease and heart failure.

In acute muscle injury, pericytes coordinate a regenerative response by creating a favorable microenvironment for muscle repair. Deposition of ECM components, including microvascular BM, provides structural scaffolding to regenerating muscle and supports satellite cell migration and myogenesis.[294.] Thus, differential deposition of ECM components by perictyes may alter the microenvironment and deter myogenesis in favor of fibrosis. Furthermore, in the setting of chronic injury, pericytes can coordinate the development and possibly initiation of pathological fibrosis.[181,191] A novel finding of this study is that in PAD muscle, αSMA$^+$ pericyte expansion and expression of TGF-β1 is coupled with alterations of microvascular architecture and perivascular deposition of Collagen I and IV. Pericytes have been shown to overproduce ECM components including Collagen I and IV in response to TGF-β1 in brain and kidney.[197,296] Therefore, it is likely that in the skeletal muscle of patients with PAD, pericytes may directly contribute to microvessel thickening by depositing products to the microvascular BM.[191] Additionally, pericytes have been implicated as a major source of collagen producing myofibroblasts in several organs, including skeletal muscle, kidney, and liver, as well as in systemic sclerosis.[191,249,289,302,317-320]

Pericytes may differentiate and migrate from the microvessel as collagen-producing myofibroblasts,[69,181,364] further exacerbating both interstitial and perivascular fibrosis in PAD muscle. Myofibroblasts express αSMA, generate contractile force, remodel and deposit excessive ECM, and are directly linked to the extent of fibrosis.[191,243] In a model of cardiac fibrosis after acute myocardial infarction, analysis of the infarcted myocardium revealed that approximately 60% of myofibroblasts were derived from pericytes.[321] TGF-β1 signaling is likely critical in the differentiation of pericytes to myofibroblasts.[284] TGF-β1 is typically involved in pericyte and vessel maturation,[196] however, TGF-β1 can also stimulate differentiation and proliferation of both endothelial

cells and pericytes.[69] Thus, enhancement of TGF-β1 expression in PAD may initially arise as a pro-angiogenic signal. Resolution of ischemia becomes progressively limited as the arterial stenosis worsens, and the intensity and duration of TGF-β1 signaling in PAD may alter pericyte responses in favor of fibrosis by stimulating pericyte αSMA expression[54] and collagen production.[284] αSMA$^+$ pericyte production of TGF-β1 may also recruit and stimulate fibroblasts to deposit collagen or enhance accumulation of the ECM by inhibiting matrix proteases and ECM degradation.[296]

The microvascular remodeling observed in PAD is strikingly similar to that observed in Pulmonary Arterial Hypertension (PAH). PAH is characterized by an increased number of TGF-β1 -producing VSMC in the pulmonary microvessels,[54,314] and TGF-β1 has been found to enhance the differentiation potential of pulmonary pericytes into αSMA$^+$ VSMC-like cells. Moreover, increased pulmonary pericyte coverage and myofibroblast differentiation were observed in association with TGF-β1 and chronic hypoxia[314] and TGF-β1 pathway overactivation was linked to PAH progression.[54] Recently, our laboratory demonstrated that PAD patients across Fontaine stages had progressively greater expression of TGF-β1 by proliferative and synthetic VSMCs of microvessels with diameters between around 50-150 μm, which suggests that the severity of occlusive disease and resulting ischemia and ischemia/reperfusion induce proliferation and greater TGF-β1 expression by subendothelial VSMC.[67] Our new finding that αSMA$^+$ pericytes of the smallest vessels also proliferate and express increased levels of TGF-β1 that is significant in Stage II PAD but even worse in Stage IV PAD patients, suggests that chronically reduced blood flow is a critical factor in the progressive alterations of the microvascular architecture and physiology observed in PAD myopathy.

Previous reports have generated conflicting results on whether or not the number or proportion of αSMA$^+$ microvessels is increased in PAD patients relative to controls.[171,173]

In our study, we observed that microvessels in PAD muscle had greater expression of αSMA, and specifically, the abundance of αSMA^+ pericytes around vessels less than 15 μm increased with PAD stage severity. We observed that microvessels between 15 - 25 μm in diameter are inappropriately muscularized in PAD muscle, and that even smaller vessels had increased αSMA^+ pericyte coverage, which was mostly absent in control muscle. Pericytes play a crucial role in vascular homeostasis and participate in vascular development, stabilization, maturation, and remodeling.[54,187,188,365] In normal physiology, pericyte density and coverage correlate with microvessel maturation during angiogenesis,[54,187,188] endothelial barrier properties, and orthostatic blood pressure,[55,181,191-193] which supports pericyte involvement in the regulation of angiogenesis, microvascular barriers, and microvascular vasomotion. It is possible that the increase in αSMA^+ pericyte abundance is initially a compensatory response to diminished blood flow across stenotic arteries. In an animal model of PAD, microperfusion was assessed in parallel with increasing arterial stenosis. Interestingly, resting skeletal muscle blood flow was preserved in moderate stenosis, and only became limited in severe stenosis. With exercise, microvascular blood volume decreased more than blood flux rate in association with increasing stenosis severity.[110] Taken together, these data suggest that the early microvascular adaptation to decreased arterial flow is to reduce microvascular blood volume, particularly during exercise, which may reflect active de-recruitment of capillary circuits, possibly *via* αSMA^+ pericyte constriction at pre-capillary sphincters, as a means to preserve precapillary pressure and maintain blood flux through a subset of capillary beds.[110,115,116]

Collagenous investment of microvessels may result in loss of flexibility, hemodynamic dysfunction, and decreased local diffusion capacity for oxygen and nutrients, exacerbating the ischemic state experienced by the myofibers and other

components of PAD muscle.[171,366] Our data support prior reports that angiogenic responses can increase the number but unfortunately not the quality of microvessels in the ischemic tissues. The architectural changes observed in this study are in line with prior reports of microperfusion deficits in PAD patients. Several studies have observed a delayed time to peak microvascular blood flow in PAD patients relative to controls after exercise and post-occlusive reactive hyperemia.[99,102,108,109,133-136] During moderate contractile exercise, microvascular blood volume was slightly lower than controls, whereas microvascular blood velocity was substantially diminished in PAD patients.[144] The BM thickening of PAD microvessels observed in this study may directly contribute to the slowing microperfusion by increasing resistance across stiffening microvascular beds.

Pericyte damage or dysfunction may directly contribute to microvascular perfusion deficits with consequent ischemic tissue damage. Pericyte expression of αSMA has been shown to be greatly enhanced in response to chronic hypoxia.[54] Ischemia-reperfusion injury triggers oxidative stress in PAD muscle and likely contributes to pathological pericyte activity. Recent studies have shown that following traumatic brain injury, αSMA expression is increased in pericytes alongside pericyte-mediated reductions of vessel diameter and hypoperfusion.[209,326] Dysfunctional pericyte contractility has also been shown in response to ischemic events. In both cerebral stroke and MI models, ischemia evoked pericyte-mediated microvascular constriction. Subsequently, pericytes perished in rigor, irreversibly constricting capillaries, a finding which may account for the “no reflow” phenomenon, in which vasoconstriction and ischemia persist even after restoration of flow through occluded vessels.[213,214] It is likely that pericyte dysfunction contributes to PAD myopathy and pericyte-mediated microcirculatory occlusion leads to localized ischemic damage that may account for the spatial heterogeneity of microvascular blood flow[114] and damage observed in PAD muscle.

The results from the multivariable general linear model showed that the main predictor variable (Control, Stage II, Stage IV) was statistically significant for each of the response variables microvascular BM thickness ($P = 0.0005$), inner BM diameter ($P = 0.0048$), microvessel total diameter ($P < 0.0001$), Collagen I density ($P = 0.0265$), sum of αSMA^{+} pericyte area ($P = 0.0003$), and total Collagen abundance ($P < 0.0001$), and marginally significant for the response variable Collagen IV abundance ($P = 0.0561$). This has helped avoiding confounding, and has added confidence to our conclusions about the predictive value of main predictor variable, PAD grouping.

A limitation of this study is the relatively small number of patients analyzed. We interrogated the contribution of DM, family history, and renal insufficiency to microvascular pathology in our covariate analysis. Although we found no significant effects, the small number of patients per group limited the statistical power of the analysis. Microvessel thickening has been observed in the microvascular beds of several organs in patients with DM and patients with renal insufficiency but in the cohorts of patients analyzed in this study, BM thickening, inner BM diameter expansion, increasing sum of pericyte area, microvascular fibrosis, and myofibrosis did not differ remarkably between patients with and without DM or renal insufficiency, which suggests that PAD alone is sufficient to induce and propagate microvascular pathology. DM microangiopathy is fairly well characterized in several organs. Death of pericytes and, consequently, microvascular instability and decreased capillary density are hallmark features of diabetic microvascular complications and are well documented features of diabetic retinopathy. Our observations that microvascular density and sum of pericyte area are increased in PAD with and without DM patients suggests that the microangiopathy of PAD is different from, and likely dominant to the microangiopathy observed in DM. Additional studies are necessary to better characterize the contribution of insulin resistance and DM to PAD microvascular pathology.

In regards to the microvascular disease several questions remain. Future research needs to address whether the microcirculatory pathology is present in other tissues of the affected PAD legs like nerves, skin, bones, joints subcutaneous fat and the degree to which it may contribute to the manifestations of PAD, including the muscle dysfunction, the neuropathy of PAD, the development of ulcers and gangrene of the ischemic limbs and their failure to heal. Understanding the relationship between microvascular pathology and microperfusion offers a unique opportunity for development of non-invasive diagnostic assessment of PAD limbs and may have great utility in the assessment of therapeutic efficacy. Furthermore, non-invasive imaging modalities, such as contrast enhanced ultrasonography, could aid in understanding the functional alterations of the microvasculature of PAD limbs and help dissociate macro- from the micro- vascular disease. Further exploration of the pathogenetic mechanisms of microvascular disease may aid in the identification of patients at risk for progressing from Stage II to Stage III or IV PAD. Understanding PAD microvascular pathology may also offer opportunities for more individualized therapies, which may include ACE-inhibitors, anti-hypertensives, statins, and DM medications, and may aid in the identification of patients who are likely to have a favorable response after revascularization surgery.

Conclusions

PAD produces a myopathy in the legs of affected patients and the myopathy is characterized by myofiber degeneration and expansion of the extracellular matrix (fibrosis). The present study introduces microvascular disease as a central component of this myopathy. Microvascular disease is characterized by thickening of the basement membrane, proliferation of TGF-β1-producing αSMA^{+} pericytes and perivascular fibrosis

and is tightly connected to both the fibrosis and the myofiber degeneration of PAD myopathy.

Chapter III: Microperfusion Deficits in Patients with PAD

Introduction:

Microvascular changes are progressive in PAD myopathy and likely lead to compromises in microvascular perfusion. In chapter II we demonstrated that microvascular architectural changes are present in PAD myopathy. Microvascular BM thickness increases with advancing severity of PAD, and in advanced PAD the inner BM diameter is significantly increased, reflecting the accommodation of increased numbers of αSMA^+ pericytes and swollen endothelial cells within the microvascular basement membrane. αSMA is considered to be a marker of contractile ability. Although the capacity of pericytes to regulate microvascular perfusion remains largely unknown, some studies have demonstrated that αSMA^+ pericytes on pre-capillary arterioles can vasoconstrict and limit perfusion through capillary beds. Hypertrophy of both VSMC, which moderate arteriolar constriction, and pericytes around the normally non-muscular microvessels of PAD skeletal muscle suggests that PAD vasculature may have an increased potential to be in a vasoconstrictive state.

Previous studies utilizing Contrast Enhanced Ultrasonography (CEU) have demonstrated that there are indeed significant alterations of microvascular perfusion. Reduced flow reserve (FR), a ratio of microvascular blood flow at reperfusion after an ischemic stress to microvascular blood flow at rest, have been observed in PAD patients. Reductions of FR could reflect either limited capacity of microvascular beds to engage in longitudinal recruitment in response to ischemia or metabolic demand. Conversely, microvascular beds may be nearly at maximal flow capacity at baseline. Endothelial

dysfunction is a well characterized feature of PAD muscle, which taken together with the proliferation of αSMA^+ pericytes suggests that microvascular hemodynamic regulation may be dysfunctional. Microvascular perfusion deficits remain poorly characterized and the relationship of these perfusion deficits to structural microvascular features is unknown. In chapter III we will test the hypothesis that microvascular perfusion is related to microvascular architectural features in PAD patients with IC. We will demonstrate that the extent of hemodynamic restriction present in the large arteries contributes to, but does not determine, the severity of microvascular architectural and perfusion changes. We will demonstrate that the microvascular architectural alterations associated with microvascular density are different between patients with IC and CLI. Additionally, we will describe the relationship between microvascular architecture and microperfusion.

Methods

Human Subjects

The experimental protocol was approved by the University of Nebraska Medical Center and the Veterans Affairs Nebraska-Western Iowa Institutional Review Boards. All subjects gave informed consent.

Control Group

We recruited 14 control patients who were undergoing vascular operations for abdominal aortic aneurysm repair. Control patients led sedentary lifestyles and had no history of

PAD symptoms. Control patients had normal blood flow to their lower limbs as indicated by normal lower extremity pulses at examination and normal ABI at rest and after stress.

PAD Patient Recruitment

We recruited 40 patients with intermittent claudication (Fontaine Stage II) and 16 patients presenting with tissue loss (Fontaine Stage IV) who were undergoing lower extremity operations for symptomatic PAD.. Medical history, physical examination, decreased ankle brachial index (ABI< 0.9), and computerized or standard arteriography that revealed stenotic and/or occluded arteries supplying the lower extremity were evaluated to establish the diagnosis for each PAD patient. Stage II PAD patients presented with intermittent claudication, but no rest pain or tissue loss. Stage IV PAD patients presented with non-healing ulcers and/or gangrene. Patients with rest pain or tissue loss were excluded from CEU analysis.

Overview of Endpoints measured in PAD patients

All forty patients underwent measurement of Ankle Brachial Index at rest and after post-occlusive Reactive Hyperemia, and Contrast Enhanced Ultrasonography for measurement of calf muscle blood flow at rest and after post-occlusive Reactive Hyperemia. A subset (N=15) of the forty patients also underwent muscle biopsies of their medial gastrocnemius belly and the muscle sample was processed for measurement of parameters of the gastrocnemius architecture (**Figure 14**). The fifteen patients in this analysis are the same as those participating in the microvascular architectural analysis studies presented in Chapter II.

Figure 14: Overview of Endpoints Measured

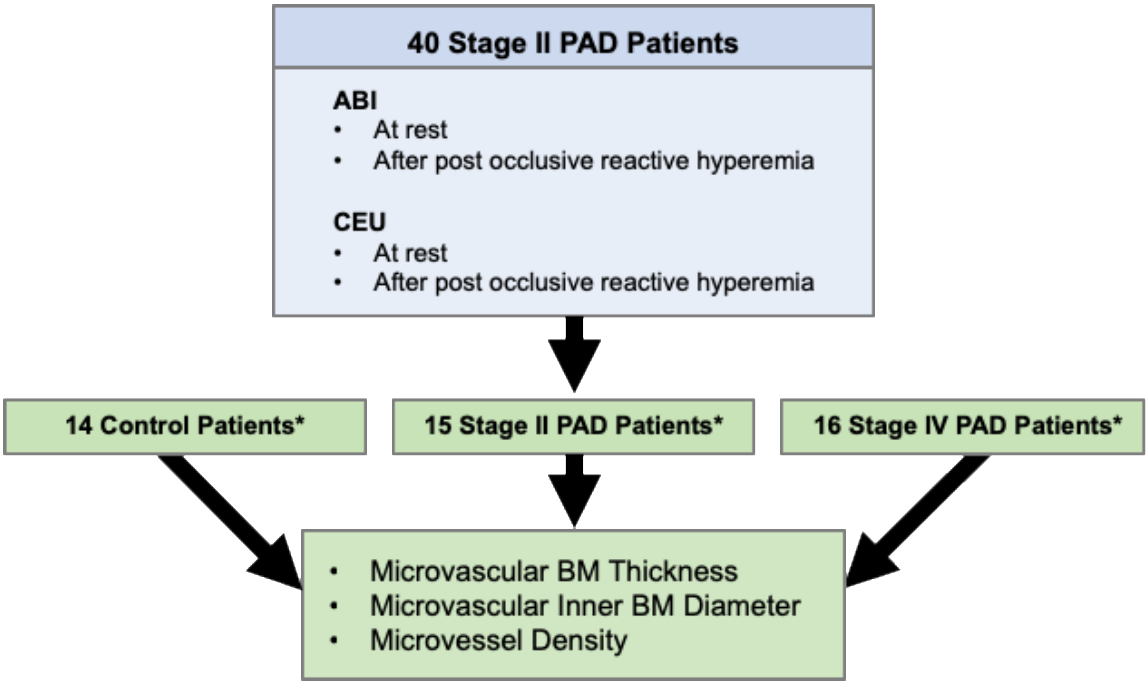

Figure 14: Overview of Endpoints Measured.
Forty Stage II PAD patients were recruited for this study and the ABI and CEU were collected at rest and during post-occlusive reactive hyperemia. A subset of these patients were evaluated for microvascular parameters. Microvessels from 14 controls, 15 Stage II PAD, and 16 Stage IV PAD patients were evaluated for microvascular BM thickness, inner BM diameter, and density.

Ankle Brachial Index and Reactive Hyperemia Assessment

ABI measurements were performed by a dedicated vascular laboratory technologist for all Stage II PAD patients. Systolic pressures were taken from the bilateral brachial, dorsalis pedis (DP), and posterior tibial (PT) arteries after a period of rest in the supine position. The maximum systolic pressure from the DP or PT was divided by the highest of the bilateral brachial systolic pressure. Following resting pressure measurements, a cuff occlusion of the superficial femoral artery was performed for five minutes at the level of the distal thigh. Occlusion was confirmed by absence of ipsilateral Doppler signal in the pedal arteries. After the cuff was released systolic pressure measurements, from the higher-pressure pedal artery at rest, were repeated every fifteen seconds until pressures returned to baseline. The ABI collected at 15 seconds after cuff release was collected and recorded as the post-occlusive reactive hyperemia ABI.

Contrast Enhanced Ultrasonography Acquisition

Continuous real time CEU perfusion imaging was performed using a phased-array transducer (S5-1, IE33; Philips Ultrasound, Andover, MA, USA) with a low mechanical index (0.19) triggered ultrasound contrast imaging with intermittent high mechanical index impulses. Definity ultrasound contrast (3%; 4ml/min) was continuously infused during the procedure. Patients were resting in a lateral recumbent position before and during the procedure. The ultrasound probe was placed on the lateral head of the gastrocnemius. Once a steady state of contrast infusion had been achieved, two minutes of baseline imaging of the lateral gastrocnemius and soleus was acquired. On completions of the resting image acquisition, a cuff was inflated around the distal thigh to 90 mmHg above the patient's systolic pressure to occlude superficial femoral artery flow and held for a 90

second period of ischemia. Reperfusion imaging began on the release of the cuff and ended after two minutes of post-occlusion imaging.

Contrast Enhanced Ultrasonography Quantification

Video intensity (VI) was measured for the whole acquired region of muscle. Sequential end-diastolic frames were obtained and imported into Image Pro Plus 8 software (Media Cybernetics, Warrendale, PA). The second frame post high mechanical index pulse was used as the background image, and was digitally subtracted from the subsequent pulse-interval images to remove large vessel signal and tissue artifacts. Time versus VI data were fit to the function:

$$y = A(1 - e^{-\beta t})$$

where y is the VI at pulsing interval t, A is the plateau value of VI that reflects microvascular blood volume, and β is the rate constant of microbubble replenishment reflecting red blood cell velocity, also known as the microvascular blood flux rate (**Figure 15**). Microvascular blood flow (MBF) was derived by the product of $A \times \beta$. Flow reserve was calculated as the ratio of reperfusion (hyperemic) MBF to resting MBF.

Figure 15: CEU Measurement Acquisition

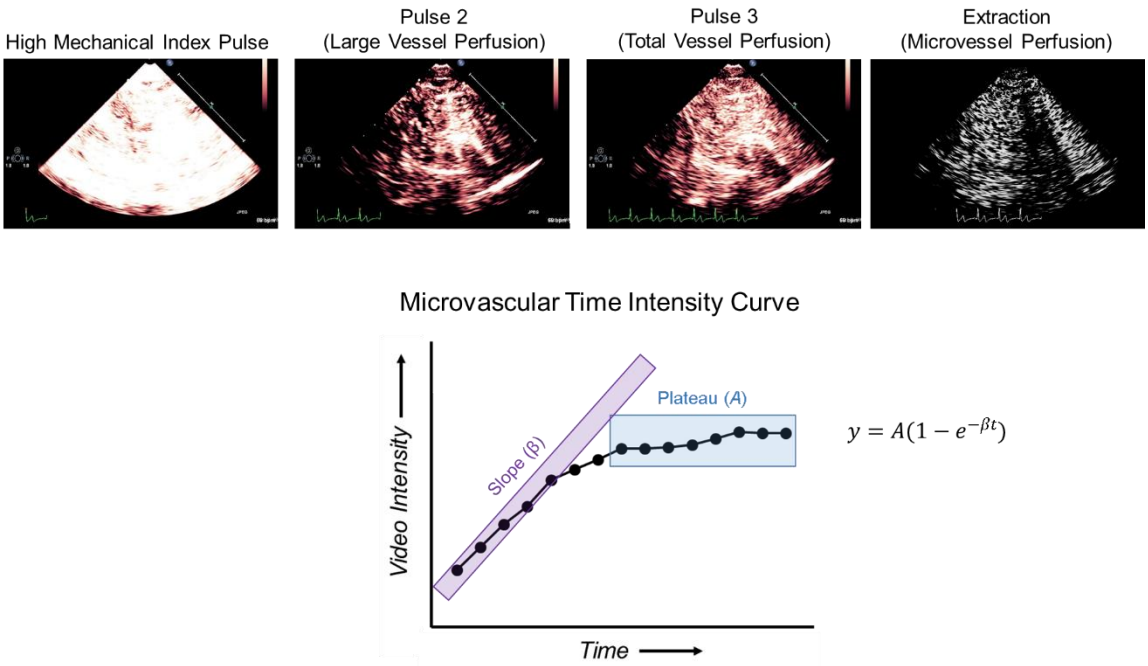

Figure 15: CEU Measurement Acquisition.
CEU images are collected during the diastolic phase of each heartbeat and represent the pulse interval. Microbubble contrast is continuously injected both at rest and during reactive hyperemia. A high mechanical index pulse destroys the microbubbles (inertial cavitation) in the imaging plane and during the subsequent pulses, new microbubbles arrive. During the initial pulses after inertial cavitation, microbubbles arrive in small vessels but very few microbubbles arrive into the microvasculature. The subsequent pulses visualize microbubbles in both small vessels and microvessels. By subtracting the initial pulse interval signal from the remaining pulse intervals, microvessel signal can be extracted and quantified. (Top panels) Time intensity curves are generated, and each measurement represents a pulse interval in the video sequence. The time intensity curve describes the kinetics of microbubble replenishment in the microvasculature after inertial cavitation. Time versus video intensity data are fit to the function $y = A(1 - e^{-\beta t})$ where the plateau value *A* estimates blood volume when contrast ingress and egress reaches a steady state and β approximates the red blood cell velocity, also known as blood flux. (Bottom panel) MBF can be calculated by the product of blood flux and volume ($A \bullet \beta$). Time intensity curves are generated for rest and reactive hyperemia, and can be used to determine the flow reserve (reperfusion MBF/resting MBF).

Biopsy

A subset (n = 15) of the 40 Stage II PAD patients underwent a biopsy of their medial gastrocnemius belly. Gastrocnemius samples weighing approximately 250 mg were obtained from the anteromedial aspect of the muscle belly, 10 cm distal to the tibial tuberosity. All biopsies were obtained with a 6 mm Bergstrom needle. Samples were immediately placed into cold methacarn and fixed for 48 hours. Specimens were transferred to cold 50% ethanol, and subsequently embedded in paraffin.

Microvascular Architecture Analysis, Microvascular Density, and Pericyte Abundance

Microvascular architecture, microvascular density, and pericyte abundance were assessed in a subset of Stage II PAD patients who underwent CEU evaluation (n=15) using the methodology described in detail in chapter II. Briefly, specimens were labeled with Collagen IV antibody and photomicrographs were collected using a 40x objective. Images were processed in Image Pro Plus software and transferred to a custom MatLab program for quantification of microvessel BM thickeness, inner BM diameter, and total microvessel diameter. Microvessels reaching a circularity criterion threshold and total diameter of <12μm were included in analysis. Approximately 50-250 microvessels were analyzed per biopsy specimen. Collagen IV labelled images were used, and partitions were created that yielded accurate vessel identification. The number of microvessels and total tissue area were determined. A ratio of microvessels per total tissue area was calculated to determine microvascular density per ROI, which were subsequently

averaged to generate a patient mean microvascular density. Specimens were labeled with Collagen IV, αSMA, and CD31 to identify and quantify αSMA^{+} pericytes.

Grey scale images were transferred into Image Pro® Plus software, and the abundance of αSMA^{+} pericytes within microvessels <15 μm in diameter was calculated as the product of event area by mean pixel intensity ($gsu \bullet \mu m^2$).

Statistical Analysis

All biological parameters were assessed for normality. Linear regression analysis was conducted. For normally distributed parameters we conducted parametric analysis using Pearson regression and reported R^2 values. Remaining parameters were assessed using non-parametric Spearman Rank correlations and reported Spearman R values. Covariate analysis was completed using multilinear regression. All statistical analyses were performed with NCSS 12 data analysis software using a 95% confidence level.

Results

Patient Demographics

The demographics of the control, Stage II and Stage IV patients assessed for microvascular architecture are presented in **Table 4**, and a summary of the age, ABI, and microvascular features are presented in **Table 6**. The demographics of the 40 patients evaluated in this chapter are presented in **Table 7.**

Table 6: ABI, Age, and Microvascular Characteristics Across Stages of PAD

	Control	Stage II PAD	Stage IV PAD	p – value *
Number of Subjects	14	15	16	
Microvascular BM Thickness	1.408 ± 0.025	1.577 ± 0.030	1.747 ± 0.060	> 0.00001
Microvascular Inner BM Diameter	3.243 ± 0.094	3.295 ± 0.064	3.972 ± 0.124	0.00007
Microvascular Total Diameter	6.058 ± 0.111	6.448 ± 0.112	7.466 ± 0.224	0.00001
Age	67.29 ± 1.34	64.27 ± 1.22	69.40 ± 1.01	0.203
Ankle Brachial Index	1.089 ± 0.027	0.604 ± 0.033	0.184 ± 0.058	>0.00001
Microvascular Density †	4.9 ± 0.2	5.8 ± 0.3	6.5 ± 0.5	0.03
αSMA⁺ Pericyte Abundance #	10210 ± 1311	23323 ± 1627	71484 ± 13259	>0.00001

Table 6: ABI, Age, and Microvascular Characteristics Across Stages of PAD
Gastrocnemius biopsy specimens were labeled with Collagen IV and microvascular architectural features were measured. Measurements were obtained for approximately 50 – 200 microvessels per each biopsy specimen. Measurements are presented as mean ± S.E.M.

* *P* values were calculated by Kruskall Wallis test

† number of microvessels per 10^3 μm^2

\# gsu • μm^2

Table 7: The Demographics of Stage II PAD Patients Included in the CEU and Biopsy Analysis

	CEU	Biopsy
Number of subjects	40	15
Mean age (years)	67.8 ± 1.1	64.3 ± 1.2
Ankle Brachial Index	0.61 ± 0.03	0.60 ± 0.03
Gender (male / female)	100 / 0	100 / 0
Smoking (never / current / former)	2.6 / 48.7 / 48.7	0 / 40 / 60
Coronary artery disease	25	20
Cerebrovascular disease	27.5	13.0
Obesity #	17.5	20
Dyslipidemia	67.5	53
Diabetes Mellitus	20	13
Chronic Obstructive Pulmonary Disease	27.5	20
Renal insufficiency †	0	0
Statins	82.5	80
Family history of cardiovascular disease	52.5	47
Hypertension	45	60

Table 7: The Demographics of Stage II PAD Patients Included in the CEU and Biopsy Analysis

Microvascular and macrovascular hemodynamics were characterized in a group of Stage II PAD patients. CEU was used to assess the microvascular hemodynamics in 40 patients, and a subset of 15 patients underwent biopsy analysis of microvascular features.

Note: Continuous variables are presented as mean ± S.E.M. All other variables are presented as percentages.

Body Mass Index > 30

† Creatinine clearance < 60 ml/min / 1.73 m^2

Microvascular Pathology is Associated with Macrovascular Disease

We investigated the relationship between macrovascular hemodynamic compromise and microvascular pathology. To assess hemodynamic compromise, we utilized ankle brachial index at rest (ABI) and after post-occlusive reactive hyperemia (RH). To quantitate microvascular pathology, we utilized histology-based microvascular architecture measurements, microvessel density, pericyte abundance, and CEU-based microperfusion parameters

ABI was assessed in control (n = 14), Stage II (n = 15) and Stage IV PAD(n = 16). ABI was progressively lower between control (1.089 $\pm$ 0.027) and Stage II PAD (0.604 $\pm$ 0.033; $p<0.0001$) and between Stage II PAD and Stage IV PAD (0.184 $\pm$ 0.058; $p = 0.001$)(**Figure 16A**). Microvascular density increased as ABI decreased ($R = -0.36$, $p = 0.02$)(**Figure 16B**). A strong linear relationship was observed between decreasing ABI and increasing αSMA^+ pericyte abundance ($R = -0.85$, $p = 0.0001$)(**Figure 16C**). An inverse linear relationship was present between ABI and microvascular architectural parameters, including BM thickness ($R = -0.66$, $p < 0.0001$), inner BM diameter ($R = -0.51$, $p = 0.0004$), and total microvessel diameter ($R = -0.63$, $p < 0.0001$) when data were pooled across control and stages of PAD (**Figure 16D-F**). This suggests that worsening macrovascular hemodynamic restriction increases the number of microvessels, although the quality of those microvessels worsens, and that advancing hemodynamic restriction is tightly linked to increasing αSMA^+ pericyte abundance.

Figure 16: Microvascular Basement Membrane Thickness Increases are Associated with Decreases in Ankle Brachial Index Across Stages of PAD.

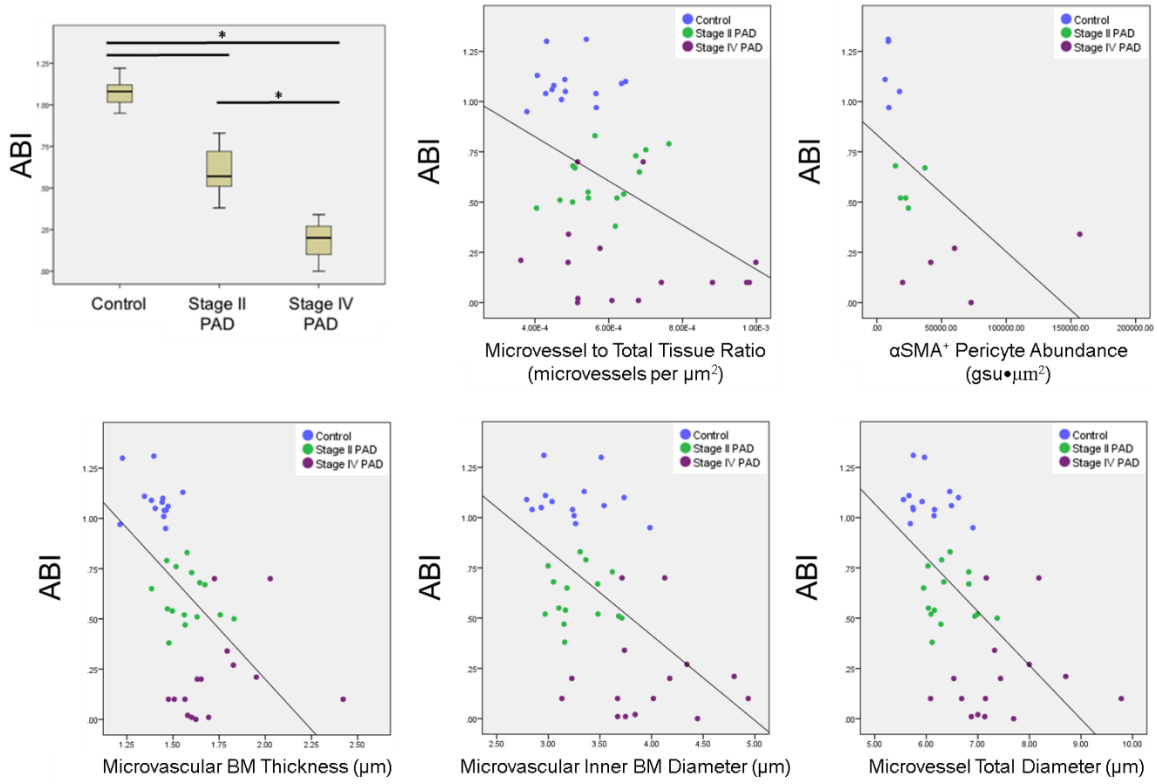

Figure 16: Microvascular Basement Membrane Thickness Increases are Associated with Decreases in Ankle Brachial Index Across Stages of PAD.

ABI was assessed in control (n = 14, blue), Stage II (n = 15, green) and Stage IV PAD(n = 16, purple). ABI was progressively lower between control (1.089), Stage II PAD (0.604), and Stage IV PAD (0.184)($p < 0.001$ between all groups)(A). There are inverse relationships between ABI and microvessel density($R = -0.36$, $p = 0.02$)(B), αSMA^+ pericyte abundance ($R = -0.85$, $p = 0.0001$)(C),microvascular BM thickness ($R = -0.66$, $p < 0.0001$)(D), inner BM diameter ($R = -0.51$, $p = 0.0004$)(E), and total microvessel diameter ($R = -0.63$, $p < 0.0001$)(F).

Microvascular BM Thickness is Strongly Linked to Microvascular Density in Stage II PAD Whereas Inner BM Diameter is Linked to Microvascular Density in Stage IV PAD

In Chapter II we demonstrated that microvascular density increases with PAD severity, which supports the presence of an angiogenic response in PAD muscle. Microvascular density may influence several parameters of microperfusion and may be related to microvascular architecture. Therefore, we assessed the relationship between the microvascular architecture and density across stages of PAD. When the patients from control and PAD groups were pooled, there was no association between microvessel density and microvascular BM thickness ($R = 0.02$, $p = 0.88$), inner BM diameter ($R = -0.08$, $p = 0.62$), and total diameter ($R = -0.05$, $p = 0.74$). However, when separated into control and PAD stages, associations between microvessel density and microvascular architecture were observed.

As microvessels became thicker, the microvascular density decreased in control ($R = -0.53$; $p = 0.05$) and Stage II PAD ($R = -0.63$; $p = 0.01$). Additionally, a trend between thicker microvascular BM and decreased microvessel density was observed in Stage IV PAD ($R = -0.43$; $p = 0.10$). Interestingly, BM thickness had a stronger association with microvascular density in Stage II PAD patients relative to control and Stage IV PAD (**Figure 17A**). Next, we assessed the relationship between microvessel density and inner BM diameter. We observed that as inner BM diameter expands, microvessel density decreases in Stage IV PAD patients ($R = -0.54$; $p = 0.03$). The relationship between increasing inner BM diameter and decreasing microvessel density was marginal in controls (($R = -0.46$; $p = 0.097$), and absent in Stage II PAD patients ($R = -0.20$, $p = 0.43$) (**Figure 17B**). Taken together, these data suggest that microvessel density is altered by PAD. In Stage II PAD, microvessel density changes in relation to BM thickness, whereas in Stage IV PAD, microvessel density changes in relation to inner BM diameter.

Figure 17: Microvascular Density is Differentially Associated with Microvascular BM Thickness and Inner BM Diameter Across Stages of PAD

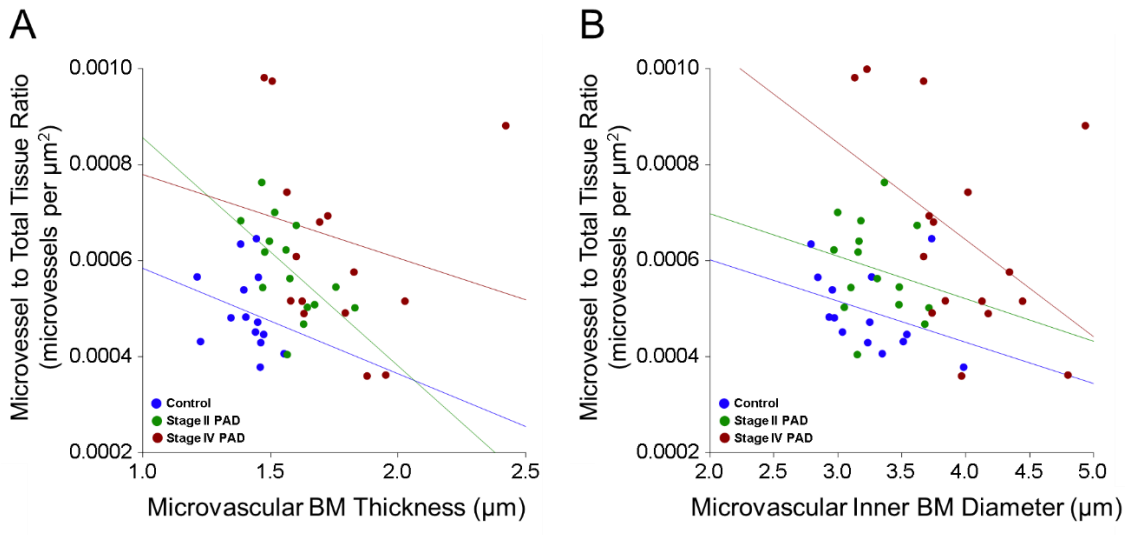

Figure 17: Microvascular Density is Differentially Associated with Microvascular BM Thickness and Inner BM Diameter Across Stages of PAD.

Microvascular density is progressively increased between control (n = 14, blue), Stage II PAD (n = 15, green), and Stage IV PAD (n = 16, purple). A stronger inverse relationship is present between microvascular density and BM thickness in Stage II PAD (R = -0. 63, p = 0.01) relative to control (R = -0.53, p = 0.05) and Stage IV PAD patients (R = -0.43, p = 0.097) (A). Conversely, the relationship between microvascular density and inner BM diameter is stronger in Stage IV PAD (R = -0.54, p = 0.032) relative to Stage II PAD (R = -0.20, p = 0.43) and control patients (R = - 0.46; p = 0.099)(B).

The Relationship Between Microperfusion and Macrovascular Hemodynamic Limitations in Stage II PAD Patients

Functional alterations within the microvascular beds may arise as a result of diminished arterial perfusion. Thus we next assessed the relationship between microperfusion (measured by CEU) and macrovascular hemodynamic limitations (measured by ABI and RH) in Stage II PAD patients (n = 40). The resting microvascular blood volume (2.14 ± 0.22 VIU) increased during reperfusion after ischemic stress (4.84 ± 0.50 VIU), whereas blood flux remained relatively constant between rest (0.43 ± 0.04 s^{-1}) and reperfusion (0.47 ± 0.05 s^{-1}). MBF was enhanced during reperfusion (1.85 ± 0.23 ml/min/g) relative to resting MBF (0.82 ± 0.09 ml/min/g), and FR was calculated (2.84 ± 0.39)(**Table 8**). An inverse relationship was observed between resting MBF and ABI (R = -0.34; R^2 = 0.12; p = 0.038)(**Figure 18A**). No linear association was observed between resting MBF and RH (p = 0.42)(**Figure 18C**). Additionally, no relationships were observed between reperfusion MBF and either ABI (p = 0.53) or RH (p = 0.57)(**Figure 18B,D**).

Table 8: Microvascular Perfusion in Stage II PAD Patients

	Resting	Reperfusion
Microvascular Blood Volume (*A*) *	2.14 ± 0.22	4.84 ± 0.50
Microvascular Blood Flux (β) †	0.43 ± 0.04	0.47 ± 0.05
Microvascular Blood Flow (*A* • β) #	0.82 ± 0.09	1.85 ± 0.23
Flow Reserve	2.84 ± 0.39	

Table 8: Microvascular Perfusion in Stage II PAD Patients

CEU parameters of microperfusion are summarized for rest and reperfusion after ischemic stress. Microvascular blood flow was calculated as the product of blood volume by flux. Flow reserve was calculated as the ratio of reperfusion MBF to resting MBF. n = 40 Stage II PAD patients.

Measurements are presented as mean ± S.E.M.

* Video Intensity Units (VIU)

† 1/seconds

\# ml/min/g

Figure 18: The Relationships Between MBF, ABI, and RH.

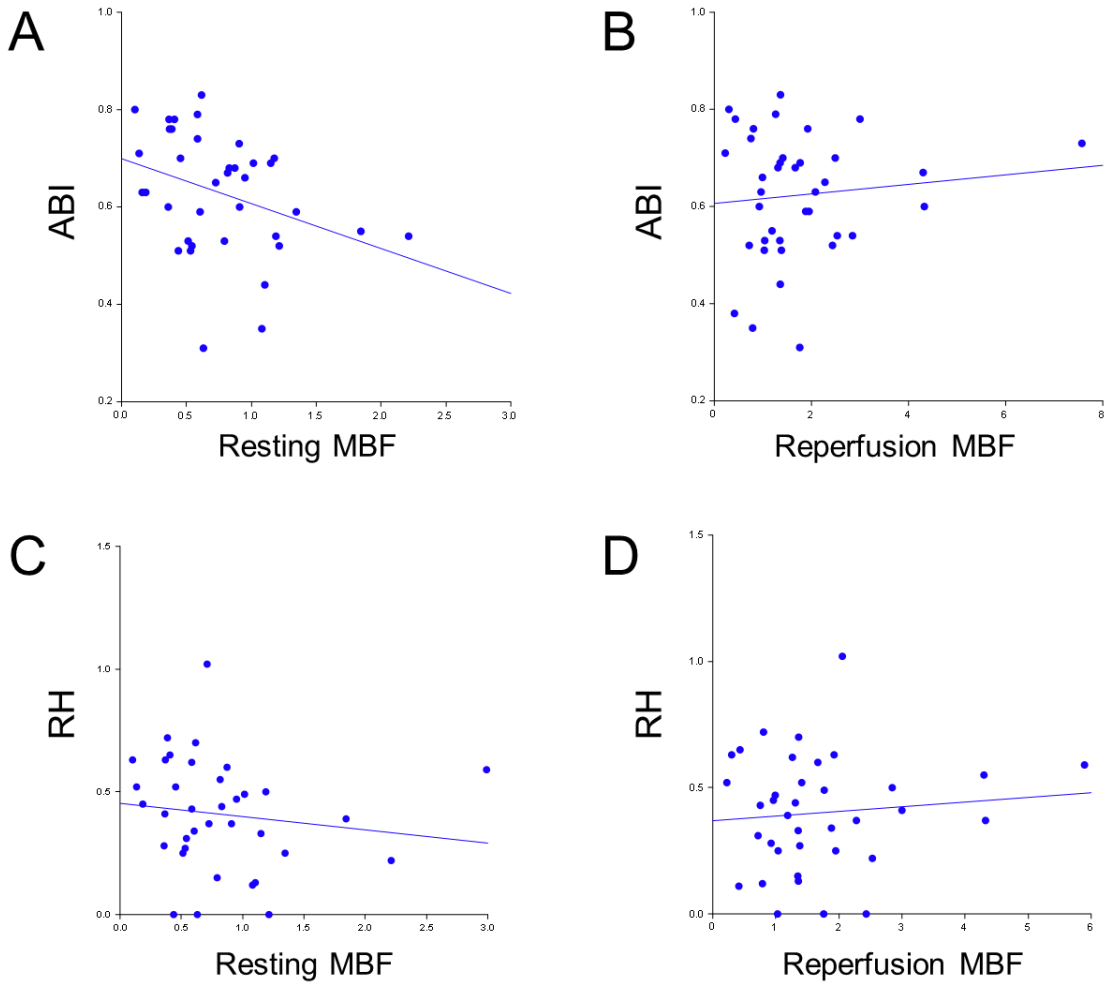

Figure 18: The Relationships Between MBF, ABI, and RH.
ABI and microperfusion were assessed at rest and during post-occlusive reactive hyperemia. As ABI decreases, resting MBF increases (n = 37; R = -0.34, p = 0.038)(A). A linear relationship is absent between ABI and reperfusion MBF (n = 38; R = 0.10, p = 0.53)(B). Both resting MBF (n = 36; R = -0.14, p = 0.42) and reperfusion MBF (n = 37, R = 0.10, p = 0.57) do not share a linear relationship with RH.

Microvascular Architecture Affects Microperfusion

ABI, but not RH, correlates with resting MBF (out of seven parameters of CEU), which suggests that macrovascular hemodynamic limitation does not fully account for the microperfusion in claudicating skeletal muscle. Thus, we assessed whether microvascular architecture (BM thickness, inner BM diameter) shared a relationship with microperfusion (as assessed by CEU). We determined that microvascular BM thickness may be associated with resting microvascular blood volume ($n = 11$, $R = -0.45$, $p = 0.16$) and resting MBF ($n = 11$, $R = -0.40$, $p = 0.23$), however these relationships did not reach statistical significance.

Review of ultrasound images revealed that qualitative differences in microperfusion were present with increasing inner BM diameter. We compared the resting microperfusion of patients with large versus small inner BM diameters and observed both lower microvascular perfusion and more areas devoid of flow in patients with greater inner BM diameters (bottom panels, **Figure 19**) relative to those with smaller inner BM diameters (top panels, **Figure 19**). Comparison of the time intensity curves demonstrated that both blood volume and flux may be diminished as inner BM diameter increases. Thus, we next assessed the relationship between inner BM diameter and resting MBF. Inner BM diameter had a strong linear correlation with microperfusion, both at rest and after ischemic stress, which was more robust than the relationships observed between BM thickness and microperfusion. As inner BM diameter increased, resting MBF decreased ($R = - 0.76$, $p = 0.006$) (**Figure 20**). Quantitative analysis revealed that the decrease in MBF may be moderated by a slowing of blood velocity through the microvascular beds, however the relationship between microvascular blood velocity and inner BM diameter was only a trend ($R = -0.44$, $p = 0.18$).

Figure 19: Microvascular Inner BM Diameter Influences Resting Microperfusion

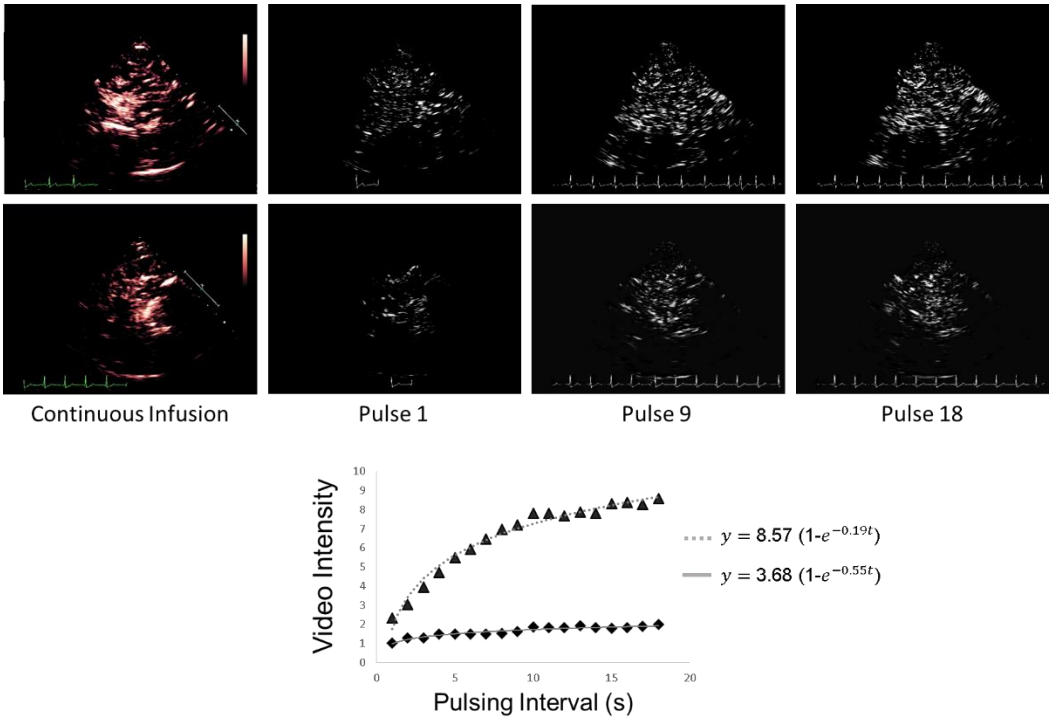

Figure 19: Microvascular Inner BM Diameter Influences Resting Microperfusion
Representative images of a patient with smaller (top panels) and larger (bottom panels) microvascular inner BM diameters. Patients are given a continuous infusion of Definity ultrasound contrast. Baseline images are acquired immediately after a high mechanical index pulse (continuous infusion) and are subsequently subtracted from the remaining frames to remove both tissue artifact and large vessel signals. Microvascular images are presented from the beginning (pulse 1), middle (pulse 9), and end (pulse 18) of the imaging interval. Greater microvascular perfusion is present in the patient with smaller inner BM diameters than the patient with larger inner BM diameters. Additionally, the patient with the larger inner BM diameters has more areas that do not receive microvascular perfusion. The corresponding time intensity curves are presented for the patient with smaller (triangles) and greater (diamonds) inner BM diameters.

Figure 20: Resting Microvascular Blood Flow is Strongly Associated with Microvascular Inner BM Diameter in PAD Gastrocnemius

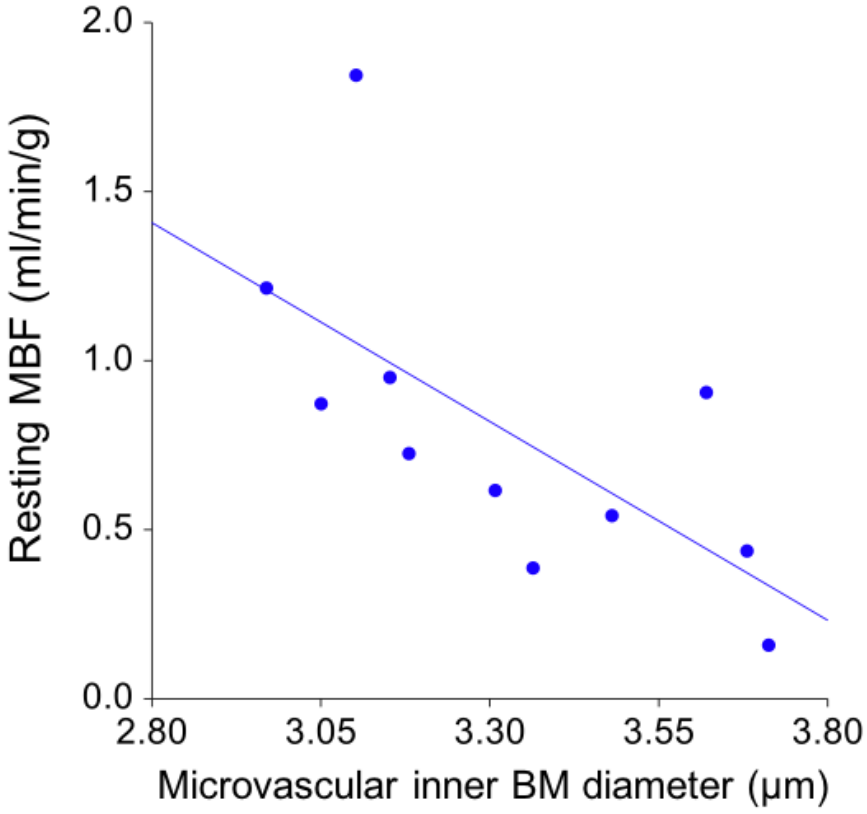

Figure 20: Microvascular Blood Flow at Rest is Strongly Associated with Microvascular Inner BM Diameter in PAD Gastrocnemius.
In stage II PAD patients (n = 11), microvascular inner BM diameter has an inverse linear relationship with resting MBF (Spearman R = -0.76, p = 0.006).

A strong positive linear association was found between inner BM diameter and RBC velocity (blood flux) during reperfusion (R = 0.7818; p =0.005) (**Figure 21A**). A trend emerged between increasing inner BM diameter and decreasing microvascular blood volume (R = -0.5091, p = 0.11) (**Figure 21B**). Although blood flux and volume appeared to be related to inner BM diameter, the reperfusion MBF was not (**Figure 21C**). Taken together, these data suggest that with increasing inner BM diameter, blood travels more rapidly through the microvascular beds at the expense of decreased microvascular blood volume in response to ischemic stress. Additionally, we observed that increases in microvascular inner BM diameter were associated with increases in FR (R = 0.65; p = 0.03) (**Figure 21D**).

Figure 21: The Relationship of Microvascular Inner BM Diameter and Microperfusion After an Ischemic Stress.

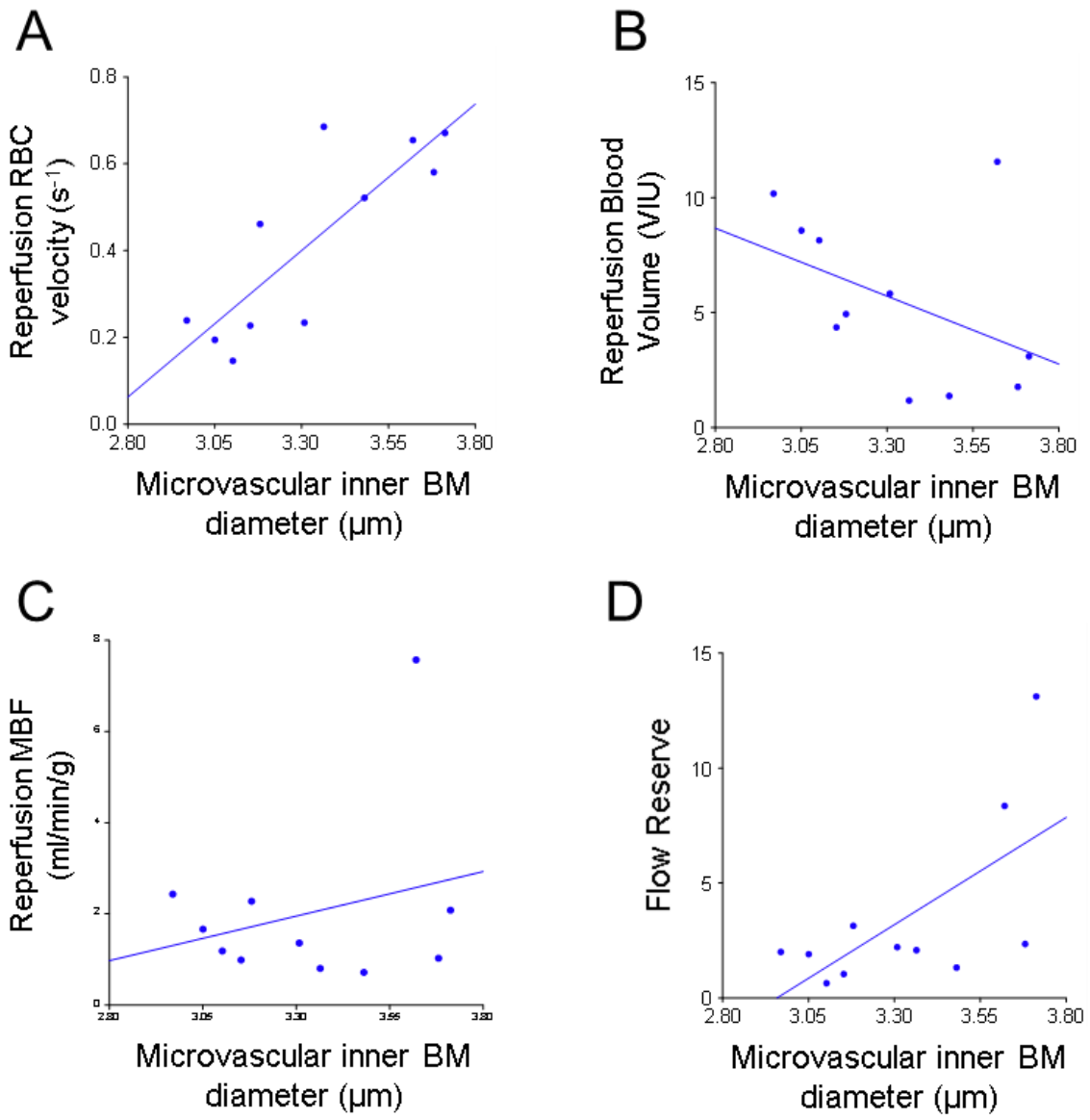

Figure 21: The Relationship of Microvascular Inner BM Diameter and Microperfusion After an Ischemic Stress.

In stage II patients (n = 11), microvascular inner BM diameter is positively correlated with RBC velocity during reperfusion (R = 0.78; p = 0.005) (A). An emerging negative trend between inner BM diameter and reperfusion blood volume was present (R = -0.51; p = 0.11) (B). Reperfusion microvascular blood flow (MBF), the product of volume by velocity, was not linearly related to microvascular inner BM diameter (R = 0.1364; p = 0.68) (C). Microvascular inner BM diameter was positively associated with flow reserve (R = 0.65; p = 0.03) (D).

Discussion

PAD begins with the atherosclerotic narrowing of peripheral large caliber arteries, including arteries supplying the legs (macrovascular disease). Increasing macrovascular atherosclerosis produces supply to demand limitations, particularly during exercise. Distal to the stenosis, our group and others have shown that vascular remodeling occurs throughout the vascular tree. Our laboratory has published the findings that microvascular remodeling occurs in PAD microvessels between 50 – 150 μm in diameter,[67] and include hypertrophy and hyperplasia of the VSMC of arterioles and perivascular collagen deposition. In Chapter II we have shown that the microvascular architecture of the terminal microvessels is also altered, and progressively worsens with PAD severity.

Arterial flow limitations are fairly well characterized in PAD, however, the structural and functional changes of the microcirculation to increasing hemodynamic restrictions remain poorly characterized. In this study we have shown that microvascular pathology worsens with decreasing ABI. We demonstrated that as ABI declines, microvessel BM thickness, inner BM diameter, and total diameter increase. Additionally, we have shown that microvessel density and αSMA^{+} pericyte abundance are increased with decreasing ABI. We have demonstrated that the presence of PAD affects capillary density in relation to microvascular structure and that Stage II PAD microvessel density changes in relation to BM thickness, whereas microvessel density changes in relation to inner BM diameter in Stage IV PAD. We have shown that resting ABI, but not reactive hyperemia ABI, is associated with resting MBF, and that reactive hyperemia MBF is not associated with ABI during rest or reactive hyperemia. Importantly, we have shown that microvascular architecture, particularly inner BM diameter, is associated with microperfusion in PAD patients. We have demonstrated that as inner BM diameter increases, resting MBF

decreases and that during reactive hyperemia, larger inner BM diameters are associated with increased blood flux and greater flow reserve.

In this study we shown that increasing arterial hemodynamic restrictions are associated with microvascular pathology. As the ABI declined, BM thickness, inner BM diameter, total diameter, microvessel density, and αSMA^+ pericyte abundance increased. Alterations of microvascular structure, number, and function may contribute to a compensatory mechanism to maintain microvascular perfusion pressure through PAD legs. We observed a strong relationship between increasing αSMA^+ pericyte abundance and declining ABI. αSMA^+ pericytes are likely proliferative and vasoconstrictive in PAD muscle. Enhanced vasoconstriction of pre-capillary sphincters by αSMA^+ pericytes may reflect a compensatory mechanism for pre-capillary pressure correction that leads to a reduction in distal resistance, increase in blood flux, and maximization of blood distribution across hypo-perfused tissues.[117] In support of this, we observed that as the inner BM diameter increased (likely reflecting the accommodation of αSMA^+ pericytes), the blood flux during reactive hyperemia increased.

Interestingly, there appeared to be a trade-off between increasing blood flux and decreasing blood volume during reperfusion, which suggests that less surface area is being perfused, thus it is possible that select terminal microvascular beds may be bypassed during whole leg ischemia. As a result, microdomains of severe ischemia may develop, especially in regions with thickened microvessels, and may account for the spatial heterogeneity of MBF distribution in PAD muscle that has been observed in this study and others.[114] Importantly, we also observed that as inner BM diameters increased in Stage II PAD patients, the resting MBF declined to very low levels, which suggests that as microvascular disease advances, microperfusion of PAD muscle worsens not only during ischemia, but also at rest.

A novel finding of our study was that macrovascular disease both at rest and during reactive hyperemia may have a rather small contribution to microperfusion in Stage II PAD muscles and that microvascular disease has a dominant effect on CEU-based parameters. Rest ABI, but not reactive hyperemia ABI, only correlated with resting MBF (out of the seven CEU parameters assessed), which suggests that macrovascular hemodynamic limitation does not account for the microperfusion defects in claudicating skeletal muscle. Paradoxically, we observed that as ABI declines, resting MBF increases. It is possible that increased MBF reflects increased microvessel density, or potentially increased vasodilation of the microcirculation at rest.

Our findings provide further evidence that microvascular disease imposes limitations on microperfusion, both at rest and during reactive hyperemia in claudicating muscle. We have demonstrated that a strong relationship exists between expanding inner BM diameter and diminishing resting MBF. We have also shown that increases in inner BM diameter are strongly associated with increased blood flux, possibly at the expense of blood volume, during reactive hyperemia. Taken together, these data support that microvascular disease (relative to macrovascular disease) is the dominant component of microperfusion limitations in claudicating muscle.

A novel finding of our study was that microvascular density is altered by PAD, and is associated with microvascular architecture. Interestingly, we observed differing relationships between microvessel density and architectural parameters between Stage II and Stage IV PAD patients. In Stage II PAD muscles, thickening BM appears to be the dominant factor in microvessel density. This suggests that as microvessels become thicker in claudicating muscle, either fewer microvessels are produced or conversely, more microvessel damage, cellular death, and consequently microvessel regression occurs. In Stage IV PAD muscles, expansion of the inner BM diameter was the dominant factor in microvessel density. The microvessels are substantially thickened in Stage IV

muscle, and additional thickening may have a relatively smaller contribution to microvessel density than observed in Stage II PAD muscle. In Chapter II we demonstrated that the abundance of αSMA^+ pericytes is substantially increased within the microvessels of Stage IV PAD muscles, and that the expansion of the inner BM diameter likely represents accommodation of more pericytes within the microvascular BM. It is possible that these αSMA^+ pericytes differentiate into myofibroblasts and subsequently migrate into the interstitial space. As a result, pericyte loss may leave the endothelium vulnerable to regression and fewer pericytes may remain to promote microvessel repair, which may account for the relationship observed between increasing inner BM diameter and decreasing microvessel density in Stage IV PAD patients.

Our findings support and expand prior studies that assessed CEU-based microperfusion in PAD patients. Several studies have observed a delayed time to peak intensity (TTP) in PAD patients relative to controls after exercise and post-occlusive reactive hyperemia.[99,102,108,109,133-136] Collagenous investment of microvessels may result in loss of flexibility, which may enhance red blood cell shear stress and vascular resistance within the capillaries, ultimately slowing the rate of blood flow through the microcirculation. We have shown that microvascular BM thickening increases between Stage II and Stage IV PAD muscle. Others have shown that as the severity of PAD increases, the TTP becomes further prolonged.[109] Moreover, Duerschmied and colleagues demonstrated that blood traversed the muscle more rapidly in the controls compared to PAD, with the greatest delays in CEU contrast transit time arising within the microvascular compartment of PAD patients,[136] which supports that worsening microvascular disease, including thickened microvascular BM, may contribute to the delayed transit across the microvascular bed.

In the current study we observed slightly larger post-occlusive flow reserves in PAD patients than previously reported.[103] Substantial variation in flow reserve has been

observed in relatively similar cohorts from both control and PAD patients,[114] which suggests that skeletal muscle flow reserve may have limited clinical utility, particularly in PAD muscle. When resting MBF values are low, small absolute differences in reperfusion flow can create deceptively large flow reserves.[114] Our findings that the patients with highest inner BM diameter had the lowest resting MBF and highest flow reserves are in agreement with prior studies that higher flow reserves may not indicate better microcirculatory health and therefore may have limited utility in determining PAD severity.[114]

There are limitations to our study. We did not have an age-matched control group for comparison. Future studies are necessary to assess the contribution of microvascular structure and pericyte coverage to normal microcirculatory physiology. Our study did not assess the extent of collateralization present, which may have an impact on microvascular disease and microperfusion. Prior studies in PAD muscle have shown that "poorly" collateralized limbs had prolonged TTP, however collateralization did not correspond to ABI,[109] which suggests that poor collateralization may accelerate microvascular disease progression. Thus, the contribution of collateral flow to microvascular disease is of particular interest for future study. Additionally, the modest number of patients included in this study limited our ability to assess confounding variables in our analysis of microperfusion. Microperfusion deficits in PAD may be exaggerated in DM.[136] Likewise, smokers experience a complex alteration in regulation of microperfusion.[137] Thus, additional studies are merited to determine the contribution of smoking status (never, former, current) on PAD microcirculatory performance in patients with and without diabetes. Alterations of PAD microcirculatory performance have also been observed during exercise and may be central to the walking limitations observed in PAD. Studies assessing the relationship between walking performance, microvascular architecture, and microperfusion are of high interest, and may yield novel treatment targets and strategies.

Conclusions

Increased arterial hemodynamic limitations (macrovascular disease) are associated with worsening microvascular disease, which is characterized by increasing microvascular BM thickness, inner BM diameter, total microvessel diameter, αSMA^{+} pericyte abundance, and microvessel density. Microvascular disease may have a dominant role relative to macrovascular disease in imposing microperfusion limitations in the muscles of PAD patients with claudication.

Chapter IV: Microvascular Architectural Features Are Associated With PAD Patient Walking Performance

Introduction

In chapter II we demonstrated that microvascular architectural changes are progressive across advancing stages of PAD. Microvascular BM thickness increases with increasing PAD stage and inner BM diameter is significantly increased in advanced disease. Expansion of the microvascular collagen ring likely reflects the increased presence of αSMA^+ pericytes, a subset of which express TGF-β1. The phenotypic change and proliferation of these pericytes suggests that pericytes are instrumental in orchestrating fibrosis, and additionally they may contribute to the microperfusion deficits present in PAD limbs.

In chapter III we described the relationship between macrovascular occlusion and microperfusion. We also determined that microvascular architecture, especially inner BM diameter, is linked to microperfusion both at rest and after occlusive hyperemia (ischemic stress) in patients with IC. Perfusion limitations caused by atheroscelerotic stenosis and narrowing of arteries supplying skeletal muscle have long been considered to be the major contributor to patient ambulation limitations. Our work and the work of others supports that microperfusion deficits may have a substantial contribution to the declining walking performance in PAD patients. Inefficient delivery of oxygen and nutrients to hypoxic tissues and removal of toxic metabolites could exacerbate oxidative damage to myocytes, subsequently compromising myocyte performance and consequently the patient's walking performance. However, morphological alterations of the microvasculature and their relationship to myocyte morphology, muscle force generation, and patient walking

limitations remain unknown. We hypothesize that alterations in the microvascular architecture of PAD patients with IC are associated with oxygen delivery deficits and are related to both qualitative and quantitative metrics of walking performance. We will demonstrate that worsening microvascular architecture accelerates the decline of oxygenation within PAD gastrocnemius. The relationship of microvascular architecture and the patient's perception of walking ability, as assessed by the WIQ, will be determined. We will also demonstrate that microvascular architectural features are associated with onset of claudication pain as well as the maximal duration of walking.

Methods

Human Subjects

The experimental protocol was approved by the University of Nebraska Medical Center and the Veterans Affairs Nebraska-Western Iowa Institutional Review Boards. All subjects gave informed consent.

PAD Patient Recruitment and Biopsy Preparation

We recruited 15 patients with intermittent claudication (Fontaine Stage II). Medical history, physical examination, decreased ankle brachial index (ABI< 0.9), and computerized or standard arteriography that revealed stenotic and/or occluded arteries supplying the lower extremity were evaluated to establish the diagnosis for each PAD patient. Patients with rest pain or tissue loss were excluded from CEU analysis. Biopsies of the gastrocnemius were acquired and prepared as described in chapters II and III.

Microvascular Architecture Analysis

Microvascular architecture was assessed in patients with IC who underwent evaluation for walking performance, which included claudication onset time (COT), peak walking time (PWT), and the scores collected from the Walking Impairment Questionnaire (WIQ). Microvascular architecture analysis was completed using the methodology described in detail in Chapter II. Briefly, specimens were labeled with Collagen IV antibody and photomicrographs were collected using a 40x objective. Images were processed in Image Pro Plus software and transferred to a custom MatLab program for quantification of microvessel BM thickness, inner BM diameter, and total microvessel diameter. Microvessels reaching a circularity criterion threshold and total diameter of <12μm were included in analysis. Approximately 50-250 microvessels were analyzed per biopsy specimen.

Near Infrared Spectroscopy

Near Infrared Spectroscopy (NIRS) measurements were taken with a wireless, continuous-wave, MOXY near-infrared spectrophotometer (Fortiori Design LLC, Hutchinson, MN) in 13 Stage II PAD patients. This device noninvasively measures oxygenated and deoxygenated heme-containing molecules (hemoglobin + myoglobin) in a target tissue. Tissue oxygen saturation (StO_2) represents the percentage of heme-containing molecules that are oxygen-bound. Muscle StO_2 measurements were relayed wirelessly in real time using the software PeriPedal (PeriPedal, Napoleon, IN). A MOXY NIRS probe was placed over the gastrocnemius bilaterally. Seated baseline measurements were taken for a minimum of three minutes or until StO_2 signal stabilized,

whichever was longer. Measurements were continuously captured during an exercise interval. Minimum StO_2 values achieved were also documented, as well as the time required to reach the minimum StO_2. In addition, specific StO_2 measurements were collected during exercise and were recorded for COT and PWT.

Claudication Onset Time and Peak Walking Time

Thirteen Stage II PAD subjects completed a Gardner treadmill walking test.[367] Subjects walked on a dynamic gait and pressure analysis treadmill (FDMT SciFit AC5000M, Noraxon USA, Inc., Scottsdale, AZ) which collects synchronized pressure measurements allowing for gait analysis and calculation of steps taken during exercise. Subjects initiated exercise at 2.0 miles per hour at 0.0% incline. With each subsequent two-minute stage, the treadmill incline was increased 2.0% to a maximum of 12.0%. Time of initial symptoms (COT) and time at which claudication symptoms were prohibitive to further walking (PWT) were recorded.

Walking Impairment Questionnaire

The WIQ has been validated in patients with IC and is qualitative physical function quality of life survey. Fourteen Stage II PAD patients completed the questionnaire. We utilized three of four subscales in this study (distance, walking speed, and stair climbing). The subscale for pain was not analyzed in this study. The WIQ is scored on a scale from 0 to 100, with lower scores representing greater functional limitations within that category.[330,332]

Statistical Analysis

All biological parameters were assessed for normality. Linear regression analysis was conducted. For normally distributed parameters we conducted parametric analysis using Pearson regression and reported R^2 values. Remaining parameters were assessed using non-parametric Spearman Rank correlations and reported Spearman R values. All statistical analyses were performed with NCSS 12 data analysis software using a 95% confidence level.

Results

Patient Demographics

Patient demographics are included in **Table 9** and include mean ABI, age, microvascular architecture measurements, COT, and PWT. For additional demographic details, please review the Stage II PAD group described **Table 4.**

Table 9: Stage II PAD Vascular Characteristics and Walking Performance

Stage II PAD	
Number of subjects	15
Ankle Brachial Index	0.61 ± 0.03
Microvascular BM thickness (μm)	1.577 ± 0.030
Microvascular inner BM diameter (μm)	3.295 ± 0.064
Microvessel total diameter (μm)	6.448 ± 0.112
Claudication onset time (s)	210.5 ± 35.4
Peak Walking Time (s)	471.0 ± 61.1

Table 9: Stage II PAD Vascular Characteristics and Walking Performance
Macrovascular (ABI) and microvascular (microvascular architecture) features and quantitative measures of walking performance (COT and PWT) are summarized. Variables are presented as mean ± S.E.M.

The Rate Decline in Oxygen Saturation During Exercise in PAD Gastrocnemius is Related to the Muscle's Microvascular Architecture

Previous work from our group has demonstrated that Stage II PAD patients exhibit distinct calf muscle NIRS profiles during exercise characterized by rapid StO_2 decline, substantial hypoxia throughout exercise, and slowed recovery to baseline StO_2 after exercise. NIRS measurements were collected during a session of graded treadmill walking (Gardner test). StO_2 was measured at rest and after 60 seconds of exercise. Additionally we measured the time period between walking onset and the point at which muscle SpO_2 reached a minimum. No linear relationships were found between resting or post occlusive ABI and StO_2 at rest, after 60 seconds of exercise, and the time interval to minimum StO_2. This suggests that arterial hemodynamic restriction is not the dominant factor determining muscle oxygen saturation in PAD legs. To determine whether limitations in muscle oxygenation were related to microvascular architecture we examined muscle oxygen saturation by NIRS in Stage II PAD patients. As BM thickness increased, the time to minimum muscle SpO_2 decreased, however this relationship was marginally significant ($n = 13$, $R = -0.49$, $p = 0.09$). A negative linear relationship was present between microvascular inner BM diameter and the time to minimum muscle SpO_2 ($n = 13$; $R = -0.58$, $R^2 = 0.34$; $p = 0.04$) (**Figure 22**). These data suggest that muscle oxygen tension reaches its minimum more rapidly with increasing microvascular pathology, and supports our previous findings that microvascular pathology worsens microperfusion deficits.

Figure 22: Microvascular Architecture Is Associated with Muscle Oxygenation

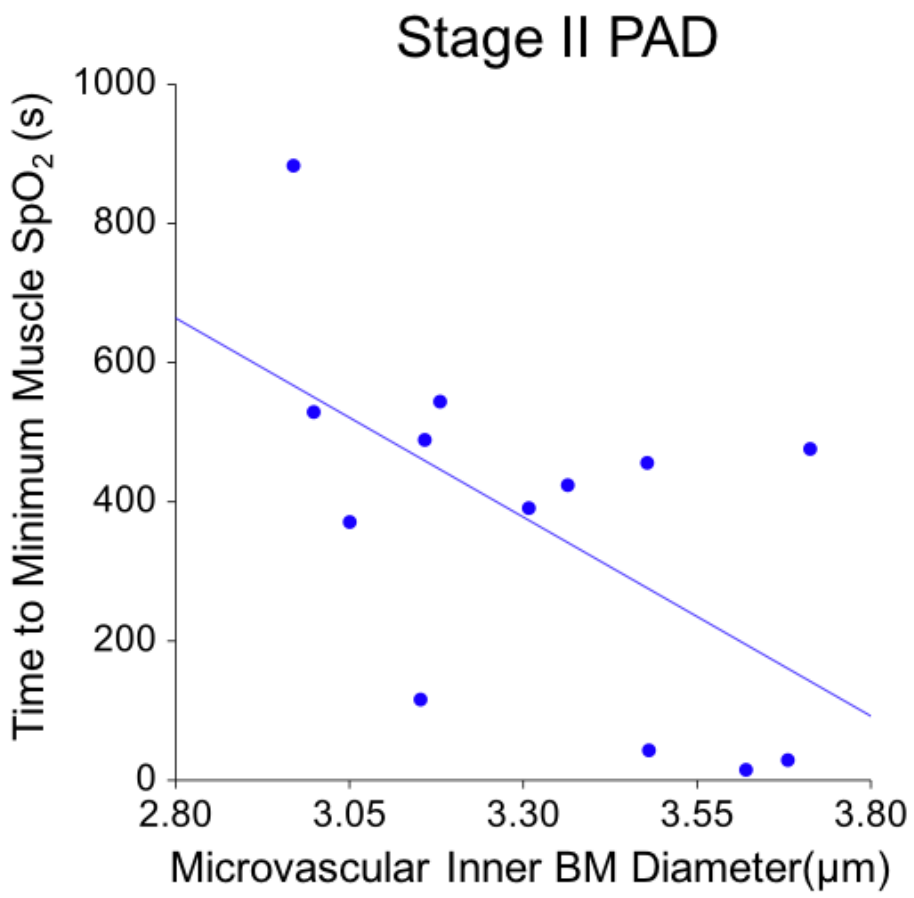

Figure 22: Microvascular Architecture is Associated with Muscle Oxygenation. A negative linear relationship exists between microvascular inner BM diameter and the time to minimum muscle SpO_2 ($n = 13$; $R = -0.58$, $R^2 = 0.34$; $p = 0.04$).

Microvascular Pathology is Associated with Patient Perception of Walking Limitations

The relationship of microvascular architectural features to both muscle oxygenation and microperfusion suggests that microvascular pathology may influence PAD patient walking performance. We explored the relationship of microvascular BM thickness and inner BM diameter with a subset of WIQ fields (walking distance, walking speed, and stair climbing) to assess whether microvascular pathology is associated with patient reported walking performance. WIQ-1 (pain) is a categorical variable and could not be assessed by linear regression methods, thus WIQ-1 was excluded from the current analysis. As BM thickness increases, patient self-reported walking performance decreases (**Figure 23**). Patients tended to report walking shorter distances as BM became thicker (n = 14; R = -0.41; p = 0.14)(**Figure 23A**). There was inverse relationship between BM thickness and patient's perception of walking speed (n = 14; R = -0.54; p = 0.05)(**Figure 23B**) and stair climbing ability (n = 14; R = -0.57; p = 0.03)(**Figure 23C**). Interestingly, the relationships between patient's perception of walking ability and inner BM diameter were stronger than those found for BM thickness (**Figure 24**). As inner BM diameter increased, patients reported walking shorter distances (n=14; R^2 = 0.31; p = 0.04)(**Figure 24A**), at slower speeds (n = 14; R^2 = 0.34; p = 0.03) (**Figure 24B**), and greater difficulty in climbing stairs (n = 14; R^2 = 0.34; p = 0.03) (**Figure 24C**).

Figure 23: Qualitative Measures of Walking Performance in PAD are Associated with Microvascular Thickness in Stage II PAD Patients

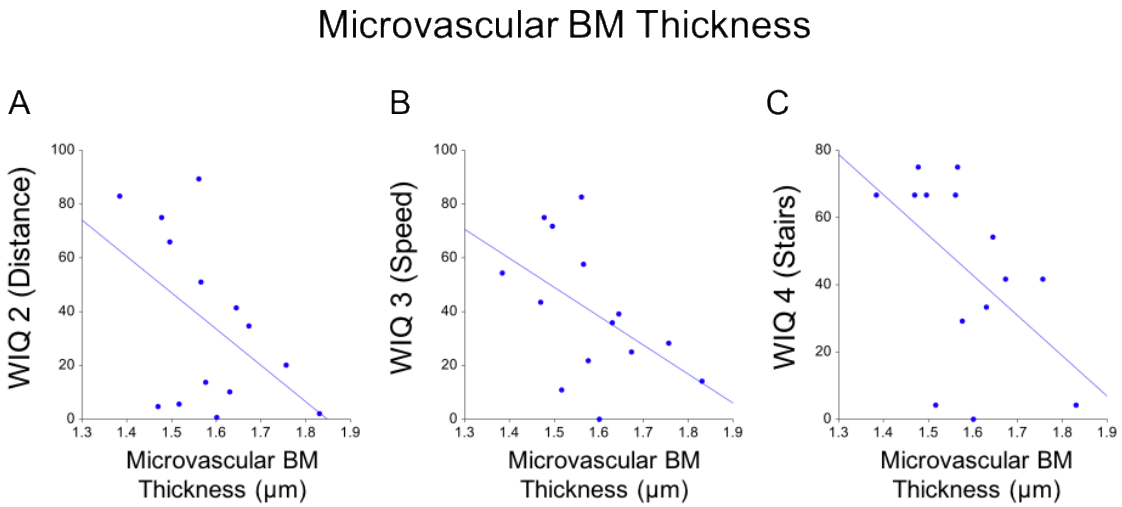

Figure 23: Qualitative Measures of Walking Performance in PAD are Associated with Microvascular Thickness.

Patient self-reported walking performance decreases as microvessels become thickened. Patients tended to report walking shorter distances as BM became thicker (n = 14; R = -0.41; p = 0.14)(**A**). As BM thickness increased, patients reported slower walking speeds (n = 14; R = -0.54; p = 0.05)(**B**) and greater difficulty climbing stairs (n = 14; R = -0.57; p = 0.03)(**C**).

Figure 24: Qualitative Measures of Walking Performance are Associated with Microvascular Inner BM Diameter in Stage II PAD Patients

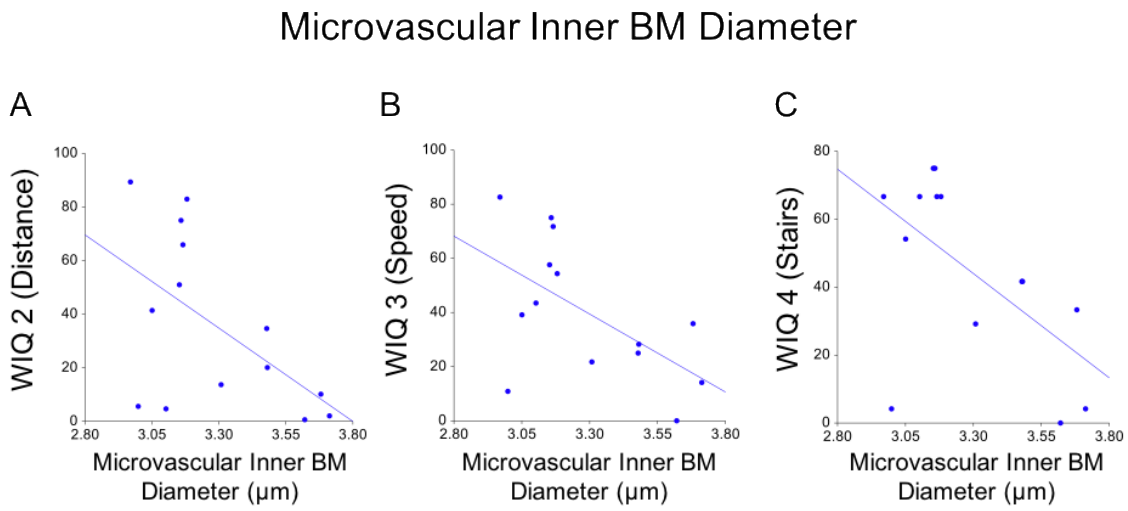

Figure 24: Qualitative measures of walking performance are associated with microvascular inner BM diameter

As inner BM diameter increased, patients reported walking shorter distances (n=14; R^2 = 0.31; p = 0.04)(**A**), at slower speeds (n = 14; R^2 = 0.34; p = 0.03) (**B**), with greater difficulty in climbing stairs (n = 14; R^2 = 0.34; p = 0.03) (**C**).

Next we explored if macrovascular disease (ABI and RH) was a stronger determinant of patient self-reported walking performance than microvascular disease. We assessed the relationship between resting and post-occlusive ABIs and WIQ subcategory scores. No linear relationship was observed between ABI at rest and walking speed ($R = -0.04$, $p = 0.82$), walking duration ($R = -0.15$, $p = 0.39$), and ability to climb stairs ($R = -0.03$, $p = 0.86$). Also absent were relations between post-occlusive ABI and walking speed ($R = -0.04$, $p = 0.82$), walking duration ($R = -0.17$, $p = 0.33$), and ability to climb stairs ($R = -0.04$, $p = 0.84$). Taken together, these data point to microvascular disease being dominant to macrovascular disease in patient self-reported walking performance.

Onset of Claudication Pain Occurs More Rapidly as Microvascular Pathology Worsens

To determine if microvascular pathology was associated with standard assessments of PAD patient walking performance, we assessed COT and microvascular architecture. We observed a trend between BM thickness and COT ($n = 13$; $R = -0.45$; $p = 0.13$). Inner BM diameter and COT had a moderate correlation ($n = 13$; $R = -0.62$; $p = 0.03$), which suggests that as inner BM diameter increases, patients experience pain more rapidly (**Figure 25**).

Figure 25: COT is Decreased with Increasing Microvascular Inner BM Diameter

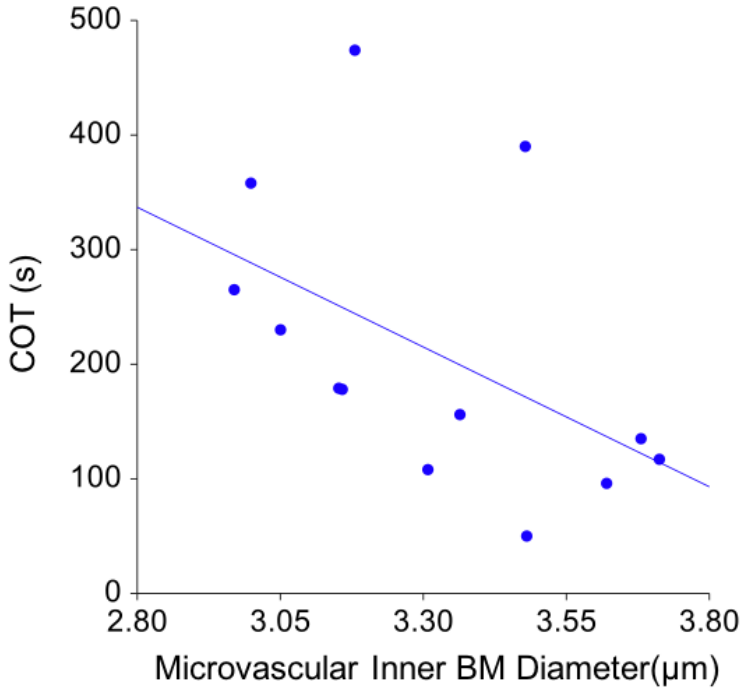

Figure 25: Claudication onset time is decreased with increasing microvascular inner BM diameter.
Patients experience pain during walking more rapidly as inner BM diameter increases (n = 13; R = -0.62; p = 0.03).

Maximal Duration of Walking is Limited by Microvascular Pathology

We next assessed the relationship between microvascular architecture and maximal walking duration. The association between PWT and BM thickness was not significant (n = 13; R = -0.41; p = 0.16). However, a negative linear relationship was present between PWT and inner BM diameter (n = 13; R = -0.67; p = 0.01)(**Figure 26**). Inner BM diameter is a stronger predictor of both COT and PWT in Stage II PAD patients than BM thickness.

Figure 26: Peak Walking Time is Influenced by Microvascular Inner BM Diameter

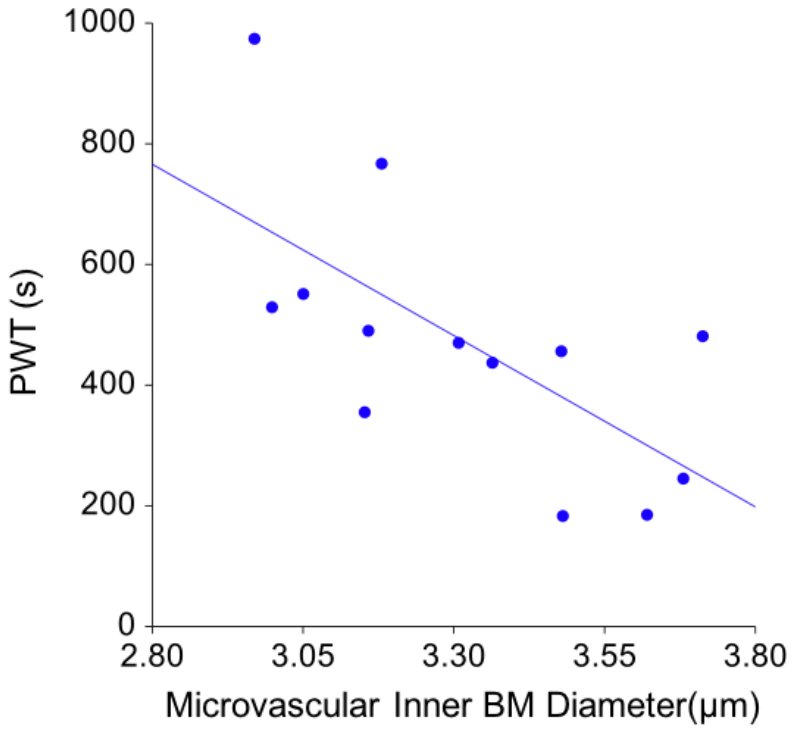

Figure 26: Peak walking time is influenced by microvascular inner BM diameter. PWT is shortened as inner BM diameter increases (n = 13; R = -0.67; p = 0.01).

Discussion

Arterial atherosclerotic occlusion impairs blood flow to the lower extremities of PAD patients, and during exercise the limitations in arterial perfusion become exaggerated and initiate pain and encumber ambulation. However, the pathophysiology of PAD limb dysfunction is complex and is not fully explained by the hemodynamic limitation produced by large artery occlusive disease (macrovascular disease). In this study we have established that microvascular disease is dominant to macrovascular disease in the correlation and likely contribution to more rapid declines in oxygen saturation and diminishing walking performance. We have demonstrated that there is a relationship between microvascular architecture (inner BM diameter and BM thickness) and both subjective and objective measures of walking performance. Interestingly, inner BM diameter appears to be a stronger predictor of walking performance than BM thickness. Taken together with the findings in the previous chapters, microvascular architectural pathology appears to be linked with myofibrosis and worsening myopathy, as well as muscle oxygenation, muscle performance, and pain responses.

Our findings support work from our groups and others that ischemic myopathy plays a central role in pathogenesis and pathophysiology in PAD legs. The microvascular disease described in this thesis may be a key component of PAD myopathy. The data presented in these studies demonstrate that microvascular disease contributes to and possibly determines the development of perivascular and muscle fibrosis, PAD muscle microperfusion limitations, and both symptoms and walking limitations in PAD patients with claudication. We have previously shown that a state of repetitive cycles of exercise-induced ischemia followed by reperfusion at rest operates in PAD patients and mediates a large number of structural and metabolic changes in the muscle (PAD myopathy). The most important myopathic changes in PAD are myofiber degeneration, fibrosis, and cytokine upregulation. In this thesis, we have shown that microvascular disease is

associated with every aspect of myopathy. We have shown that microvascular disease may contribute to muscle hypoperfusion. Microvascular disease appears to be involved in the fibrotic process, and fibrosis appears to originate around pathologic microvessels and subsequently spread to involve myofibers and myofascicles of the affected muscles. Therefore, it is highly likely that microvascular pathology is an important contributer to PAD myopathy. In this study, we have shown that as microvascular pathology worsens, muscle oxygenation during exercise diminishes more rapidly. Thus, alterations of microvascular architecture may predispose muscle to ischemia, particularly during ambulation. Rapid decline of muscle oxygen tension in PAD limbs may hasten pain initiation and escalation with consequent decreases in walking performance. The inability to efficiently deliver blood and the limitation in diffusion of oxygen predispose working myocytes to oxidative stress, damage, and degeneration. Therefore, microvascular architectural alterations may also contribute to myopathy propagation with subsequent deterioration of muscle function and walking performance.

In Chapter II we demonstrated that the inner BM diameter expands to accommodate αSMA^+ pericytes. αSMA^+ pericyte abundance increased in association with increasing BM thickness, inner BM diameter, peri-microvascular Collagen IV abundance and peri-microvascular Collagen I density. In Chapter III we observed that as the BM becomes thickened in Stage II PAD patients, the microvascular density decreases. Thickening of the BM and deposition of collagens around the microvessels may alter their hemodynamic properties, as well as the ability to deliver oxygen (diffusion capacity) to myocytes. Oxygen delivery may be further challenged by the reduction in microvessel density as Stage II PAD microvessels becomes thicker. Initiation of walking increases metabolic demands in PAD skeletal muscle and the combination of macro- and microvascular disease leads to a drop in tissue oxygenation and an increase in the byproducts of alternative fuel consumption, such as lactic acid. In addition to hypoxia

signals, these metabolites may contribute to the induction of C-fiber-mediated pain signals, which grow in intensity as the patient continues to walk. Additionally, αSMA^+ pericytes are likely proliferative and vasoconstrictive in PAD muscle. Enhanced vasoconstriction of pre-capillary sphincters by αSMA^+ pericytes may reflect a compensatory mechanism for pre-capillary pressure correction that leads to a reduction in distal resistance, increase in blood flux, and maximization of blood distribution across hypo-perfused tissues[117] but may also create microdomains of severe ischemia in PAD muscle. We have observed a non-uniform pattern of perfusion by CEU imaging of claudicating muscle, which supports that blood flow may be shunted around select capillary beds. Taken together, these data suggest that microvascular disease may contribute to local ischemia and may directly contribute to myocyte ischemia/reperfusion injury.

Our observation that microvascular architectural alterations correlate with the walking impairment and severity of the symptoms experienced by patients with claudication is significant. Patients report walking shorter distances at slower speeds, and climbing stairs with greater difficulty as inner BM diameter increases, suggesting that microvascular pathology contributes to limitations of executing routine daily activities. The decline in ambulation speed and duration suggest a behavioral modification to limit microvascular-mediated ischemia in PAD muscle. Moderate correlations between inner BM diameter and both COT and PWT suggest that microvascular pathology directly contributes to patient walking limitations, including the initiation and worsening of pain during walking. This further points to the possibility that microvascular architectural alterations are not limited to skeletal muscle, but rather may be a ubiquitous finding across tissues of PAD limbs, such as nerves and skin, which may contribute to the well documented neuropathy of PAD and the loss of hair follicles, oil- and sweat- glands and

overall thinning and dryness of PAD skin. Declines in microvascular density are concordant with microvascular architectural alterations, suggesting that angiogenesis becomes exhausted, which, when coupled to perfusion and oxygenation deficits, may account for the poorer wound healing observed in PAD patients, particularly in advanced stages.

This study has several limitations. We used the WIQ to assess the patient's ability to perform normal activities of daily living. Additional studies that quantitatively assess ambulation and duration of activity throughout the day using objective methodology (*e.g.* with the use of an accelerometer) may provide insight on the impact of microvascular pathology during routine activities. In our assessment of tissue oxygenation, we used NIRS probes which are portable and allow measurements during ambulation but have a limited spatial resolution. Higher resolution modalities, such as BOLD MRI, may provide additional characterization of the oxygenation deficits in PAD and clarify the functional contribution of microvascular pathology to oxygenation limitations across PAD muscles.

Future studies are needed to better understand the role of microvascular pathology in both PAD myopathy progression and walking limitations. In this study we characterized the correlation of microvascular structural alterations to oxygenation and ambulation deficits. However, functional alterations in blood flow regulation remain poorly characterized, particularly within the microvasculature. Our findings suggest that microvascular pathology may contribute to ischemic damage within PAD muscle, and studies that assess the relationship between microvascular architecture, oxidative damage, and mitochondrial dysfunction are warranted. Furthermore, the potential of standard and currently developing therapies to reverse microvascular architectural pathology and thereby improve symptoms and ambulatory ability of PAD patients remains to be tested.

Conclusions

Microvascular remodeling in PAD, particularly the expansion of the inner BM diameter, are linked to worsening muscle oxygenation, walking performance, and pain responses in PAD limbs. Microvascular pathology may contribute to ischemia/reperfusion injury and myopathy propagation.

Chapter V: Discussion

In this dissertation, we have demonstrated that there is a progressive alteration of the microvascular architecture across stages of PAD that corresponds to increases in microvascular density, αSMA^+ pericyte abundance, and decreasing ABI across stages of PAD. These studies also reveal an association between microvascular pathology and not only perivascular collagen deposition, but also total fibrotic burden. We have also shown that microvascular architecture, particularly inner BM diameter, is linked to oxygen tension and microperfusion in PAD muscle, as well as PAD patient walking performance. Taken together, the results of these studies indicate that microvascular pathology may have a substantial role in the pathogenesis of PAD myopathy, particularly fibrogenesis, and may have a direct contribution to the walking limitations experienced by patients with PAD.

Although these studies are observational in nature, they provide a solid foundation for future studies to explore in greater depth the mechanisms by which microvascular pathology arises in PAD muscle. Of particular interest are studies that explore the impact of treatment interventions in PAD, such as revascularization surgery, supervised exercise, or pharmacological interventions. Such studies would assist in understanding the mechanisms by which microvascular architecture and perfusion are altered, potentially enabling the development of more effective treatment strategies for PAD. Additionally, they offer the unique opportunity to characterize with greater accuracy and validity the utility of non-invasive imaging modalities that assess microperfusion, particularly CEU. Defining the relationships between microvascular pathology, myopathy, and CEU parameters could aid clinical decision making, and may one day be of use in tailoring individualized therapeutic strategies. We hypothesis that the extent of microvascular pathology is linked to the risk of failure of revascularization surgery. To clarify, there may be a threshold of microvascular pathology, that once exceeded, will not regress upon

reinstitution of arterial flow, which would thus result in poorer outcomes and limited benefit of performing a risky and invasive operation.

An ongoing study in our laboratory is assessing the impact of six months Ramipril (ACE-inhibitor) intervention on the microvascular of Stage II PAD muscles. Comparing pre and post Ramipril parameters allows the opportunity to begin understanding causality between microvascular architectural features and outcomes. Preliminary data from our lab suggests that after six months of Ramipril treatment, patients have a significant increase in inner BM diameter and total microvascular diameter, but BM thickness remains unchanged (**Table 10**). However, CEU parameters were not significantly altered (**Table 11**).

Table 10: Microvascular Architecture Before and After Ramipril Treatment

	Pre Ramipril	Post Ramipril	p – value *
Microvascular BM Thickness	1.577 ± 0.030	1.619 ± 0.038	0.15
Microvascular Inner BM Diameter	3.295 ± 0.064	3.497 ± 0.099	0.049
Microvascular Total Diameter	6.448 ± 0.112	6.734 ± 0.162	0.047

Table 10: Microvascular Architecture Before and After Six Months of Ramipril Treatment.

Patients (n = 15) were assessed before and after six months of treatment with Ramipril. Gastrocnemius biopsy specimens were labeled with Collagen IV and microvascular architectural features were measured. Measurements were obtained for approximately 50 – 200 microvessels per each biopsy specimen. Measurements are presented as mean ± S.E.M.

* *p* values were calculated by parametric paired t-test

Table 11: Microperfusion Characteristics Before and After Ramipril Treatment

	Pre Ramipril	Post Ramipril	p – value *
Resting Microvascular Blood Volume (*A*)	1.51 ± 0.30	1.93 ± 0.21	0.22
Resting Microvascular Blood Flux (β)	0.52 ± 0.09	0.55 ± 0.13	0.83
Resting Microvascular Blood Flow (*A* • β)	0.67 ± 0.13	1.12 ± 0.34	0.22
Reperfusion Microvascular Blood Volume (*A*)	3.57 ± 0.72	3.90 ± 0.64	0.63
Reperfusion Microvascular Blood Flux (β)	0.42 ± 0.09	0.33 ± 0.04	0.24
Reperfusion Microvascular Blood Flow (*A* • β)	1.15 ± 0.22	1.08 ± 0.10	0.78
Flow Reserve	2.25 ± 0.54	1.75 ± 0.43	0.48

Table 11: Microperfusion Characteristics Before and After Ramipril Treatment
CEU imaging was performed on Stage II PAD patients (n = 13) both before and after six months of treatment with Ramipril. CEU parameter measurements are presented as mean ± S.E.M.

* *p* values were calculated by parametric paired t-test

Comparison of the percent change of across parameters revealed several interesting relationships that support that microvascular pathology is indeed central to PAD myopathy. Our early results show that there may be robust relationships between microvascular architecture and blood flux (**Figure 27**). The patients who had an increase in BM thickness also experienced an increase in blood flux at rest (R = 0.77), though currently this association is marginally significant (n = 6, p = 0.07)(**Figure 27A**). The patients that experienced an inner BM diameter expansion had an increase in reperfusion blood flux (n = 6, R = 0.89, p = 0.02)(**Figure 27B**). We also observed emerging relationships between microvascular architecture, microperfusion, and oxygen saturation. A trend was observed between increasing inner BM diameter and decreasing time to minimum SpO_2 (n = 12, R = -0.55, p = 0.07)(**Figure 28A**). Additionally, we observed a strong inverse relationship between resting MBF and time to minimum SpO_2 (n = 10, R = -0.85, p = 0.002)(**Figure 28B**). These data support that oxygen saturation becomes increasing limited as BM thickness and resting MBF increase.

Furthermore, emerging correlations are also present between changes in microvascular architecture, microperfusion, and PWT. Although marginally significant, there is evidence that increasing inner BM diameter (n = 12, R = -0.52, p = 0.08)(**Figure 29A**) and increasing resting MBF (n = 10, R = -0.60, p = 0.07)(**Figure 29B**) are moderately associated with declines in walking duration. Given our observations that blood flux is increased with increasing microvascular architectural alterations, it is possible that microvascular pathology has advanced in the Ramipril treated patients. Thus it is possible that the blood may remain in larger vessels with lower resistance and may be diverted around capillary beds. Alternatively, six months of Ramipril treatment may improve collateralization and the quality and function of the arterioles, which may increase resting MBF without improving terminal microvascular pathology, and consequently without improving walking performance.

Figure 27: Alterations in Microvascular Association are Associated with Changes in Blood Flux

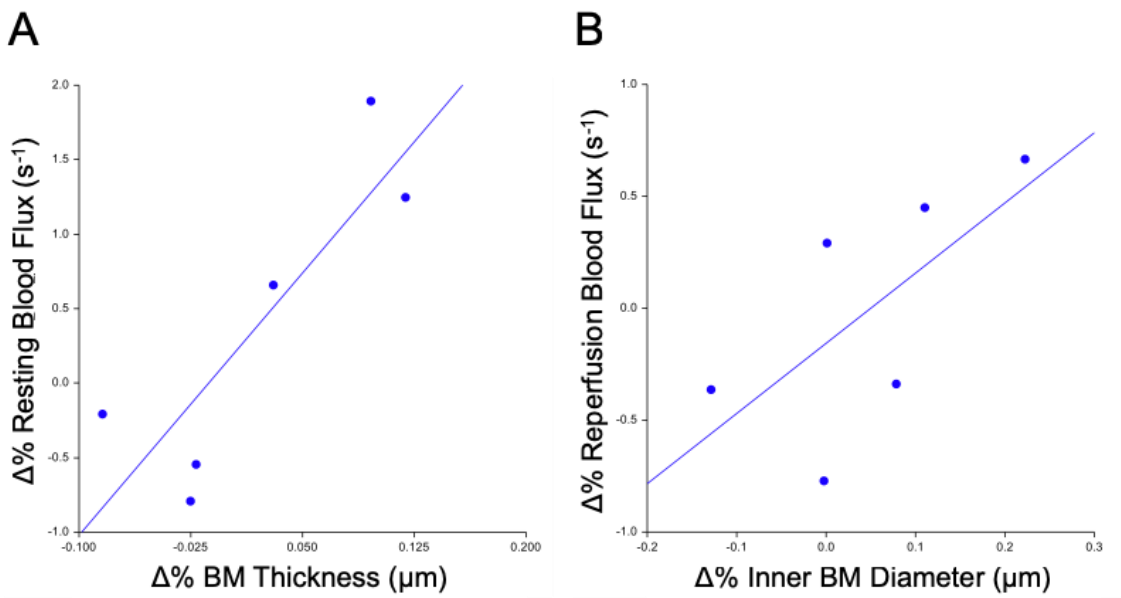

Figure 27: Alterations in Microvascular Architecture are Associated with Changes in Blood Flux.

Quantification of microvascular architecture and microperfusion by CEU were obtained in PAD patients with IC (n = 6) before and six months after Ramipril treatment. The percent change (Δ%) was calculated. A trend was observed between increasing BM thickness and increases in resting blood flux (R = 0.77, p = 0.07) (A). A strong linear relationship was observed between enlarging inner BM diameter and reperfusion blood flux (R = 0.89, p = 0.02). Relationships were assessed by non-parametric correlation analysis, and Spearman R values are reported.

Figure 28: The Relationship Between Oxygen Tension, Inner BM Diameter, and Resting MBF

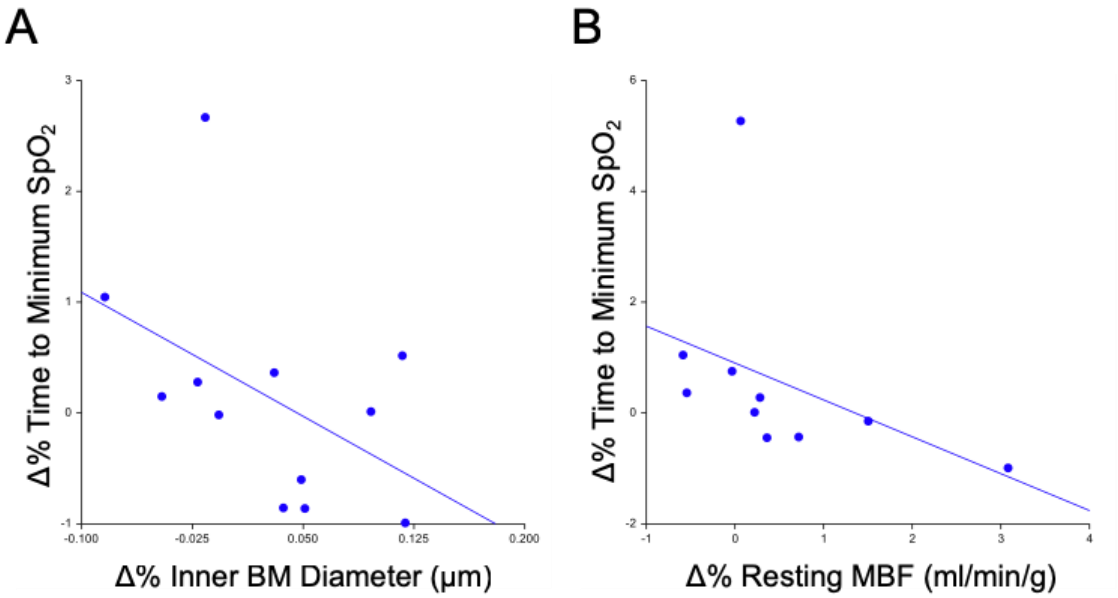

Figure 28: The Relationship Between Oxygen Tension, Inner BM Diameter, and Resting MBF.

Quantification of microvascular architecture, microperfusion by CEU, and oxygen saturation by NIRS were obtained in PAD patients with IC before and six months after Ramipril treatment. The percent change (Δ%) was calculated. A trend was observed between increasing inner BM diameter and shortening of the interval to minimum SpO_2 ($R = -0.55$, $n = 12$, $p = 0.07$) (A). A strong linear relationship was observed between enlarging inner BM diameter and reperfusion blood flux ($R = 0.85$, $n = 10$, $p = 0.002$). Relationships were assessed by non-parametric correlation analysis, and Spearman R values are reported.

Figure 29: Alterations of Microvascular Architecture and Resting MBF are Related to Declines in PWT

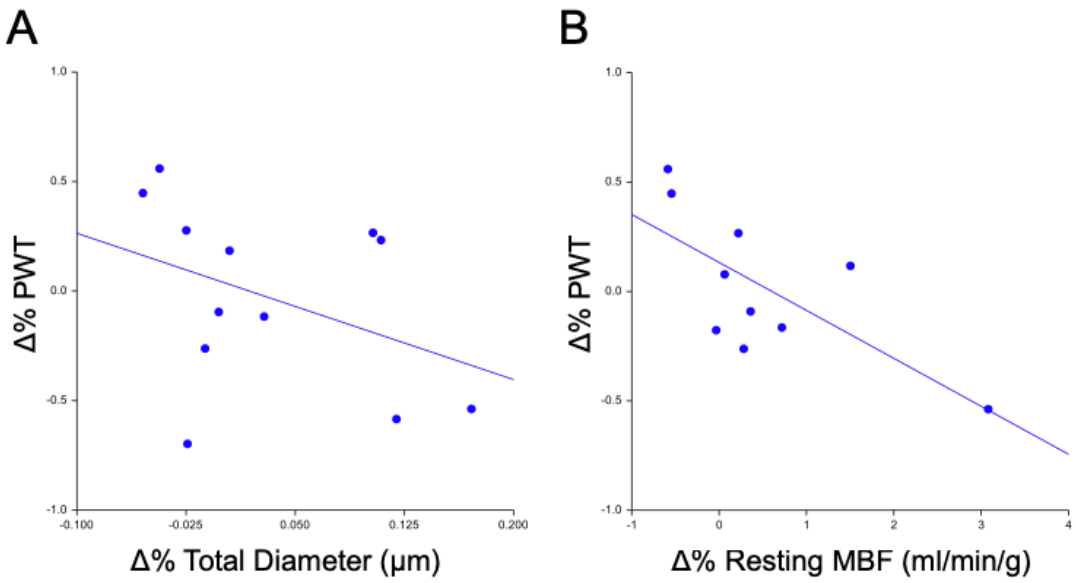

Figure 29: Alterations of Microvascular Architecture and Resting MBF are Related to Declines in PWT.

Quantification of microvascular architecture and microperfusion by CEU were performed in PAD patients with IC before and six months after Ramipril treatment. The percent change (Δ%) was calculated. A trend was observed between increasing microvascular total diameter and declining PWT ($R = -0.52$, $n = 12$, $p = 0.08$) (A). A marginally significant linear relationship was observed between increasing resting MBF and declining PWT ($R = -0.60$, $n = 10$, $p = 0.07$). Relationships were assessed by non-parametric correlation analysis, and Spearman R values are reported.

It is possible that improvements of the arterioles may precede improvements of the microvascular beds. Therefore, six months of Ramipril treatment may be too short of an interval to capture beneficial alterations of microvascular architecture or function in the legs of PAD patients. Future studies are merited in exploring the changes in terminal microvasculature against alterations of larger microvasculature and the relationship of these features to microperfusion, muscle strength, and walking performance.

Collectively, the data presented in this thesis point to a mechanism of progressive deterioration of the microvasculature and subsequently microperfusion and walking performance. Microvascular BM thickening appears to be an early event in PAD myopathy and is likely initiated by inflammatory and ischemic cues from early atherosclerotic narrowing of the arteries. As inflammation and hypoxia become more frequent, the endothelium swells, endothelial dysfunction arises, and the likely consequence is endothelial cell and pericyte damage and cell death. Thus, the first step in PAD microvascular pathology includes microvascular regression, which contributes to local ischemia and subsequent initiation of an angiogenic response.

Our data support that an angiogenic response is mounted in PAD muscle and becomes more robust with PAD severity. Studies of more proximal muscle groups consistently demonstrate non-significant alterations of microvascular density. Two possible explanations for the divergent results between our studies and theirs include: 1) blood traveling through more proximal muscle may have better oxygen tension than blood arriving in distal microvascular beds; 2) the atherosclerotic burden across a larger arterial area leads to more dramatic reductions in arterial flow to distal muscle and drives more significant pathological changes to the microvasculature.

Increasing microvascular density leads to the second step in PAD microvascular pathology, where the loss of microvascular constituents stimulates repair, and consequently BM thickening. Prolonged exposure to inflammation and

ischemia/reperfusion injury predispose the muscles of PAD patients to repetitive cycles of microvascular to damage, death, and regeneration. With each iteration, fragments of lost cells, such as the pericyte ghosts that have been reported, become incorporated into the BM. As incoming endothelial cells interact with pericytes, they form a new layer of BM, in effect adding a layer with each attempt at microvascular repair. Thus, perpetual damage and repair cycles may account for the progressive nature of the BM thickening we have observed in our studies. As the BM continues to expand, the deleterious sequelae of deteriorating oxygen diffusion and microperfusion arise and worsen.

In our studies we observed that the fibrotic burden parallels the microvascular architectural alterations, which supports that the origin of fibrosis may be the microvasculature. Thus, the third step in PAD microvascular pathology includes the abnormal accumulation of TGF-β1-producing αSMA$^+$ pericytes to the microvasculature. These pericytes are likely capable of vasoconstriction and may be involved in the initiation and propagation of fibrosis. Pericytes can synthesize collagens, but they can also recruit and direct fibroblasts to deposit collagen *via* TGF-β1signaling. Additionally, αSMA$^+$ pericytes may be able to differentiate into myofibroblasts.

Pericyte-mediated constriction may be a response to chronically low arterial flow, where shunting of blood around terminal microvascular beds maintains adequate perfusion pressure and better distribution of blood throughout the microvascular network. However, with chronic intermittent hypoxia, oxidative damage cumulatively injures pericytes, and may ultimately induce αSMA$^+$ pericyte death, resulting in pericyte rigor and loss of perfusion of selected capillary beds. This mechanism may in part account for the spatial heterogeneity observed in Stage II PAD muscle, both for myopathic changes and microdomains devoid of microvascular blood flow in CEU studies.

In advanced stage PAD muscle, microvascular remodeling is pronounced, and includes substantial increases in αSMA^{+} pericyte abundance (and consequently expansion of the inner BM diameter) around the microvasculature, which gives the appearance of "arteriolization" of the smallest microvessels. The significance of this observation is two-fold. Muscularization of capillaries may reflect additional shunting of blood around microvascular beds. It may also represent pericytes that are differentiating into myofibroblasts. Acellular capillaries appear to be limited to vessels that had substantial BM thickening. This supports the notion that pericyte egress as myofibroblasts, leaving in their wake an unstable endothelium prone to regression. An alternative explanation for the increased frequency of acellular capillaries is that angiogenesis becomes "exhausted", leading to a late stage regression of microvessels, and further ischemia and myocyte damage.

Undoubtedly, microvascular pathology contributes to PAD myopathy. Our findings that associations are present between microvascular architecture, particularly inner BM diameter, and both subjective and objective measures of walking performance are significant. Targeting microvascular pathology, potentially by coaxing pericytes from a pro-fibrotic to a pro-regenerative phenotype may improve outcomes in PAD patients. A better understanding of PAD microvascular pathology may prove to be a meaningful predictor of disease progression and response to interventions. For example, assessment of microvascular pathology, possibly by CEU, may have clinical utility in the selection of revascularization surgery candidates.

Threats to the internal validity in this study, and the ongoing study of pre/post Ramipril intervention, include history, maturation, testing, measurement, and selection. The relatively short duration of Ramipril intervention (24 weeks) limits the influence of maturation. However, we anticipate some effects from history and testing, as continuous interactions with our clinical staff allow multiple points of education about their disease

process, and thus may affect the motivation of the patients to engage in new behaviours, such as decreased smoking, increased exercise, and better diet. Our collection of data is not completed in one clinic visit. Instead, separate sessions are scheduled for clinical assessment, biopsy, CEU acquisition, and biomechanics data acquisition. Thus, history and testing are still relevant concerns to consider in the assessment of our native PAD and control cohorts. Although the impact of maturation should be very low across studies of native Stage II PAD, there may be a non-negligible contribution to the interventional study of Ramipril. Selection bias may occur, as patients who volunteer to take part in the study may have better access to clinical care, and thus better management of comorbidities than the general population. Quantitative measurements of microvascular architecture and microvascular density have been tested for reliability in this study, with test-retest values agreeing within 10% of each other. However, our measurements may not be as accurate as those acquired by evaluation of higher resolution electron micrographs.

A threat to external validity exists in our limited sampling of patients within eastern Nebraska and western Iowa. Since our recruitment is limited to UNMC and the VA Hospitals within Omaha, Nebraska, it is possible that our effects may have a loss in generalizability due to our convenience sampling. Our patient population is fairly homogeneous and is predominantly male. Follow up studies may be necessary in additional centers with access to more women and minority patients with PAD. We do not anticipate a large effect from the interaction of treatment and setting, as the UNMC hospital and VA Hospital do not differ greatly. As was discussed for internal validity, history may affect the generalizability of this study, as future studies may not involve as much opportunity for patient education and lifestyle modification.

Future Studies

Microvascular pathology remains poorly characterized in PAD limbs. However, the potential for discovery of pharmacological targets is high, as well as the clinical relevance for diagnostic and therapeutic approaches. Elucidation of the mechanisms involved in microvascular pathology can also have a broad impact on other pathologies, such as the microvascular pathology observed in transplant organs, MI, congestive heart failure, and PAH. Pericytes, in particular, have a very unclear role in PAD pathophysiology. Future studies should be targeted towards the characterization of the role of pericytes in fibrogenesis. Animal models may provide clarification of the lineage of myofibroblasts in hindlimb ischemia and determine if the contribution of pericytes to the myofibroblast pool is significant. Additionally, these studies may identify markers that may be of use in conformational studies in human PAD muscle. Tissue culture may also provide mechanistic insights to the contribution of pro-inflammatory cytokines, alterations in shear stress, and hypoxia to pericyte function and adaptation.

Studies that assess the impact of current interventions to microvascular pathology are needed. Revascularization surgery and supervised exercise interventions are of great interest, as these studies may assist in understanding the physiologic responses of the microvasculature in human muscle, which can provide mechanistic insights in microvascular pathogenesis. It is highly recommended that these studies be conducted in a way such that tissue oxygenation, microperfusion, and microvascular architecture can be concurrently analyzed.

References

1. Mozaffarian D. Dietary and Policy Priorities for Cardiovascular Disease, Diabetes, and Obesity: A Comprehensive Review. *Circulation.* 2016;133(2):187-225.

2. Barquera S, Pedroza-Tobias A, Medina C, et al. Global Overview of the Epidemiology of Atherosclerotic Cardiovascular Disease. *Arch Med Res.* 2015;46(5):328-338.

3. Criqui MH, Aboyans V. Epidemiology of peripheral artery disease. *Circ Res.* 2015;116(9):1509-1526.

4. Gardner AW, Afaq A. Management of lower extremity peripheral arterial disease. *J Cardiopulm Rehabil Prev.* 2008;28(6):349-357.

5. Fowkes FG, Rudan D, Rudan I, et al. Comparison of global estimates of prevalence and risk factors for peripheral artery disease in 2000 and 2010: a systematic review and analysis. *Lancet.* 2013;382(9901):1329-1340.

6. Benjamin EJ, Virani SS, Callaway CW, et al. Heart Disease and Stroke Statistics-2018 Update: A Report From the American Heart Association. *Circulation.* 2018;137(12):e67-e492.

7. Roger VL, Go AS, Lloyd-Jones DM, et al. Heart disease and stroke statistics--2011 update: a report from the American Heart Association. *Circulation.* 2011;123(4):e18-e209.

8. Mahoney EM, Wang K, Keo HH, et al. Vascular hospitalization rates and costs in patients with peripheral artery disease in the United States. *Circ Cardiovasc Qual Outcomes.* 2010;3(6):642-651.

9. Mahoney EM, Wang K, Cohen DJ, et al. One-year costs in patients with a history of or at risk for atherothrombosis in the United States. *Circ Cardiovasc Qual Outcomes.* 2008;1(1):38-45.

10. Myers SA, Johanning JM, Stergiou N, Lynch TG, Longo GM, Pipinos, II. Claudication distances and the Walking Impairment Questionnaire best describe the ambulatory limitations in patients with symptomatic peripheral arterial disease. *J Vasc Surg.* 2008;47(3):550-555.

11. Liles DR, Kallen MA, Petersen LA, Bush RL. Quality of life and peripheral arterial disease. *J Surg Res.* 2006;136(2):294-301.

12. Menard JR, Smith HE, Riebe D, Braun CM, Blissmer B, Patterson RB. Long-term results of peripheral arterial disease rehabilitation. *J Vasc Surg.* 2004;39(6):1186-1192.

13. Hirsch AT, Duval S. The global pandemic of peripheral artery disease. *Lancet.* 2013;382(9901):1312-1314.

14. Atkins LM, Gardner AW. The relationship between lower extremity functional strength and severity of peripheral arterial disease. *Angiology.* 2004;55(4):347-355.

15. Gardner AW, Clancy RJ. The relationship between ankle-brachial index and leisure-time physical activity in patients with intermittent claudication. *Angiology.* 2006;57(5):539-545.

16. Lassila R, Lepantalo M, Lindfors O. Peripheral arterial disease--natural outcome. *Acta Med Scand.* 1986;220(4):295-301.

17. Selvin E, Erlinger TP. Prevalence of and risk factors for peripheral arterial disease in the United States: results from the National Health and Nutrition Examination Survey, 1999-2000. *Circulation.* 2004;110(6):738-743.

18. Shammas NW. Epidemiology, classification, and modifiable risk factors of peripheral arterial disease. *Vasc Health Risk Manag.* 2007;3(2):229-234.

19. Fontaine R, Kim M, Kieny R. [Surgical treatment of peripheral circulation disorders]. *Helv Chir Acta.* 1954;21(5-6):499-533.

20. Chen SJ, Pipinos I, Johanning J, et al. Bilateral claudication results in alterations in the gait biomechanics at the hip and ankle joints. *J Biomech.* 2008;41(11):2506-2514.

21. Dormandy JA, Rutherford RB. Management of peripheral arterial disease (PAD). TASC Working Group. TransAtlantic Inter-Society Consensus (TASC). *J Vasc Surg.* 2000;31(1 Pt 2):S1-S296.

22. Novo S. Classification, epidemiology, risk factors, and natural history of peripheral arterial disease. *Diabetes Obes Metab.* 2002;4 Suppl 2:S1-6.

23. Norgren L, Hiatt WR, Dormandy JA, et al. Inter-Society Consensus for the Management of Peripheral Arterial Disease (TASC II). *J Vasc Surg.* 2007;45 Suppl S:S5-67.

24. Hernandez H, Myers SA, Schieber M, et al. Quantification of Daily Physical Activity and Sedentary Behavior of Claudicating Patients. *Ann Vasc Surg.* 2018.

25. Muluk SC, Muluk VS, Kelley ME, et al. Outcome events in patients with claudication: a 15-year study in 2777 patients. *J Vasc Surg.* 2001;33(2):251-257; discussion 257-258.

26. Cassar K. Intermittent claudication. *BMJ.* 2006;333(7576):1002-1005.

27. Nehler MR, Duval S, Diao L, et al. Epidemiology of peripheral arterial disease and critical limb ischemia in an insured national population. *J Vasc Surg.* 2014;60(3):686-695 e682.

28. Rothwell PM, Coull AJ, Silver LE, et al. Population-based study of event-rate, incidence, case fatality, and mortality for all acute vascular events in all arterial territories (Oxford Vascular Study). *Lancet.* 2005;366(9499):1773-1783.

29. Griffiths RI, O'Malley CD, Herbert RJ, Danese MD. Misclassification of incident conditions using claims data: impact of varying the period used to exclude pre-existing disease. *BMC Med Res Methodol.* 2013;13:32.

30. Hiatt WR, Hoag S, Hamman RF. Effect of diagnostic criteria on the prevalence of peripheral arterial disease. The San Luis Valley Diabetes Study. *Circulation.* 1995;91(5):1472-1479.

31. Kardia SL, Greene MT, Boerwinkle E, Turner ST, Kullo IJ. Investigating the complex genetic architecture of ankle-brachial index, a measure of peripheral arterial disease, in non-Hispanic whites. *BMC Med Genomics.* 2008;1:16.

32. Chang P, Nead KT, Olin JW, Cooke JP, Leeper NJ. Clinical and socioeconomic factors associated with unrecognized peripheral artery disease. *Vasc Med.* 2014;19(4):289-296.

33. Khaleghi M, Isseh IN, Bailey KR, Kullo IJ. Family history as a risk factor for peripheral arterial disease. *Am J Cardiol.* 2014;114(6):928-932.

34. Wahlgren CM, Magnusson PK. Genetic influences on peripheral arterial disease in a twin population. *Arterioscler Thromb Vasc Biol.* 2011;31(3):678-682.

35. Kullo IJ, Leeper NJ. The genetic basis of peripheral arterial disease: current knowledge, challenges, and future directions. *Circ Res.* 2015;116(9):1551-1560.

36. Levy PJ, Gonzalez MF, Hornung CA, Chang WW, Haynes JL, Rush DS. A prospective evaluation of atherosclerotic risk factors and hypercoagulability in young adults with premature lower extremity atherosclerosis. *J Vasc Surg.* 1996;23(1):36-43, discussion 43-35.

37. Gudmundsson G, Matthiasson SE, Arason H, et al. Localization of a gene for peripheral arterial occlusive disease to chromosome 1p31. *Am J Hum Genet.* 2002;70(3):586-592.

38. Willigendael EM, Teijink JA, Bartelink ML, et al. Influence of smoking on incidence and prevalence of peripheral arterial disease. *J Vasc Surg.* 2004;40(6):1158-1165.

39. Lu L, Mackay DF, Pell JP. Meta-analysis of the association between cigarette smoking and peripheral arterial disease. *Heart.* 2014;100(5):414-423.

40. Muntner P, Wildman RP, Reynolds K, Desalvo KB, Chen J, Fonseca V. Relationship between HbA1c level and peripheral arterial disease. *Diabetes Care.* 2005;28(8):1981-1987.

41. Hayes KL, Messina LM, Schwartz LM, Yan J, Burnside AS, Witkowski S. Type 2 diabetes impairs the ability of skeletal muscle pericytes to augment postischemic

neovascularization in db/db mice. *Am J Physiol Cell Physiol.* 2018;314(5):C534-C544.

42. Thiruvoipati T, Kielhorn CE, Armstrong EJ. Peripheral artery disease in patients with diabetes: Epidemiology, mechanisms, and outcomes. *World J Diabetes.* 2015;6(7):961-969.

43. Selvin E, Marinopoulos S, Berkenblit G, et al. Meta-analysis: glycosylated hemoglobin and cardiovascular disease in diabetes mellitus. *Ann Intern Med.* 2004;141(6):421-431.

44. Arya S, Binney ZO, Khakharia A, et al. High hemoglobin A1c associated with increased adverse limb events in peripheral arterial disease patients undergoing revascularization. *J Vasc Surg.* 2018;67(1):217-228 e211.

45. Jude EB, Oyibo SO, Chalmers N, Boulton AJ. Peripheral arterial disease in diabetic and nondiabetic patients: a comparison of severity and outcome. *Diabetes Care.* 2001;24(8):1433-1437.

46. Humphries MD, Brunson A, Li CS, Melnikow J, Romano PS. Amputation trends for patients with lower extremity ulcers due to diabetes and peripheral artery disease using statewide data. *J Vasc Surg.* 2016;64(6):1747-1755 e1743.

47. Jones WS, Patel MR, Dai D, et al. Temporal trends and geographic variation of lower-extremity amputation in patients with peripheral artery disease: results from U.S. Medicare 2000-2008. *J Am Coll Cardiol.* 2012;60(21):2230-2236.

48. Hingorani A, LaMuraglia GM, Henke P, et al. The management of diabetic foot: A clinical practice guideline by the Society for Vascular Surgery in collaboration with the American Podiatric Medical Association and the Society for Vascular Medicine. *J Vasc Surg.* 2016;63(2 Suppl):3S-21S.

49. Richards OC, Raines SM, Attie AD. The role of blood vessels, endothelial cells, and vascular pericytes in insulin secretion and peripheral insulin action. *Endocr Rev.* 2010;31(3):343-363.

50. Baron AD. Hemodynamic actions of insulin. *Am J Physiol.* 1994;267(2 Pt 1):E187-202.

51. Barrett EJ, Eggleston EM, Inyard AC, et al. The vascular actions of insulin control its delivery to muscle and regulate the rate-limiting step in skeletal muscle insulin action. *Diabetologia.* 2009;52(5):752-764.

52. Clark MG. Impaired microvascular perfusion: a consequence of vascular dysfunction and a potential cause of insulin resistance in muscle. *Am J Physiol Endocrinol Metab.* 2008;295(4):E732-750.

53. Lillioja S, Young AA, Culter CL, et al. Skeletal muscle capillary density and fiber type are possible determinants of in vivo insulin resistance in man. *J Clin Invest.* 1987;80(2):415-424.

54. Ricard N, Tu L, Le Hiress M, et al. Increased pericyte coverage mediated by endothelial-derived fibroblast growth factor-2 and interleukin-6 is a source of smooth muscle-like cells in pulmonary hypertension. *Circulation.* 2014;129(15):1586-1597.

55. Tilton RG, Faller AM, Burkhardt JK, Hoffmann PL, Kilo C, Williamson JR. Pericyte degeneration and acellular capillaries are increased in the feet of human diabetic patients. *Diabetologia.* 1985;28(12):895-900.

56. Schieber MN, Hasenkamp RM, Pipinos, II, et al. Muscle strength and control characteristics are altered by peripheral artery disease. *J Vasc Surg.* 2017;66(1):178-186 e112.

57. Myers SA, Applequist BC, Huisinga JM, Pipinos, II, Johanning JM. Gait kinematics and kinetics are affected more by peripheral arterial disease than by age. *J Rehabil Res Dev.* 2016;53(2):229-238.

58. Koutakis P, Johanning JM, Haynatzki GR, et al. Abnormal joint powers before and after the onset of claudication symptoms. *J Vasc Surg.* 2010;52(2):340-347.

59. Koutakis P, Miserlis D, Myers SA, et al. Abnormal accumulation of desmin in gastrocnemius myofibers of patients with peripheral artery disease: associations with altered myofiber morphology and density, mitochondrial dysfunction and impaired limb function. *J Histochem Cytochem.* 2015;63(4):256-269.

60. Long CA, Timmins LH, Koutakis P, et al. An endovascular model of ischemic myopathy from peripheral arterial disease. *J Vasc Surg.* 2017;66(3):891-901.

61. Weiss DJ, Casale GP, Koutakis P, et al. Oxidative damage and myofiber degeneration in the gastrocnemius of patients with peripheral arterial disease. *J Transl Med.* 2013;11:230.

62. Garg PK, Liu K, Ferrucci L, et al. Lower extremity nerve function, calf skeletal muscle characteristics, and functional performance in peripheral arterial disease. *J Am Geriatr Soc.* 2011;59(10):1855-1863.

63. Pipinos, II, Swanson SA, Zhu Z, et al. Chronically ischemic mouse skeletal muscle exhibits myopathy in association with mitochondrial dysfunction and oxidative damage. *Am J Physiol Regul Integr Comp Physiol.* 2008;295(1):R290-296.

64. Pipinos, II, Judge AR, Selsby JT, et al. The myopathy of peripheral arterial occlusive disease: part 1. Functional and histomorphological changes and evidence for mitochondrial dysfunction. *Vasc Endovascular Surg.* 2007;41(6):481-489.

65. Makris KI, Nella AA, Zhu Z, et al. Mitochondriopathy of peripheral arterial disease. *Vascular.* 2007;15(6):336-343.

66. Brass EP, Hiatt WR. Acquired skeletal muscle metabolic myopathy in atherosclerotic peripheral arterial disease. *Vasc Med.* 2000;5(1):55-59.

67. Ha DM, Carpenter LC, Koutakis P, et al. Transforming growth factor-beta 1 produced by vascular smooth muscle cells predicts fibrosis in the gastrocnemius of patients with peripheral artery disease. *J Transl Med.* 2016;14:39.

68. Xu J, Shi GP. Vascular wall extracellular matrix proteins and vascular diseases. *Biochim Biophys Acta.* 2014;1842(11):2106-2119.

69. Armulik A, Abramsson A, Betsholtz C. Endothelial/pericyte interactions. *Circ Res.* 2005;97(6):512-523.

70. Laughlin MH, Schrage WG. Effects of muscle contraction on skeletal muscle blood flow: when is there a muscle pump? *Med Sci Sports Exerc.* 1999;31(7):1027-1035.

71. Eltzschig HK, Eckle T. Ischemia and reperfusion--from mechanism to translation. *Nat Med.* 2011;17(11):1391-1401.

72. Zhang X, Zhang W, Ma SF, et al. Hypoxic response contributes to altered gene expression and precapillary pulmonary hypertension in patients with sickle cell disease. *Circulation.* 2014;129(16):1650-1658.

73. Zhou X, Yuan P, He Y. Role of microRNAs in peripheral artery disease (review). *Mol Med Rep.* 2012;6(4):695-700.

74. Pipinos, II, Judge AR, Zhu Z, et al. Mitochondrial defects and oxidative damage in patients with peripheral arterial disease. *Free Radic Biol Med.* 2006;41(2):262-269.

75. Rontoyanni VG, Nunez Lopez O, Fankhauser GT, Cheema ZF, Rasmussen BB, Porter C. Mitochondrial Bioenergetics in the Metabolic Myopathy Accompanying Peripheral Artery Disease. *Front Physiol.* 2017;8:141.

76. Hiatt WR, Wolfel EE, Regensteiner JG, Brass EP. Skeletal muscle carnitine metabolism in patients with unilateral peripheral arterial disease. *J Appl Physiol (1985).* 1992;73(1):346-353.

77. Hiatt WR, Armstrong EJ, Larson CJ, Brass EP. Pathogenesis of the limb manifestations and exercise limitations in peripheral artery disease. *Circ Res.* 2015;116(9):1527-1539.

78. Conley KE. Mitochondria to motion: optimizing oxidative phosphorylation to improve exercise performance. *J Exp Biol.* 2016;219(Pt 2):243-249.

79. Koutakis P, Weiss DJ, Miserlis D, et al. Oxidative damage in the gastrocnemius of patients with peripheral artery disease is myofiber type selective. *Redox Biol.* 2014;2:921-928.

80. Pipinos, II, Sharov VG, Shepard AD, et al. Abnormal mitochondrial respiration in skeletal muscle in patients with peripheral arterial disease. *J Vasc Surg.* 2003;38(4):827-832.

81. Kemp GJ, Hands LJ, Ramaswami G, et al. Calf muscle mitochondrial and glycogenolytic ATP synthesis in patients with claudication due to peripheral vascular disease analysed using 31P magnetic resonance spectroscopy. *Clin Sci (Lond).* 1995;89(6):581-590.

82. Baum O, Torchetti E, Malik C, et al. Capillary ultrastructure and mitochondrial volume density in skeletal muscle in relation to reduced exercise capacity of patients with intermittent claudication. *Am J Physiol Regul Integr Comp Physiol.* 2016;310(10):R943-951.

83. Angquist KA, Sjostrom M. Intermittent claudication and muscle fiber fine structure: morphometric data on mitochondrial volumes. *Ultrastruct Pathol.* 1980;1(4):461-470.

84. Elander A, Sjostrom M, Lundgren F, Schersten T, Bylund-Fellenius AC. Biochemical and morphometric properties of mitochondrial populations in human muscle fibres. *Clin Sci (Lond).* 1985;69(2):153-164.

85. Makitie J, Teravainen H. Histochemical changes in striated muscle in patients with intermittent claudication. *Arch Pathol Lab Med.* 1977;101(12):658-663.

86. Marbini A, Gemignani F, Scoditti U, Rustichelli P, Bragaglia MM, Govoni E. Abnormal muscle mitochondria in ischemic claudication. *Acta Neurol Belg.* 1986;86(5):304-310.

87. Cluff K, Miserlis D, Naganathan GK, et al. Morphometric analysis of gastrocnemius muscle biopsies from patients with peripheral arterial disease: objective grading of muscle degeneration. *Am J Physiol Regul Integr Comp Physiol.* 2013;305(3):R291-299.

88. Hedberg B, Angquist KA, Henriksson-Larsen K, Sjostrom M. Fibre loss and distribution in skeletal muscle from patients with severe peripheral arterial insufficiency. *Eur J Vasc Surg.* 1989;3(4):315-322.

89. Hedberg B, Langstrom M, Angquist KA, Fugl-Meyer AR. Isokinetic plantar flexor performance and fatiguability in peripheral arterial insufficiency. Effects of training vs. vascular surgery. *Acta Chir Scand.* 1988;154(5-6):363-369.

90. McDermott MM, Criqui MH, Greenland P, et al. Leg strength in peripheral arterial disease: associations with disease severity and lower-extremity performance. *J Vasc Surg.* 2004;39(3):523-530.

91. McDermott MM, Liu K, Tian L, et al. Calf muscle characteristics, strength measures, and mortality in peripheral arterial disease: a longitudinal study. *J Am Coll Cardiol.* 2012;59(13):1159-1167.

92. Regensteiner JG, Wolfel EE, Brass EP, et al. Chronic changes in skeletal muscle histology and function in peripheral arterial disease. *Circulation.* 1993;87(2):413-421.

93. Wynn TA. Cellular and molecular mechanisms of fibrosis. *J Pathol.* 2008;214(2):199-210.

94. Farinon AM, Marbini A, Gemignani F, et al. Skeletal muscle and peripheral nerve changes caused by chronic arterial insufficiency--significance and clinical correlations--histological, histochemical and ultrastructural study. *Clin Neuropathol.* 1984;3(6):240-252.

95. Serrano AL, Mann CJ, Vidal B, Ardite E, Perdiguero E, Munoz-Canoves P. Cellular and molecular mechanisms regulating fibrosis in skeletal muscle repair and disease. *Curr Top Dev Biol.* 2011;96:167-201.

96. Mann CJ, Perdiguero E, Kharraz Y, et al. Aberrant repair and fibrosis development in skeletal muscle. *Skelet Muscle.* 2011;1(1):21.

97. J.R. Thompson GPC, S.A. Swanson, P. Koutakis, K.Kim, E. Papoutsi, Z. Zhu, D. Miserlis, D. Ha, J.M Johanning, I. Pipinos. Quantification of Cytokines in the Gastrocnemius and Serum of Claudicating Patients with Peripheral Arterial Disease. *J Surg Res.* 2013;179(2):281-282.

98. Richter K, Konzack A, Pihlajaniemi T, Heljasvaara R, Kietzmann T. Redox-fibrosis: Impact of TGFbeta1 on ROS generators, mediators and functional consequences. *Redox Biol.* 2015;6:344-352.

99. Aschwanden M, Partovi S, Jacobi B, et al. Assessing the end-organ in peripheral arterial occlusive disease-from contrast-enhanced ultrasound to blood-oxygen-level-dependent MR imaging. *Cardiovasc Diagn Ther.* 2014;4(2):165-172.

100. Versluis B, Backes WH, van Eupen MG, et al. Magnetic resonance imaging in peripheral arterial disease: reproducibility of the assessment of morphological and functional vascular status. *Invest Radiol.* 2011;46(1):11-24.

101. Ledermann HP, Schulte AC, Heidecker HG, et al. Blood oxygenation level-dependent magnetic resonance imaging of the skeletal muscle in patients with peripheral arterial occlusive disease. *Circulation.* 2006;113(25):2929-2935.

102. Amarteifio E, Krix M, Wormsbecher S, et al. Dynamic contrast-enhanced ultrasound for assessment of therapy effects on skeletal muscle microcirculation in peripheral arterial disease: pilot study. *Eur J Radiol.* 2013;82(4):640-646.

103. Lindner JR, Womack L, Barrett EJ, et al. Limb stress-rest perfusion imaging with contrast ultrasound for the assessment of peripheral arterial disease severity. *JACC Cardiovasc Imaging.* 2008;1(3):343-350.

104. Kaspar M, Partovi S, Aschwanden M, et al. Assessment of microcirculation by contrast-enhanced ultrasound: a new approach in vascular medicine. *Swiss Med Wkly.* 2015;145:w14047.

105. Seol SH, Lindner JR. A primer on the methods and applications for contrast echocardiography in clinical imaging. *J Cardiovasc Ultrasound.* 2014;22(3):101-110.

106. Mehta KS, Lee JJ, Taha AG, Avgerinos E, Chaer RA. Vascular applications of contrast-enhanced ultrasound imaging. *J Vasc Surg.* 2017;66(1):266-274.

107. Krix M, Weber MA, Kauczor HU, Delorme S, Krakowski-Roosen H. Changes in the micro-circulation of skeletal muscle due to varied isometric exercise assessed by contrast-enhanced ultrasound. *Eur J Radiol.* 2010;76(1):110-116.

108. Amarteifio E, Wormsbecher S, Krix M, et al. Dynamic contrast-enhanced ultrasound and transient arterial occlusion for quantification of arterial perfusion reserve in peripheral arterial disease. *Eur J Radiol.* 2012;81(11):3332-3338.

109. Duerschmied D, Zhou Q, Rink E, et al. Simplified contrast ultrasound accurately reveals muscle perfusion deficits and reflects collateralization in PAD. *Atherosclerosis.* 2009;202(2):505-512.

110. Bragadeesh T, Sari I, Pascotto M, Micari A, Kaul S, Lindner JR. Detection of peripheral vascular stenosis by assessing skeletal muscle flow reserve. *J Am Coll Cardiol.* 2005;45(5):780-785.

111. Wei K, Jayaweera AR, Firoozan S, Linka A, Skyba DM, Kaul S. Quantification of myocardial blood flow with ultrasound-induced destruction of microbubbles administered as a constant venous infusion. *Circulation.* 1998;97(5):473-483.

112. Ghanem A, DeMaria AN, Lohmaier S, et al. Triggered replenishment imaging reduces variability of quantitative myocardial contrast echocardiography and allows assessment of myocardial blood flow reserve. *Echocardiography.* 2007;24(2):149-158.

113. Kuntz-Hehner S, Goenechea J, Pohl C, et al. Continuous-infusion contrast-enhanced US: in vitro studies of infusion techniques with different contrast agents. *Radiology.* 2001;220(3):647-654.

114. Davidson BP, Hodovan J, Belcik JT, et al. Rest-Stress Limb Perfusion Imaging in Humans with Contrast Ultrasound Using Intermediate-Power Imaging and Microbubbles Resistant to Inertial Cavitation. *J Am Soc Echocardiogr.* 2017;30(5):503-510 e501.

115. Rucker M, Strobel O, Vollmar B, Roesken F, Menger MD. Vasomotion in critically perfused muscle protects adjacent tissues from capillary perfusion failure. *Am J Physiol Heart Circ Physiol.* 2000;279(2):H550-558.

116. Jayaweera AR, Wei K, Coggins M, Bin JP, Goodman C, Kaul S. Role of capillaries in determining CBF reserve: new insights using myocardial contrast echocardiography. *Am J Physiol.* 1999;277(6):H2363-2372.

117. Pascotto M, Leong-Poi H, Kaufmann B, et al. Assessment of ischemia-induced microvascular remodeling using contrast-enhanced ultrasound vascular anatomic mapping. *J Am Soc Echocardiogr.* 2007;20(9):1100-1108.

118. Clerk LH, Vincent MA, Barrett EJ, Lankford MF, Lindner JR. Skeletal muscle capillary responses to insulin are abnormal in late-stage diabetes and are

restored by angiotensin-converting enzyme inhibition. *Am J Physiol Endocrinol Metab.* 2007;293(6):E1804-1809.

119. Damon DH, Duling BR. Evidence that capillary perfusion heterogeneity is not controlled in striated muscle. *Am J Physiol.* 1985;249(2 Pt 2):H386-392.

120. Honig CR, Odoroff CL, Frierson JL. Capillary recruitment in exercise: rate, extent, uniformity, and relation to blood flow. *Am J Physiol.* 1980;238(1):H31-42.

121. Slaaf DW, Oude Egbrink MG. Capillaries and flow redistribution play an important role in muscle blood flow reserve capacity. *J Mal Vasc.* 2002;27(2):63-67.

122. Murrant CL, Sarelius IH. Coupling of muscle metabolism and muscle blood flow in capillary units during contraction. *Acta Physiol Scand.* 2000;168(4):531-541.

123. Clifford PS, Hellsten Y. Vasodilatory mechanisms in contracting skeletal muscle. *J Appl Physiol (1985).* 2004;97(1):393-403.

124. Abe T, Kearns CF, Sato Y. Muscle size and strength are increased following walk training with restricted venous blood flow from the leg muscle, Kaatsu-walk training. *J Appl Physiol (1985).* 2006;100(5):1460-1466.

125. Bearden SE. Effect of aging on the structure and function of skeletal muscle microvascular networks. *Microcirculation.* 2006;13(4):279-288.

126. Black MA, Cable NT, Thijssen DH, Green DJ. Importance of measuring the time course of flow-mediated dilatation in humans. *Hypertension.* 2008;51(2):203-210.

127. Muller-Delp JM. Aging-induced adaptations of microvascular reactivity. *Microcirculation.* 2006;13(4):301-314.

128. Taddei S, Virdis A, Ghiadoni L, et al. Age-related reduction of NO availability and oxidative stress in humans. *Hypertension.* 2001;38(2):274-279.

129. Lyons D, Roy S, Patel M, Benjamin N, Swift CG. Impaired nitric oxide-mediated vasodilatation and total body nitric oxide production in healthy old age. *Clin Sci (Lond).* 1997;93(6):519-525.

130. Proctor DN, Parker BA. Vasodilation and vascular control in contracting muscle of the aging human. *Microcirculation.* 2006;13(4):315-327.

131. Ferrari AU, Radaelli A, Centola M. Invited review: aging and the cardiovascular system. *J Appl Physiol (1985).* 2003;95(6):2591-2597.

132. Thomas KN, Cotter JD, Lucas SJ, Hill BG, van Rij AM. Reliability of contrast-enhanced ultrasound for the assessment of muscle perfusion in health and peripheral arterial disease. *Ultrasound Med Biol.* 2015;41(1):26-34.

133. Kundi R, Prior SJ, Addison O, Lu M, Ryan AS, Lal BK. Contrast-Enhanced Ultrasound Reveals Exercise-Induced Perfusion Deficits in Claudicants. *J Vasc Endovasc Surg.* 2017;2(1).

134. Amarteifio E, Weber MA, Wormsbecher S, et al. Dynamic contrast-enhanced ultrasound for assessment of skeletal muscle microcirculation in peripheral arterial disease. *Invest Radiol.* 2011;46(8):504-508.

135. Duerschmied D, Olson L, Olschewski M, et al. Contrast ultrasound perfusion imaging of lower extremities in peripheral arterial disease: a novel diagnostic method. *Eur Heart J.* 2006;27(3):310-315.

136. Duerschmied D, Maletzki P, Freund G, et al. Analysis of muscle microcirculation in advanced diabetes mellitus by contrast enhanced ultrasound. *Diabetes Res Clin Pract.* 2008;81(1):88-92.

137. Mancini M, Di Donato O, Saldalamacchia G, Liuzzi R, Rivellese A, Salvatore M. Contrast-enhanced ultrasound evaluation of peripheral microcirculation in diabetic patients: effects of cigarette smoking. *Radiol Med.* 2013;118(2):206-214.

138. Meneses AL, Nam MCY, Bailey TG, et al. Leg Blood Flow and Skeletal Muscle Microvascular Perfusion Responses to Submaximal Exercise in Peripheral Arterial Disease. *Am J Physiol Heart Circ Physiol.* 2018.

139. Duerschmied D, Maletzki P, Freund G, Olschewski M, Bode C, Hehrlein C. Success of arterial revascularization determined by contrast ultrasound muscle perfusion imaging. *J Vasc Surg.* 2010;52(6):1531-1536.

140. Celermajer DS, Adams MR, Clarkson P, et al. Passive smoking and impaired endothelium-dependent arterial dilatation in healthy young adults. *N Engl J Med.* 1996;334(3):150-154.

141. Pellaton C, Kubli S, Feihl F, Waeber B. Blunted vasodilatory responses in the cutaneous microcirculation of cigarette smokers. *Am Heart J.* 2002;144(2):269-274.

142. Binder S, Navratil K, Halek J. Chronic smoking and its effect on arterial stiffness. *Biomed Pap Med Fac Univ Palacky Olomouc Czech Repub.* 2008;152(2):299-302.

143. Stefanadis C, Tsiamis E, Vlachopoulos C, et al. Unfavorable effect of smoking on the elastic properties of the human aorta. *Circulation.* 1997;95(1):31-38.

144. Davidson BP, Belcik JT, Landry G, Linden J, Lindner JR. Exercise versus vasodilator stress limb perfusion imaging for the assessment of peripheral artery disease. *Echocardiography.* 2017;34(8):1187-1194.

145. Belcik JT, Mott BH, Xie A, et al. Augmentation of limb perfusion and reversal of tissue ischemia produced by ultrasound-mediated microbubble cavitation. *Circ Cardiovasc Imaging.* 2015;8(4).

146. Bachle AC, Morsdorf P, Rezaeian F, Ong MF, Harder Y, Menger MD. N-acetylcysteine attenuates leukocytic inflammation and microvascular perfusion failure in critically ischemic random pattern flaps. *Microvasc Res.* 2011;82(1):28-34.

147. Ozmen S, Ayhan S, Demir Y, Siemionow M, Atabay K. Impact of gradual blood flow increase on ischaemia-reperfusion injury in the rat cremaster microcirculation model. *J Plast Reconstr Aesthet Surg.* 2008;61(8):939-948.

148. Krishna SM, Moxon JV, Golledge J. A review of the pathophysiology and potential biomarkers for peripheral artery disease. *Int J Mol Sci.* 2015;16(5):11294-11322.

149. Creager MA, Roddy MA. Effect of captopril and enalapril on endothelial function in hypertensive patients. *Hypertension.* 1994;24(4):499-505.

150. Guzik TJ, Mussa S, Gastaldi D, et al. Mechanisms of increased vascular superoxide production in human diabetes mellitus: role of NAD(P)H oxidase and endothelial nitric oxide synthase. *Circulation.* 2002;105(14):1656-1662.

151. Ruschitzka F, Shaw S, Gygi D, Noll G, Barton M, Luscher TF. Endothelial dysfunction in acute renal failure: role of circulating and tissue endothelin-1. *J Am Soc Nephrol.* 1999;10(5):953-962.

152. Girn HR, Orsi NM, Homer-Vanniasinkam S. An overview of cytokine interactions in atherosclerosis and implications for peripheral arterial disease. *Vasc Med.* 2007;12(4):299-309.

153. McDermott MM, Liu K, Ferrucci L, et al. Circulating blood markers and functional impairment in peripheral arterial disease. *J Am Geriatr Soc.* 2008;56(8):1504-1510.

154. Cheng CH, Chen YS, Shu KH, Chang HR, Chou MC. Higher serum levels of soluble intracellular cell adhesion molecule-1 and soluble vascular cell adhesion molecule predict peripheral artery disease in haemodialysis patients. *Nephrology (Carlton).* 2012;17(8):718-724.

155. Gardner AW, Parker DE, Montgomery PS, et al. Gender and racial differences in endothelial oxidative stress and inflammation in patients with symptomatic peripheral artery disease. *J Vasc Surg.* 2015;61(5):1249-1257.

156. Casey DP, Joyner MJ. Local control of skeletal muscle blood flow during exercise: influence of available oxygen. *J Appl Physiol (1985).* 2011;111(6):1527-1538.

157. Loffredo L, Pignatelli P, Cangemi R, et al. Imbalance between nitric oxide generation and oxidative stress in patients with peripheral arterial disease: effect of an antioxidant treatment. *J Vasc Surg.* 2006;44(3):525-530.

158. Boger RH, Bode-Boger SM, Thiele W, Junker W, Alexander K, Frolich JC. Biochemical evidence for impaired nitric oxide synthesis in patients with peripheral arterial occlusive disease. *Circulation.* 1997;95(8):2068-2074.

159. Phillips SA, Mahmoud AM, Brown MD, Haus JM. Exercise interventions and peripheral arterial function: implications for cardio-metabolic disease. *Prog Cardiovasc Dis.* 2015;57(5):521-534.

160. Li JM, Shah AM. Endothelial cell superoxide generation: regulation and relevance for cardiovascular pathophysiology. *Am J Physiol Regul Integr Comp Physiol.* 2004;287(5):R1014-1030.

161. Thomson IA, Egginton S, Simms MH, Hudlicka O. Effect of muscle ischaemia and iloprost during femorodistal reconstruction on capillary endothelial swelling. *Int J Microcirc Clin Exp.* 1996;16(6):284-290.

162. Hudlicka O, Garnham A, Shiner R, Egginton S. Attenuation of changes in capillary fine structure and leukocyte adhesion improves muscle performance following chronic ischaemia in rats. *J Physiol.* 2008;586(20):4961-4975.

163. Strock PE, Majno G. Microvascular changes in acutely ischemic rat muscle. *Surg Gynecol Obstet.* 1969;129(6):1213-1224.

164. Gidlof A, Lewis DH, Hammersen F. The effect of prolonged total ischemia on the ultrastructure of human skeletal muscle capillaries. A morphometric analysis. *Int J Microcirc Clin Exp.* 1988;7(1):67-86.

165. Mazzoni MC, Intaglietta M, Cragoe EJ, Jr., Arfors KE. Amiloride-sensitive Na+ pathways in capillary endothelial cell swelling during hemorrhagic shock. *J Appl Physiol (1985).* 1992;73(4):1467-1473.

166. Mazzoni MC, Cragoe EJ, Jr., Arfors KE. Systemic blood acidosis in low-flow ischemia induces capillary luminal narrowing. *Int J Microcirc Clin Exp.* 1994;14(3):144-150.

167. Hickey NC, Hudlicka O, Simms MH. Claudication induces systemic capillary endothelial swelling. *Eur J Vasc Surg.* 1992;6(1):36-40.

168. Egginton S, Hudlicka O. Early changes in performance, blood flow and capillary fine structure in rat fast muscles induced by electrical stimulation. *J Physiol.* 1999;515 (Pt 1):265-275.

169. Hughes S, Gardiner T, Hu P, Baxter L, Rosinova E, Chan-Ling T. Altered pericyte-endothelial relations in the rat retina during aging: implications for vessel stability. *Neurobiol Aging.* 2006;27(12):1838-1847.

170. Vracko R, Benditt EP. Basal lamina: the scaffold for orderly cell replacement. Observations on regeneration of injured skeletal muscle fibers and capillaries. *J Cell Biol.* 1972;55(2):406-419.

171. Baum O, Djonov V, Ganster M, Widmer M, Baumgartner I. Arteriolization of capillaries and FGF-2 upregulation in skeletal muscles of patients with chronic peripheral arterial disease. *Microcirculation.* 2005;12(6):527-537.

172. Baum O, Bigler M. Pericapillary basement membrane thickening in human skeletal muscles. *Am J Physiol Heart Circ Physiol.* 2016;311(3):H654-666.

173. Ho TK, Rajkumar V, Black CM, Abraham DJ, Baker DM. Increased angiogenic response but deficient arteriolization and abnormal microvessel ultrastructure in critical leg ischaemia. *Br J Surg.* 2006;93(11):1368-1376.

174. Makitie J. Skeletal muscle capillaries in intermittent claudication. *Arch Pathol Lab Med.* 1977;101(9):500-503.

175. Bigler M, Koutsantonis D, Odriozola A, et al. Morphometry of skeletal muscle capillaries: the relationship between capillary ultrastructure and ageing in humans. *Acta Physiol (Oxf).* 2016;218(2):98-111.

176. Galatius S, Bent-Hansen L, Wroblewski H, Sorensen VB, Norgaard T, Kastrup J. Plasma disappearance of albumin and impact of capillary thickness in idiopathic dilated cardiomyopathy and after heart transplantation. *Circulation.* 2000;102(3):319-325.

177. Baum O, Gubeli J, Frese S, et al. Angiogenesis-related ultrastructural changes to capillaries in human skeletal muscle in response to endurance exercise. *J Appl Physiol (1985).* 2015;119(10):1118-1126.

178. Baum O, Ganster M, Baumgartner I, Nieselt K, Djonov V. Basement membrane remodeling in skeletal muscles of patients with limb ischemia involves regulation of matrix metalloproteinases and tissue inhibitor of matrix metalloproteinases. *J Vasc Res.* 2007;44(3):202-213.

179. Kemeny SF, Figueroa DS, Andrews AM, Barbee KA, Clyne AM. Glycated collagen alters endothelial cell actin alignment and nitric oxide release in response to fluid shear stress. *J Biomech.* 2011;44(10):1927-1935.

180. Tilton RG, Kilo C, Williamson JR. Pericyte-endothelial relationships in cardiac and skeletal muscle capillaries. *Microvasc Res.* 1979;18(3):325-335.

181. Murray IR, Baily JE, Chen WCW, et al. Skeletal and cardiac muscle pericytes: Functions and therapeutic potential. *Pharmacol Ther.* 2017;171:65-74.

182. Campagnolo P, Cesselli D, Al Haj Zen A, et al. Human adult vena saphena contains perivascular progenitor cells endowed with clonogenic and proangiogenic potential. *Circulation.* 2010;121(15):1735-1745.

183. Norrmen C, Tammela T, Petrova TV, Alitalo K. Biological basis of therapeutic lymphangiogenesis. *Circulation.* 2011;123(12):1335-1351.

184. Shepro D, Morel NM. Pericyte physiology. *FASEB J.* 1993;7(11):1031-1038.

185. Hirschi KK, D'Amore PA. Pericytes in the microvasculature. *Cardiovasc Res.* 1996;32(4):687-698.

186. LaBarbera KE, Hyldahl RD, O'Fallon KS, Clarkson PM, Witkowski S. Pericyte NF-kappaB activation enhances endothelial cell proliferation and proangiogenic cytokine secretion in vitro. *Physiol Rep.* 2015;3(4).

187. Gokcinar-Yagci B, Uckan-Cetinkaya D, Celebi-Saltik B. Pericytes: Properties, Functions and Applications in Tissue Engineering. *Stem Cell Rev.* 2015;11(4):549-559.

188. von Tell D, Armulik A, Betsholtz C. Pericytes and vascular stability. *Exp Cell Res.* 2006;312(5):623-629.

189. Reigstad LJ, Sande HM, Fluge O, et al. Platelet-derived growth factor (PDGF)-C, a PDGF family member with a vascular endothelial growth factor-like structure. *J Biol Chem.* 2003;278(19):17114-17120.

190. Andrae J, Gallini R, Betsholtz C. Role of platelet-derived growth factors in physiology and medicine. *Genes Dev.* 2008;22(10):1276-1312.

191. Armulik A, Genove G, Betsholtz C. Pericytes: developmental, physiological, and pathological perspectives, problems, and promises. *Dev Cell.* 2011;21(2):193-215.

192. Diaz-Flores L, Gutierrez R, Madrid JF, et al. Pericytes. Morphofunction, interactions and pathology in a quiescent and activated mesenchymal cell niche. *Histol Histopathol.* 2009;24(7):909-969.

193. Sims DE. Diversity within pericytes. *Clin Exp Pharmacol Physiol.* 2000;27(10):842-846.

194. Gerhardt H, Betsholtz C. Endothelial-pericyte interactions in angiogenesis. *Cell Tissue Res.* 2003;314(1):15-23.

195. Bergers G, Song S. The role of pericytes in blood-vessel formation and maintenance. *Neuro Oncol.* 2005;7(4):452-464.

196. van Dijk CG, Nieuweboer FE, Pei JY, et al. The complex mural cell: pericyte function in health and disease. *Int J Cardiol.* 2015;190:75-89.

197. Winkler EA, Bell RD, Zlokovic BV. Central nervous system pericytes in health and disease. *Nat Neurosci.* 2011;14(11):1398-1405.

198. Vezzani B, Pierantozzi E, Sorrentino V. Not All Pericytes Are Born Equal: Pericytes from Human Adult Tissues Present Different Differentiation Properties. *Stem Cells Dev.* 2016.

199. Nees S, Weiss DR, Senftl A, et al. Isolation, bulk cultivation, and characterization of coronary microvascular pericytes: the second most frequent myocardial cell type in vitro. *Am J Physiol Heart Circ Physiol.* 2012;302(1):H69-84.

200. Larson DM, Carson MP, Haudenschild CC. Junctional transfer of small molecules in cultured bovine brain microvascular endothelial cells and pericytes. *Microvasc Res.* 1987;34(2):184-199.

201. Diaz-Flores L, Gutierrez R, Varela H, Rancel N, Valladares F. Microvascular pericytes: a review of their morphological and functional characteristics. *Histol Histopathol.* 1991;6(2):269-286.

202. Dalkara T, Gursoy-Ozdemir Y, Yemisci M. Brain microvascular pericytes in health and disease. *Acta Neuropathol.* 2011;122(1):1-9.

203. Allt G, Lawrenson JG. Pericytes: cell biology and pathology. *Cells Tissues Organs.* 2001;169(1):1-11.

204. Fernandez-Klett F, Offenhauser N, Dirnagl U, Priller J, Lindauer U. Pericytes in capillaries are contractile in vivo, but arterioles mediate functional hyperemia in the mouse brain. *Proc Natl Acad Sci U S A.* 2010;107(51):22290-22295.

205. Dai M, Nuttall A, Yang Y, Shi X. Visualization and contractile activity of cochlear pericytes in the capillaries of the spiral ligament. *Hear Res.* 2009;254(1-2):100-107.

206. Bichsel CA, Hall SR, Schmid RA, Guenat OT, Geiser T. Primary Human Lung Pericytes Support and Stabilize In Vitro Perfusable Microvessels. *Tissue Eng Part A.* 2015;21(15-16):2166-2176.

207. Papetti M, Shujath J, Riley KN, Herman IM. FGF-2 antagonizes the TGF-beta1-mediated induction of pericyte alpha-smooth muscle actin expression: a role for myf-5 and Smad-mediated signaling pathways. *Invest Ophthalmol Vis Sci.* 2003;44(11):4994-5005.

208. Kotecki M, Zeiger AS, Van Vliet KJ, Herman IM. Calpain- and talin-dependent control of microvascular pericyte contractility and cellular stiffness. *Microvasc Res.* 2010;80(3):339-348.

209. Dore-Duffy P, Wang S, Mehedi A, et al. Pericyte-mediated vasoconstriction underlies TBI-induced hypoperfusion. *Neurol Res.* 2011;33(2):176-186.

210. Kamouchi M, Ago T, Kitazono T. Brain pericytes: emerging concepts and functional roles in brain homeostasis. *Cell Mol Neurobiol.* 2011;31(2):175-193.

211. Kamouchi M, Kitazono T, Ago T, et al. Hydrogen peroxide-induced Ca2+ responses in CNS pericytes. *Neurosci Lett.* 2007;416(1):12-16.

212. Rucker HK, Wynder HJ, Thomas WE. Cellular mechanisms of CNS pericytes. *Brain Res Bull.* 2000;51(5):363-369.

213. Hall CN, Reynell C, Gesslein B, et al. Capillary pericytes regulate cerebral blood flow in health and disease. *Nature.* 2014;508(7494):55-60.

214. O'Farrell FM, Attwell D. A role for pericytes in coronary no-reflow. *Nat Rev Cardiol.* 2014;11(7):427-432.

215. Yemisci M, Gursoy-Ozdemir Y, Vural A, Can A, Topalkara K, Dalkara T. Pericyte contraction induced by oxidative-nitrative stress impairs capillary reflow despite

successful opening of an occluded cerebral artery. *Nat Med.* 2009;15(9):1031-1037.

216. Kamouchi M, Ago T, Kuroda J, Kitazono T. The possible roles of brain pericytes in brain ischemia and stroke. *Cell Mol Neurobiol.* 2012;32(2):159-165.

217. Birbrair A, Zhang T, Wang ZM, et al. Type-2 pericytes participate in normal and tumoral angiogenesis. *Am J Physiol Cell Physiol.* 2014;307(1):C25-38.

218. Dar A, Domev H, Ben-Yosef O, et al. Multipotent vasculogenic pericytes from human pluripotent stem cells promote recovery of murine ischemic limb. *Circulation.* 2012;125(1):87-99.

219. Gubernator M, Slater SC, Spencer HL, et al. Epigenetic profile of human adventitial progenitor cells correlates with therapeutic outcomes in a mouse model of limb ischemia. *Arterioscler Thromb Vasc Biol.* 2015;35(3):675-688.

220. Vono R, Fuoco C, Testa S, et al. Activation of the Pro-Oxidant PKCbetaII-p66Shc Signaling Pathway Contributes to Pericyte Dysfunction in Skeletal Muscles of Patients With Diabetes With Critical Limb Ischemia. *Diabetes.* 2016;65(12):3691-3704.

221. Yan J, Tie G, Wang S, et al. Type 2 diabetes restricts multipotency of mesenchymal stem cells and impairs their capacity to augment postischemic neovascularization in db/db mice. *J Am Heart Assoc.* 2012;1(6):e002238.

222. Volz KS, Jacobs AH, Chen HI, et al. Pericytes are progenitors for coronary artery smooth muscle. *Elife.* 2015;4.

223. Crisan M, Yap S, Casteilla L, et al. A perivascular origin for mesenchymal stem cells in multiple human organs. *Cell Stem Cell.* 2008;3(3):301-313.

224. Corselli M, Crisan M, Murray IR, et al. Identification of perivascular mesenchymal stromal/stem cells by flow cytometry. *Cytometry A.* 2013;83(8):714-720.

225. Crisan M, Chen CW, Corselli M, Andriolo G, Lazzari L, Peault B. Perivascular multipotent progenitor cells in human organs. *Ann N Y Acad Sci.* 2009;1176:118-123.

226. Caplan AI, Correa D. The MSC: an injury drugstore. *Cell Stem Cell.* 2011;9(1):11-15.

227. Chen WC, Peault B, Huard J. Regenerative Translation of Human Blood-Vessel-Derived MSC Precursors. *Stem Cells Int.* 2015;2015:375187.

228. Katare R, Riu F, Mitchell K, et al. Transplantation of human pericyte progenitor cells improves the repair of infarcted heart through activation of an angiogenic program involving micro-RNA-132. *Circ Res.* 2011;109(8):894-906.

229. Avolio E, Meloni M, Spencer HL, et al. Combined intramyocardial delivery of human pericytes and cardiac stem cells additively improves the healing of mouse

infarcted hearts through stimulation of vascular and muscular repair. *Circ Res.* 2015;116(10):e81-94.

230. Dellavalle A, Sampaolesi M, Tonlorenzi R, et al. Pericytes of human skeletal muscle are myogenic precursors distinct from satellite cells. *Nat Cell Biol.* 2007;9(3):255-267.

231. Kostallari E, Baba-Amer Y, Alonso-Martin S, et al. Pericytes in the myovascular niche promote post-natal myofiber growth and satellite cell quiescence. *Development.* 2015;142(7):1242-1253.

232. Farup J, De Lisio M, Rahbek SK, et al. Pericyte response to contraction mode-specific resistance exercise training in human skeletal muscle. *J Appl Physiol (1985).* 2015;119(10):1053-1063.

233. Birbrair A, Zhang T, Wang ZM, Messi ML, Mintz A, Delbono O. Type-1 pericytes participate in fibrous tissue deposition in aged skeletal muscle. *Am J Physiol Cell Physiol.* 2013;305(11):C1098-1113.

234. Birbrair A, Zhang T, Wang ZM, et al. Skeletal muscle neural progenitor cells exhibit properties of NG2-glia. *Exp Cell Res.* 2013;319(1):45-63.

235. Lange S, Trost A, Tempfer H, et al. Brain pericyte plasticity as a potential drug target in CNS repair. *Drug Discov Today.* 2013;18(9-10):456-463.

236. Jacobs AH, Tavitian B, consortium IN. Noninvasive molecular imaging of neuroinflammation. *J Cereb Blood Flow Metab.* 2012;32(7):1393-1415.

237. Hung C, Linn G, Chow YH, et al. Role of lung pericytes and resident fibroblasts in the pathogenesis of pulmonary fibrosis. *Am J Respir Crit Care Med.* 2013;188(7):820-830.

238. Olson LE, Soriano P. PDGFRbeta signaling regulates mural cell plasticity and inhibits fat development. *Dev Cell.* 2011;20(6):815-826.

239. Voisin MB, Nourshargh S. Neutrophil transmigration: emergence of an adhesive cascade within venular walls. *J Innate Immun.* 2013;5(4):336-347.

240. Alon R, Nourshargh S. Learning in motion: pericytes instruct migrating innate leukocytes. *Nat Immunol.* 2013;14(1):14-15.

241. Campanholle G, Mittelsteadt K, Nakagawa S, et al. TLR-2/TLR-4 TREM-1 signaling pathway is dispensable in inflammatory myeloid cells during sterile kidney injury. *PLoS One.* 2013;8(7):e68640.

242. Proebstl D, Voisin MB, Woodfin A, et al. Pericytes support neutrophil subendothelial cell crawling and breaching of venular walls in vivo. *J Exp Med.* 2012;209(6):1219-1234.

243. Barron L, Gharib SA, Duffield JS. Lung Pericytes and Resident Fibroblasts: Busy Multitaskers. *Am J Pathol.* 2016;186(10):2519-2531.

244. Wong SP, Rowley JE, Redpath AN, Tilman JD, Fellous TG, Johnson JR. Pericytes, mesenchymal stem cells and their contributions to tissue repair. *Pharmacol Ther.* 2015;151:107-120.

245. Stark K, Eckart A, Haidari S, et al. Capillary and arteriolar pericytes attract innate leukocytes exiting through venules and 'instruct' them with pattern-recognition and motility programs. *Nat Immunol.* 2013;14(1):41-51.

246. Chen WC, Park TS, Murray IR, et al. Cellular kinetics of perivascular MSC precursors. *Stem Cells Int.* 2013;2013:983059.

247. Ma J, Wang Q, Fei T, Han JD, Chen YG. MCP-1 mediates TGF-beta-induced angiogenesis by stimulating vascular smooth muscle cell migration. *Blood.* 2007;109(3):987-994.

248. Rustenhoven J, Scotter EL, Jansson D, et al. An anti-inflammatory role for C/EBPdelta in human brain pericytes. *Sci Rep.* 2015;5:12132.

249. Rowley JE, Johnson JR. Pericytes in chronic lung disease. *Int Arch Allergy Immunol.* 2014;164(3):178-188.

250. Duffield JS, Lupher M, Thannickal VJ, Wynn TA. Host responses in tissue repair and fibrosis. *Annu Rev Pathol.* 2013;8:241-276.

251. Okabe Y, Medzhitov R. Tissue biology perspective on macrophages. *Nat Immunol.* 2016;17(1):9-17.

252. Balabanov R, Washington R, Wagnerova J, Dore-Duffy P. CNS microvascular pericytes express macrophage-like function, cell surface integrin alpha M, and macrophage marker ED-2. *Microvasc Res.* 1996;52(2):127-142.

253. Thomas WE. Brain macrophages: on the role of pericytes and perivascular cells. *Brain Res Brain Res Rev.* 1999;31(1):42-57.

254. Abbott NJ. Astrocyte-endothelial interactions and blood-brain barrier permeability. *J Anat.* 2002;200(6):629-638.

255. Tak PP, Firestein GS. NF-kappaB: a key role in inflammatory diseases. *J Clin Invest.* 2001;107(1):7-11.

256. Baldwin AS, Jr. The NF-kappa B and I kappa B proteins: new discoveries and insights. *Annu Rev Immunol.* 1996;14:649-683.

257. Mourkioti F, Kratsios P, Luedde T, et al. Targeted ablation of IKK2 improves skeletal muscle strength, maintains mass, and promotes regeneration. *J Clin Invest.* 2006;116(11):2945-2954.

258. Cai D, Frantz JD, Tawa NE, Jr., et al. IKKbeta/NF-kappaB activation causes severe muscle wasting in mice. *Cell.* 2004;119(2):285-298.

259. Hyldahl RD, Xin L, Hubal MJ, Moeckel-Cole S, Chipkin S, Clarkson PM. Activation of nuclear factor-kappaB following muscle eccentric contractions in humans is localized primarily to skeletal muscle-residing pericytes. *FASEB J.* 2011;25(9):2956-2966.

260. Huntsman HD, Zachwieja N, Zou K, et al. Mesenchymal stem cells contribute to vascular growth in skeletal muscle in response to eccentric exercise. *Am J Physiol Heart Circ Physiol.* 2013;304(1):H72-81.

261. Sava P, Cook IO, Mahal RS, Gonzalez AL. Human microvascular pericyte basement membrane remodeling regulates neutrophil recruitment. *Microcirculation.* 2015;22(1):54-67.

262. Siwik DA, Chang DL, Colucci WS. Interleukin-1beta and tumor necrosis factor-alpha decrease collagen synthesis and increase matrix metalloproteinase activity in cardiac fibroblasts in vitro. *Circ Res.* 2000;86(12):1259-1265.

263. Summers L, Kangwantas K, Rodriguez-Grande B, et al. Activation of brain endothelial cells by interleukin-1 is regulated by the extracellular matrix after acute brain injury. *Mol Cell Neurosci.* 2013;57:93-103.

264. Sciorati C, Clementi E, Manfredi AA, Rovere-Querini P. Fat deposition and accumulation in the damaged and inflamed skeletal muscle: cellular and molecular players. *Cell Mol Life Sci.* 2015;72(11):2135-2156.

265. Miyata M, Sakuma F, Yoshimura A, Ishikawa H, Nishimaki T, Kasukawa R. Pulmonary hypertension in rats. 2. Role of interleukin-6. *Int Arch Allergy Immunol.* 1995;108(3):287-291.

266. Golembeski SM, West J, Tada Y, Fagan KA. Interleukin-6 causes mild pulmonary hypertension and augments hypoxia-induced pulmonary hypertension in mice. *Chest.* 2005;128(6 Suppl):572S-573S.

267. Dvorak HF, Mihm MC, Jr., Dvorak AM, et al. Morphology of delayed type hypersensitivity reactions in man. I. Quantitative description of the inflammatory response. *Lab Invest.* 1974;31(2):111-130.

268. Dvorak HF, Mihm MC, Jr., Dvorak AM. Morphology of delayed-type hypersensitivity reactions in man. *J Invest Dermatol.* 1976;67(3):391-401.

269. Dvorak AM, Mihm MC, Jr., Dvorak HF. Morphology of delayed-type hypersensitivity reactions in man. II. Ultrastructural alterations affecting the microvasculature and the tissue mast cells. *Lab Invest.* 1976;34(2):179-191.

270. Torres SH, Finol HJ, Montes de Oca M, Vasquez F, Puigbo JJ, Loyo JG. Capillary damage in skeletal muscle in advanced Chagas' disease patients. *Parasitol Res.* 2004;93(5):364-368.

271. Jerusalem F, Rakusa M, Engel AG, MacDonald RD. Morphometric analysis of skeletal muscle capillary ultrastructure in inflammatory myopathies. *J Neurol Sci.* 1974;23(3):391-402.

272. Finol HJ, Gonzalez N, Marquez A. Effects of simultaneous denervation and tenotomy on the ultrastructure of a rat slow twitch muscle. *Acta Cient Venez.* 1992;43(1):26-33.

273. Finol HJ, Muller B, Montes de Oca I, Marquez A. Ultrastructure of skeletal muscle in rheumatoid myositis. *J Rheumatol.* 1988;15(4):552-555.

274. Finol HJ, Marquez A, Montes de Oca I, Muller B. Skeletal muscle ultrastructural alterations in a case of Guillain-Barre syndrome. *Acta Cient Venez.* 1991;42(1):39-44.

275. Pallis M, Hopkinson N, Lowe J, Powell R. An electron microscopic study of muscle capillary wall thickening in systemic lupus erythematosus. *Lupus.* 1994;3(5):401-407.

276. Pallis M, Robson DK, Haskard DO, Powell RJ. Distribution of cell adhesion molecules in skeletal muscle from patients with systemic lupus erythematosus. *Ann Rheum Dis.* 1993;52(9):667-671.

277. Johnson JR, Folestad E, Rowley JE, et al. Pericytes contribute to airway remodeling in a mouse model of chronic allergic asthma. *Am J Physiol Lung Cell Mol Physiol.* 2015;308(7):L658-671.

278. Siemionow M, Demir Y. Diabetic neuropathy: pathogenesis and treatment. *J Reconstr Microsurg.* 2004;20(3):241-252.

279. Tilton RG, Kilo C, Williamson JR, Murch DW. Differences in pericyte contractile function in rat cardiac and skeletal muscle microvasculatures. *Microvasc Res.* 1979;18(3):336-352.

280. Rattigan S, Bradley EA, Richards SM, Clark MG. Muscle metabolism and control of capillary blood flow: insulin and exercise. *Essays Biochem.* 2006;42:133-144.

281. Coggins M, Lindner J, Rattigan S, et al. Physiologic hyperinsulinemia enhances human skeletal muscle perfusion by capillary recruitment. *Diabetes.* 2001;50(12):2682-2690.

282. Rattigan S, Clark MG, Barrett EJ. Hemodynamic actions of insulin in rat skeletal muscle: evidence for capillary recruitment. *Diabetes.* 1997;46(9):1381-1388.

283. Zhang L, Vincent MA, Richards SM, et al. Insulin sensitivity of muscle capillary recruitment in vivo. *Diabetes.* 2004;53(2):447-453.

284. Marriott S, Baskir RS, Gaskill C, et al. ABCG2pos lung mesenchymal stem cells are a novel pericyte subpopulation that contributes to fibrotic remodeling. *Am J Physiol Cell Physiol.* 2014;307(8):C684-698.

285. Mitchell TS, Bradley J, Robinson GS, Shima DT, Ng YS. RGS5 expression is a quantitative measure of pericyte coverage of blood vessels. *Angiogenesis.* 2008;11(2):141-151.

286. Cho H, Kozasa T, Bondjers C, Betsholtz C, Kehrl JH. Pericyte-specific expression of Rgs5: implications for PDGF and EDG receptor signaling during vascular maturation. *FASEB J.* 2003;17(3):440-442.

287. Goritz C, Dias DO, Tomilin N, Barbacid M, Shupliakov O, Frisen J. A pericyte origin of spinal cord scar tissue. *Science.* 2011;333(6039):238-242.

288. Schrimpf C, Xin C, Campanholle G, et al. Pericyte TIMP3 and ADAMTS1 modulate vascular stability after kidney injury. *J Am Soc Nephrol.* 2012;23(5):868-883.

289. Ren S, Johnson BG, Kida Y, et al. LRP-6 is a coreceptor for multiple fibrogenic signaling pathways in pericytes and myofibroblasts that are inhibited by DKK-1. *Proc Natl Acad Sci U S A.* 2013;110(4):1440-1445.

290. Hernandez N, Torres SH, Finol HJ, Vera O. Capillary changes in skeletal muscle of patients with essential hypertension. *Anat Rec.* 1999;256(4):425-432.

291. Stratman AN, Schwindt AE, Malotte KM, Davis GE. Endothelial-derived PDGF-BB and HB-EGF coordinately regulate pericyte recruitment during vasculogenic tube assembly and stabilization. *Blood.* 2010;116(22):4720-4730.

292. Stratman AN, Malotte KM, Mahan RD, Davis MJ, Davis GE. Pericyte recruitment during vasculogenic tube assembly stimulates endothelial basement membrane matrix formation. *Blood.* 2009;114(24):5091-5101.

293. Sa-Pereira I, Brites D, Brito MA. Neurovascular unit: a focus on pericytes. *Mol Neurobiol.* 2012;45(2):327-347.

294. DiMario J, Buffinger N, Yamada S, Strohman RC. Fibroblast growth factor in the extracellular matrix of dystrophic (mdx) mouse muscle. *Science.* 1989;244(4905):688-690.

295. Hallmann R, Horn N, Selg M, Wendler O, Pausch F, Sorokin LM. Expression and function of laminins in the embryonic and mature vasculature. *Physiol Rev.* 2005;85(3):979-1000.

296. Ziyadeh FN. Mediators of diabetic renal disease: the case for tgf-Beta as the major mediator. *J Am Soc Nephrol.* 2004;15 Suppl 1:S55-57.

297. Finol HJ, Muller B, Torres SH, Dominguez JJ, Perdomo P, Montes de Oca I. Ultrastructural abnormalities in muscular vessels of hyperthyroid patients. *Acta Neuropathol.* 1986;71(1-2):64-69.

298. Vlodavsky EA, Ludatscher RM, Sabo E, Kerner H. Evaluation of muscle capillary basement membrane in inflammatory myopathy. A morphometric ultrastructural study. *Virchows Arch.* 1999;435(1):58-61.

299. Ludatscher RM. Patterns of regeneration in vessels of human diseased muscle and skin. An ultrastructural study. *Virchows Arch B Cell Pathol Incl Mol Pathol.* 1981;36(1):65-75.

300. Uezumi A, Ikemoto-Uezumi M, Tsuchida K. Roles of nonmyogenic mesenchymal progenitors in pathogenesis and regeneration of skeletal muscle. *Front Physiol.* 2014;5:68.

301. Dulauroy S, Di Carlo SE, Langa F, Eberl G, Peduto L. Lineage tracing and genetic ablation of ADAM12(+) perivascular cells identify a major source of profibrotic cells during acute tissue injury. *Nat Med.* 2012;18(8):1262-1270.

302. Lin SL, Kisseleva T, Brenner DA, Duffield JS. Pericytes and perivascular fibroblasts are the primary source of collagen-producing cells in obstructive fibrosis of the kidney. *Am J Pathol.* 2008;173(6):1617-1627.

303. Ito I, Fixman ED, Asai K, et al. Platelet-derived growth factor and transforming growth factor-beta modulate the expression of matrix metalloproteinases and migratory function of human airway smooth muscle cells. *Clin Exp Allergy.* 2009;39(9):1370-1380.

304. Cambier S, Gline S, Mu D, et al. Integrin alpha(v)beta8-mediated activation of transforming growth factor-beta by perivascular astrocytes: an angiogenic control switch. *Am J Pathol.* 2005;166(6):1883-1894.

305. Wipff PJ, Hinz B. Integrins and the activation of latent transforming growth factor beta1 - an intimate relationship. *Eur J Cell Biol.* 2008;87(8-9):601-615.

306. Shi M, Zhu J, Wang R, et al. Latent TGF-beta structure and activation. *Nature.* 2011;474(7351):343-349.

307. Hirschi KK, Burt JM, Hirschi KD, Dai C. Gap junction communication mediates transforming growth factor-beta activation and endothelial-induced mural cell differentiation. *Circ Res.* 2003;93(5):429-437.

308. Sato Y, Rifkin DB. Inhibition of endothelial cell movement by pericytes and smooth muscle cells: activation of a latent transforming growth factor-beta 1-like molecule by plasmin during co-culture. *J Cell Biol.* 1989;109(1):309-315.

309. Antonelli-Orlidge A, Saunders KB, Smith SR, D'Amore PA. An activated form of transforming growth factor beta is produced by cocultures of endothelial cells and pericytes. *Proc Natl Acad Sci U S A.* 1989;86(12):4544-4548.

310. Carvalho RL, Jonker L, Goumans MJ, et al. Defective paracrine signalling by TGFbeta in yolk sac vasculature of endoglin mutant mice: a paradigm for hereditary haemorrhagic telangiectasia. *Development.* 2004;131(24):6237-6247.

311. Goumans MJ, Valdimarsdottir G, Itoh S, Rosendahl A, Sideras P, ten Dijke P. Balancing the activation state of the endothelium via two distinct TGF-beta type I receptors. *EMBO J.* 2002;21(7):1743-1753.

312. Chen S, Kulik M, Lechleider RJ. Smad proteins regulate transcriptional induction of the SM22alpha gene by TGF-beta. *Nucleic Acids Res.* 2003;31(4):1302-1310.

313. Ota T, Fujii M, Sugizaki T, et al. Targets of transcriptional regulation by two distinct type I receptors for transforming growth factor-beta in human umbilical vein endothelial cells. *J Cell Physiol.* 2002;193(3):299-318.

314. Wang S, Zeng H, Xie XJ, et al. Loss of prolyl hydroxylase domain protein 2 in vascular endothelium increases pericyte coverage and promotes pulmonary arterial remodeling. *Oncotarget.* 2016;7(37):58848-58861.

315. Rock JR, Barkauskas CE, Cronce MJ, et al. Multiple stromal populations contribute to pulmonary fibrosis without evidence for epithelial to mesenchymal transition. *Proc Natl Acad Sci U S A.* 2011;108(52):E1475-1483.

316. Noble PW, Barkauskas CE, Jiang D. Pulmonary fibrosis: patterns and perpetrators. *J Clin Invest.* 2012;122(8):2756-2762.

317. Fabris L, Strazzabosco M. Epithelial-mesenchymal interactions in biliary diseases. *Semin Liver Dis.* 2011;31(1):11-32.

318. Schrimpf C, Duffield JS. Mechanisms of fibrosis: the role of the pericyte. *Curr Opin Nephrol Hypertens.* 2011;20(3):297-305.

319. Wei J, Bhattacharyya S, Tourtellotte WG, Varga J. Fibrosis in systemic sclerosis: emerging concepts and implications for targeted therapy. *Autoimmun Rev.* 2011;10(5):267-275.

320. Mahoney WM, Jr., Fleming JN, Schwartz SM. A unifying hypothesis for scleroderma: identifying a target cell for scleroderma. *Curr Rheumatol Rep.* 2011;13(1):28-36.

321. Kramann R, Schneider RK, DiRocco DP, et al. Perivascular Gli1+ progenitors are key contributors to injury-induced organ fibrosis. *Cell Stem Cell.* 2015;16(1):51-66.

322. Venkatachalam MA, Griffin KA, Lan R, Geng H, Saikumar P, Bidani AK. Acute kidney injury: a springboard for progression in chronic kidney disease. *Am J Physiol Renal Physiol.* 2010;298(5):F1078-1094.

323. Hammes HP, Feng Y, Pfister F, Brownlee M. Diabetic retinopathy: targeting vasoregression. *Diabetes.* 2011;60(1):9-16.

324. Yuan K, Shao NY, Hennigs JK, et al. Increased Pyruvate Dehydrogenase Kinase 4 Expression in Lung Pericytes Is Associated with Reduced Endothelial-Pericyte Interactions and Small Vessel Loss in Pulmonary Arterial Hypertension. *Am J Pathol.* 2016;186(9):2500-2514.

325. Kim JW, Tchernyshyov I, Semenza GL, Dang CV. HIF-1-mediated expression of pyruvate dehydrogenase kinase: a metabolic switch required for cellular adaptation to hypoxia. *Cell Metab.* 2006;3(3):177-185.

326. Dore-Duffy P, Owen C, Balabanov R, Murphy S, Beaumont T, Rafols JA. Pericyte migration from the vascular wall in response to traumatic brain injury. *Microvasc Res.* 2000;60(1):55-69.

327. Watson L, Ellis B, Leng GC. Exercise for intermittent claudication. *Cochrane Database Syst Rev.* 2008(4):CD000990.

328. Dachun X, Jue L, Liling Z, et al. Sensitivity and specificity of the ankle--brachial index to diagnose peripheral artery disease: a structured review. *Vasc Med.* 2010;15(5):361-369.

329. Nam SC, Han SH, Lim SH, et al. Factors affecting the validity of ankle-brachial index in the diagnosis of peripheral arterial obstructive disease. *Angiology.* 2010;61(4):392-396.

330. Coyne KS, Margolis MK, Gilchrist KA, et al. Evaluating effects of method of administration on Walking Impairment Questionnaire. *J Vasc Surg.* 2003;38(2):296-304.

331. Murphy TP, Cutlip DE, Regensteiner JG, et al. Supervised exercise versus primary stenting for claudication resulting from aortoiliac peripheral artery disease: six-month outcomes from the claudication: exercise versus endoluminal revascularization (CLEVER) study. *Circulation.* 2012;125(1):130-139.

332. Chetter IC, Spark JI, Kent PJ, Berridge DC, Scott DJ, Kester RC. Percutaneous transluminal angioplasty for intermittent claudication: evidence on which to base the medicine. *Eur J Vasc Endovasc Surg.* 1998;16(6):477-484.

333. Verspaget M, Nicolai SP, Kruidenier LM, Welten RJ, Prins MH, Teijink JA. Validation of the Dutch version of the Walking Impairment Questionnaire. *Eur J Vasc Endovasc Surg.* 2009;37(1):56-61.

334. McDermott MM, Mehta S, Liu K, et al. Leg symptoms, the ankle-brachial index, and walking ability in patients with peripheral arterial disease. *J Gen Intern Med.* 1999;14(3):173-181.

335. Sagar SP, Brown PM, Zelt DT, Pickett WL, Tranmer JE. Further clinical validation of the walking impairment questionnaire for classification of walking performance in patients with peripheral artery disease. *Int J Vasc Med.* 2012;2012:190641.

336. Nicolai SP, Kruidenier LM, Rouwet EV, Graffius K, Prins MH, Teijink JA. The walking impairment questionnaire: an effective tool to assess the effect of treatment in patients with intermittent claudication. *J Vasc Surg.* 2009;50(1):89-94.

337. Gardner AW, Skinner JS, Cantwell BW, Smith LK. Progressive vs single-stage treadmill tests for evaluation of claudication. *Med Sci Sports Exerc.* 1991;23(4):402-408.

338. Bennell K, Dobson F, Hinman R. Measures of physical performance assessments: Self-Paced Walk Test (SPWT), Stair Climb Test (SCT), Six-Minute

Walk Test (6MWT), Chair Stand Test (CST), Timed Up & Go (TUG), Sock Test, Lift and Carry Test (LCT), and Car Task. *Arthritis Care Res (Hoboken).* 2011;63 Suppl 11:S350-370.

339. Montgomery PS, Gardner AW. The clinical utility of a six-minute walk test in peripheral arterial occlusive disease patients. *J Am Geriatr Soc.* 1998;46(6):706-711.

340. Labs KH, Nehler MR, Roessner M, Jaeger KA, Hiatt WR. Reliability of treadmill testing in peripheral arterial disease: a comparison of a constant load with a graded load treadmill protocol. *Vasc Med.* 1999;4(4):239-246.

341. Hiatt WR, Rogers RK, Brass EP. The treadmill is a better functional test than the 6-minute walk test in therapeutic trials of patients with peripheral artery disease. *Circulation.* 2014;130(1):69-78.

342. Shimada YJ, Passeri JJ, Baggish AL, et al. Effects of losartan on left ventricular hypertrophy and fibrosis in patients with nonobstructive hypertrophic cardiomyopathy. *JACC Heart Fail.* 2013;1(6):480-487.

343. Song JH, Cha SH, Lee HJ, et al. Effect of low-dose dual blockade of renin-angiotensin system on urinary TGF-beta in type 2 diabetic patients with advanced kidney disease. *Nephrol Dial Transplant.* 2006;21(3):683-689.

344. Shahin Y, Cockcroft JR, Chetter IC. Randomized clinical trial of angiotensin-converting enzyme inhibitor, ramipril, in patients with intermittent claudication. *Br J Surg.* 2013;100(9):1154-1163.

345. Stevens JW, Simpson E, Harnan S, et al. Systematic review of the efficacy of cilostazol, naftidrofuryl oxalate and pentoxifylline for the treatment of intermittent claudication. *Br J Surg.* 2012;99(12):1630-1638.

346. Coppola G, Romano G, Corrado E, Grisanti RM, Novo S. Peripheral artery disease: potential role of ACE-inhibitor therapy. *Vasc Health Risk Manag.* 2008;4(6):1179-1187.

347. Hunter MR, Cahoon WD, Jr., Lowe DK. Angiotensin-converting enzyme inhibitors for intermittent claudication associated with peripheral arterial disease. *Ann Pharmacother.* 2013;47(11):1552-1557.

348. Kurklinsky AK, Levy M. Effect of ramipril on walking times and quality of life among patients with peripheral artery disease and intermittent claudication: a randomized controlled trial. Journal of the American Medical Association 2013; 309: 453-460. *Vasc Med.* 2013;18(4):234-236.

349. Hobbs SD, Thomas ME, Bradbury AW. Manipulation of the renin angiotensin system in peripheral arterial disease. *Eur J Vasc Endovasc Surg.* 2004;28(6):573-582.

350. Brown NJ, Vaughan DE. Angiotensin-converting enzyme inhibitors. *Circulation.* 1998;97(14):1411-1420.

351. Shahin Y, Khan JA, Chetter I. Angiotensin converting enzyme inhibitors effect on arterial stiffness and wave reflections: a meta-analysis and meta-regression of randomised controlled trials. *Atherosclerosis.* 2012;221(1):18-33.

352. Givertz MM. Manipulation of the renin-angiotensin system. *Circulation.* 2001;104(5):E14-18.

353. Montezano AC, Nguyen Dinh Cat A, Rios FJ, Touyz RM. Angiotensin II and vascular injury. *Curr Hypertens Rep.* 2014;16(6):431.

354. Roberts DH, Tsao Y, McLoughlin GA, Breckenridge A. Placebo-controlled comparison of captopril, atenolol, labetalol, and pindolol in hypertension complicated by intermittent claudication. *Lancet.* 1987;2(8560):650-653.

355. Sonecha TN, Nicolaides AN, Kyprianou P, et al. The effect of enalapril on leg muscle blood flow in patients with claudication. *Int Angiol.* 1990;9(1):22-24.

356. Bernardi D, Bartoli P, Ferreri A, Geri AB, Ieri A. Assessment of captopril and nicardipine effects on chronic occlusive arterial disease of the lower extremity using Doppler ultrasound. *Angiology.* 1988;39(11):942-952.

357. Kranzhofer R, Schmidt J, Pfeiffer CA, Hagl S, Libby P, Kubler W. Angiotensin induces inflammatory activation of human vascular smooth muscle cells. *Arterioscler Thromb Vasc Biol.* 1999;19(7):1623-1629.

358. Hernandez-Presa M, Bustos C, Ortego M, et al. Angiotensin-converting enzyme inhibition prevents arterial nuclear factor-kappa B activation, monocyte chemoattractant protein-1 expression, and macrophage infiltration in a rabbit model of early accelerated atherosclerosis. *Circulation.* 1997;95(6):1532-1541.

359. Tummala PE, Chen XL, Sundell CL, et al. Angiotensin II induces vascular cell adhesion molecule-1 expression in rat vasculature: A potential link between the renin-angiotensin system and atherosclerosis. *Circulation.* 1999;100(11):1223-1229.

360. Brevetti G, Giugliano G, Brevetti L, Hiatt WR. Inflammation in peripheral artery disease. *Circulation.* 2010;122(18):1862-1875.

361. Eagle KA, Rihal CS, Foster ED, Mickel MC, Gersh BJ. Long-term survival in patients with coronary artery disease: importance of peripheral vascular disease. The Coronary Artery Surgery Study (CASS) Investigators. *J Am Coll Cardiol.* 1994;23(5):1091-1095.

362. Pipinos, II, Judge AR, Selsby JT, et al. The myopathy of peripheral arterial occlusive disease: Part 2. Oxidative stress, neuropathy, and shift in muscle fiber type. *Vasc Endovascular Surg.* 2008;42(2):101-112.

363. Birbrair A, Delbono O. Pericytes are Essential for Skeletal Muscle Formation. *Stem Cell Rev.* 2015;11(4):547-548.

364. Sundberg C, Ivarsson M, Gerdin B, Rubin K. Pericytes as collagen-producing cells in excessive dermal scarring. *Lab Invest.* 1996;74(2):452-466.

365. Rajkumar VS, Shiwen X, Bostrom M, et al. Platelet-derived growth factor-beta receptor activation is essential for fibroblast and pericyte recruitment during cutaneous wound healing. *Am J Pathol.* 2006;169(6):2254-2265.

366. Coutinho T, Rooke TW, Kullo IJ. Arterial dysfunction and functional performance in patients with peripheral artery disease: a review. *Vasc Med.* 2011;16(3):203-211.

367. Gardner AW, Parker DE, Webb N, Montgomery PS, Scott KJ, Blevins SM. Calf muscle hemoglobin oxygen saturation characteristics and exercise performance in patients with intermittent claudication. *J Vasc Surg.* 2008;48(3):644-649.